

Geometric Variations of Local Systems

by

Jordan Allan Kostiuk

A thesis submitted in partial fulfilment of the requirements for the degree of

Doctor of Philosophy

in

Mathematics

Department of Mathematics and Statistical Sciences

University of Alberta

Abstract

The formalism of variations of local systems is applied in a geometric setting to define a notion of *geometric variation of local systems*; this provides a natural framework with which to study families of fibrations of Kähler manifolds. We apply this formalism in various contexts, starting with an examination of the moduli space of rational elliptic surfaces with four singular fibres. From there, we use the quadratic twist operation to construct families of K3 surfaces and examine the resulting geometric variations of local systems. We then proceed to study families of K3 surface fibrations. Specifically, we study families of M -polarized K3 surface fibrations and M_n -polarized K3 surface fibrations in the context of geometric variations of local systems; in particular, we are able to show how to obtain the fourteenth-case of integral variation of Hodge structures from the Doran-Morgan classification in this setting. Finally, we explain the connection to geometric isomonodromic deformations and, more generally, to solutions of the Schlesinger equations.

Dedication

To my wife, Rosie. I cannot imagine having completed this program without your unremitting support. Over the last eight years, you have played the role of cheerleader, audience member, and muse, as I have explored my passion for mathematics. When doubt crept in and brought me down, you brought me back up; when inspiration struck, you stoked the fires. You were there for it all, and I cannot wait to share the rest with you.

Acknowledgements

I would like to acknowledge the support of the large group of mathematicians at the University of Alberta that have shaped my views on the subject. In the beginning of my studies, Vladimir Troitsky, Adi Tcaciuc, and Paul Buckingham inspired and encouraged me to pursue my passion for mathematics and for that, I am eternally grateful. Sean Graves has instilled in me a passion for education that goes hand in hand with my research. There are simply no words to express the gratitude I have for my advisor, Chuck Doran, who has helped me in all matters of life, both mathematical and personal. To everyone at the University of Alberta: Thank You.

Finally, I would like to acknowledge NSERC, PIMS, and the government of Alberta for funding my studies and research throughout my time at the University of Alberta.

Contents

1	Introduction	1
2	Geometric Variations of Local Systems	4
2.1	Variations of Local Systems and Parabolic Cohomology	4
2.1.1	Fuchsian Differential Equations	5
2.1.2	Local Systems and Parabolic Cohomology	7
2.1.3	Variations of Local Systems	10
2.1.4	Computing the Monodromy Representation of Parabolic Cohomology	11
2.2	Variations of Hodge Structures	14
2.2.1	Hodge structures	15
2.2.2	Variation of Hodge Structure and Parabolic Cohomology	17
2.2.3	Geometric Variations of Local Systems	19
3	Elliptic Fibrations	21
3.1	Elliptic Surfaces and Parabolic Cohomology	22
3.1.1	Geometry of Elliptic Surfaces	22
3.1.2	The Structure of $H^2(E, \mathbf{Z})$ and Parabolic Cohomology	29
3.2	Elliptic Surfaces with Four Singular Fibres	32
3.2.1	Families of Rational Elliptic Surfaces	33
3.2.2	Families of K3 Surfaces from Herfurtner's List	40

4	K3 Surface Fibrations	49
4.1	The 14th Case VHS of Doran-Morgan	50
4.1.1	M -polarized K3-surfaces	50
4.1.2	The $\sigma = 1$ Locus	58
4.1.3	A New Perspective on the 14th Case	62
4.2	M_n -Polarized K3 Surface-Fibrations	67
4.2.1	General Theory	67
4.2.2	The Dwork Pencil	71
4.2.3	An Interesting Example	76
5	Isomonodromic Deformations	81
5.1	Isomonodromy	81
5.2	The Schlesinger Equations	84
5.3	The Sixth Painlevé Equation	86
6	Conclusion/Future Work	90
	Bibliography	92
	Appendix A Sage Code	97
	Appendix B Monodromy Representations	104

List of Tables

3.1	Kodaira's Classification	24
3.2	The five families.	34
3.3	Generating sections for Mordell-Weil of Families 2-4.	38
3.4	The seven families with I_0^* fibres.	39
3.5	Monodromies for the seven I_0^* families.	40
3.6	The 11 examples with one additive fibre.	42
3.7	Monodromy representations associated to examples in Table 3.6	45
B.1	Monodromy matrices for the two-parameter family of K3 surfaces generated by the eleven entries on Herfurtner's list with exactly one additive fibre. (Entries 1-6)	105
B.2	Monodromy matrices for the two-parameter family of K3 surfaces generated by the eleven entries on Herfurtner's list with exactly one additive fibre. (Entries 7-11)	106
B.3	Monodromy representations for the three-parameter family of K3 surfaces obtained from the seven families of rational elliptic surfaces with an I_0^* fibre on Herfurtner's list.	107
B.4	The monodromy representations for the one-parameter families of K3 surfaces obtained by twisting two non- I_0^* fibres in the I_0^* -families.	108

List of Figures

- 3.1 Branch cuts and transformations for Φ 27
- 3.2 Initial configuration for Family 1. 35
- 3.3 The braiding action for Family 1. 36
- 3.4 The loops $\gamma_1, \dots, \gamma_5$ 41

- 4.1 The standard fibration when $[a : b : d] = [1 : 1 : -1]$ 55
- 4.2 The alternate fibration when $[a : b : d] = [1 : 1 : -1]$ 57
- 4.3 The standard fibration variation. 60
- 4.4 The alternate fibration variation. 63
- 4.5 The M -polarized fibration variation. 65
- 4.6 The graph representing the functional invariant for the elliptic fibration (4.36). 72
- 4.7 The graph representing the initial elliptic fibration (4.38) on the quartic mirror
family. 72
- 4.8 The braid $\varphi(\sigma_0)$ 73
- 4.9 The braid $\varphi(\sigma_1)$ 73
- 4.10 The quintic mirror fibration 74
- 4.11 The initial configuration. 78
- 4.12 The motion of poles. 79

Chapter 1

Introduction

In his own thesis [21], Doran described a class of isomonodromic deformations of Fuchsian equations coming from geometry and named them *geometric isomonodromic deformations*. His interest at the time was in finding interesting algebraic solutions to the Schlesinger equations, of which the sixth Painlevé equation is a special case. By examining the kinds of geometric isomonodromic deformations that arise from Herfurtner’s classification of the moduli space of rational elliptic surfaces with four singular fibres [23], Doran was able to determine the totality of geometric isomonodromic deformations that gave rise to solutions to Painlevé VI—there were essentially only five of them. The perspective taken in [21], and the follow-up article [15] was tailored to the period map associated to the differential equation. This has the effect of inducing an equivalence relation, known as *projective equivalence* on the kinds of differential equations in consideration. Such an equivalence relation is also natural from the standpoint of isomonodromy, but it is not so well-behaved geometrically. For example, it is possible for two elliptic surfaces to have projectively equivalent Picard-Fuchs equations without themselves being isomorphic. Indeed, consider any elliptic surface and apply a quadratic twist.

The goal of this thesis is to refine the notion of geometric isomonodromic deformations in such a way that we remain sensitive to the underlying geometric structures involved. This is accomplished in the following manner. Dettweiler-Wewers in [12] have developed a formalism for studying *variations of local systems* of R -modules where R is a ring with unit. Roughly speaking, a variation of local systems is a family of local systems \mathcal{V}_a parameterized by a topological space A where each \mathcal{V}_a is a local system on a punctured sphere. The sheaf of R -modules on A whose stalks are equal to the parabolic cohomology groups of the local systems \mathcal{V}_a is a local system on A that captures information about the variation.

In the setting where $f: \mathcal{X} \rightarrow A$ is a family of Kähler manifolds for which each \mathcal{X}_a itself admits a fibration of Kähler manifolds, we then imagine the local systems \mathcal{V}_a as describing structures related to the “internal” fibration on each \mathcal{X}_a and then the parabolic cohomology local system \mathcal{W} on A is a local system capturing information about the “external” fibration $f: \mathcal{X} \rightarrow A$. These parabolic cohomology groups have already proved useful in studying K3 surface-fibred Calabi-Yau threefolds. Indeed, the article [18] explains how the parabolic cohomology of a single K3 surface fibration can be used to compute the hodge numbers of the total-space threefold. A key component in these computations was the fact that the parabolic cohomology groups involved admitted polarizable Hodge structures, thanks to results of Zucker [45]. While it was observed in [18] that several of these K3 fibrations move in families, the investigation of the corresponding *family* of parabolic cohomology groups was left open. Zucker’s results are quite general and equip the parabolic cohomology groups of “geometric” local systems with Hodge structures in a general setting. By combining these results with the variation of local system formalism, we are led to the notion of *geometric variation of local systems*. In short, this is a family of variations of Hodge structures whose parabolic cohomology local system is itself a variation of Hodge structure. This is the natural successor the notion of geometric isomonodromic deformations and allows us to capture more of the underlying geometric structures.

Just as important to the subject as the formalism are the algorithms developed in [12] to compute the corresponding parabolic cohomology groups and the monodromy representations for the corresponding local systems. By implementing these algorithms in sage, we are able use these algorithms to compute monodromy representations for many interesting variations of local systems. Since the algorithms developed in [12] are valid for rings with unit, we are able to work with \mathbf{Z} -bases of parabolic cohomology and obtain \mathbf{Z} -valued monodromy matrices. In this way, we remain sensitive to the integral structure underlying the geometry.

Chapter 2 of the thesis is devoted to recalling and developing the formalism needed to introduce geometric variations of local systems. In Chapter 3 we explore many of the geometric variations of local systems that come from Herfurtner’s list. As it turns out, there is a whole array of interesting geometric variations of local systems that can be found in Herfurtner’s list, despite the fact that it led to so few interesting geometric isomonodromic deformations. From the Herfurtner list we consider families of K3 surfaces that are obtained by applying quadratic twists. By computing the monodromy representations of the corresponding parabolic cohomology groups, we are able to compute the Picard number for many of these families by deciding whether or not the representation is irreducible.

Chapter 4 moves up a dimension and considers geometric variations of local systems

corresponding to K3 surface fibrations. Specifically, we study manifolds that are fibred by M -polarized K3 surfaces, where M is the rank eighteen unimodular lattice $H \oplus E_8 \oplus E_8$, as well as M_n -polarized K3 surfaces, where $M_n = M \oplus \langle -2n \rangle$. Starting with the two generic fibration structures on the family of M -polarized K3 surfaces, we show that the parabolic cohomology of the corresponding geometric variations of local systems gives rise to the rank four two-parameter transcendental lattice local system on the M -polarized moduli space \mathcal{M}_M . By restricting to a special “ $\sigma = 1$ ” sub-locus, we are able to apply the Dettweiler-Wewers algorithm to compute the monodromy representation in two different ways. In turn, we show how to obtain the fourteenth case of integral variations of Hodge structure classified in [20] by constructing a one-parameter geometric variation of local systems corresponding to a family of Calabi-Yau threefolds fibred by M -polarized K3 surfaces in the $\sigma = 1$ locus.

After constructing the fourteenth case variation, we examine M_n -polarized K3 surfaces. We state a definition of generalized “ K -equation” that captures the structure of the kinds of differential equations that arise from studying the corresponding mirror-map and prove a similar structural result to the result of Stiller [42]. We then consider the Dwork pencil of mirror hypersurfaces and the “iterative” geometric variations of local systems therein. Starting with the family of mirror cubic elliptic curves, we are able to construct the variation of Hodge structure on the family of mirror quartic surfaces using our techniques; in turn, we construct the variation of Hodge structure on the family of mirror quintic hypersurfaces from this.

Chapter 5 brings us back to Doran’s original motivations: the Schlesinger equations. We explain precisely the close relationship between isomonodromy and variations of local systems. By considering the Schlesinger equations, we use results of [27] and [32] to show that geometric variations of local systems will always give rise to “Schlesinger” deformations, as opposed to “non-Schlesinger.” We end the thesis by noting that associating to each solution of the Schlesinger equations its parabolic cohomology may be an interesting invariant to study from the point of view of the classification problem of the algebraic solutions. It is shown by example how this can be implemented for solutions to Painlevé VI, which now has a complete classification of solutions [33].

Finally, Chapter 6 describes some of the various directions in which we will continue to apply the tools developed in this thesis.

Chapter 2

Geometric Variations of Local Systems

In this chapter, we review the necessary prerequisite material to develop the notion of geometric variations of local systems. We start with Fuchsian differential equations, local systems and flat connections, and then review the theory of variations of local systems as discussed in [12], going over in some details their algorithm that will be used extensively in this thesis. After reviewing local systems and their variations, we discuss Hodge structure, their variations, and the result of Zucker that allow us to endow our parabolic cohomology groups with a Hodge structure. Finally, we combine these notions and define *geometric variations of local systems* in an abstract setting, laying the groundwork for the rest of the thesis.

2.1 Variations of Local Systems and Parabolic Cohomology

Here we review local systems and differential equations. Our conventions on the fundamental group of a topological space are the following: the product of two loops $\alpha \cdot \beta$ denotes the loop obtained by first traveling along α , and then along β , i.e., we read loops from the left to the right. With this convention on the fundamental group, it is most natural to consider *right* actions when speaking about group actions, and we do this for most of the thesis, pointing out when/if we stray from this. These are the conventions that are used by Dettweiler-Wewers in their papers on the subject, making it easier for the reader to transition between our work and theirs.

2.1.1 Fuchsian Differential Equations

We begin with a quick discussion of the necessary background of Fuchsian differential equations and differential systems. For references, the reader is encouraged to consult [26] for a careful treatment of the subject. Consider the n -th order differential equation

$$\frac{d^n f}{dt^n} + a_1(t) \frac{d^{n-1} f}{dt^{n-1}} + \cdots + a_n(t) f = 0. \quad (2.1)$$

The singular points of equation (2.1) are the points at which the coefficients $a_i(t)$ fail to be holomorphic. We say that (2.1) is *Fuchsian*, or is in the *Fuchsian class* if each singular point of (2.1) is *regular*. This means that solutions to (2.1) obey certain growth conditions near each singular point. In turn, this condition is equivalent to growth conditions on the coefficients: equation (2.1) is Fuchsian with regular singularities at $t_1, \dots, t_{m+1} = \infty$ if and only if the coefficients are of the form

$$a_k(t) = \frac{p_k(t)}{\prod_{i=1}^m (t - t_i)^k},$$

where each $p_k(t)$ is a polynomial of degree at most $k(m - 1)$.

The solution space in a neighbourhood of each regular point to (2.1) is a complex vector space of dimension n . A basis $\{f_1, \dots, f_n\}$ of solutions is known as a *fundamental set* of solutions to (2.1). Two differential equations of the form (2.1) are called *projectively equivalent* if there is function $\lambda(t)$ for which the map $f \mapsto \lambda \cdot f$ maps the solution space of the first equation to the other. In particular, if we scale by the n -th root of the Wronskian, which is defined to be the determinant of the matrix whose columns consist of the first $n - 1$ derivatives of a fundamental set of solutions, then we obtain the *projective normal form* of (2.1)—this is the unique n -th order Fuchsian equation that is projectively equivalent to (2.1) for which the coefficient a_1 vanishes.

Suppose now that $\{f_1, \dots, f_n\}$ is a fundamental set of solutions defined in a neighbourhood of t_0 , and let $S = \mathbf{P}_t^1 - \{t_1, \dots, t_m, \infty\}$, and $G = \pi_1(S, t_0)$ be the fundamental group. The solutions f_i are functions on the universal cover \tilde{S} and G acts as deck transformations. For each solution f of (2.1), the function f^γ is also a solution. If we fix a fundamental set $\{f_1, \dots, f_n\}$ of solutions and write them as a column vector, then for each $\gamma \in G$, there is a uniquely determined matrix $\rho(\gamma) \in \mathrm{GL}_n(\mathbf{C})$ satisfying

$$\begin{pmatrix} f_1 \\ \vdots \\ f_n \end{pmatrix}^\gamma = \rho(\gamma) \begin{pmatrix} f_1 \\ \vdots \\ f_n \end{pmatrix},$$

known as the *monodromy matrix*. The map $\rho: G \rightarrow \mathrm{GL}_n(\mathbf{C})$ is a homomorphism and is called the *monodromy representation* of (2.1) with respect to the basis $\{f_1, \dots, f_n\}$.

Suppose that $t = 0$ is a regular singular point of the differential equation (2.1) and introduce the operator

$$\delta := t \frac{d}{dt}.$$

Using the fact that $t^k \frac{d^k}{dt^k} = \delta(\delta - 1) \cdots (\delta - k + 1)$, we can re-write (2.1) as

$$L(f) = 0, \quad L = \sum_{i=0}^n b_i(t) \delta^{n-i},$$

where $b_0(t) = 1$ and the other b_i are convergent power series in t . The polynomial $g := \sum_{i=0}^n b_i(0) s^{n-i}$ is called the *characteristic equation* of (2.1) at $t = 0$ and its roots are called the *characteristic exponents* at $t = 0$. We define the characteristic equations and exponents for an arbitrary point $t \in \mathbf{C}$ by making the appropriate change of variable.

The data of the characteristic exponents and the singular points of a differential equations is typically tabulated as follows, in a table known as the *Riemann-scheme*:

t_1	\cdots	t_{m+1}
s_1^1	\cdots	s_1^{m+1}
\vdots	\vdots	\vdots
s_n^1	\cdots	s_n^{m+1}

The Riemann-scheme tells us information about the local solutions near each singular point. One can use the Fröbenius method to find power-series solutions to (2.1) near each singular point and determine the local monodromy transformation [26]. If s_1, \dots, s_n are the characteristic exponents of (2.1) at the singular point $t = t_i$, then the eigenvalues of the monodromy transformation along a small loop around t_i are equal to $e^{2\pi i s_1}, \dots, e^{2\pi i s_n}$ [26]. Thus, the determinant and trace of each monodromy transformation is determined by the Riemann-scheme. In particular, if the exponent differences $s_i - s_j$ are all non-integers, the monodromy transformation is diagonalizable.

If the exponent differences are all integers, then many things can happen. First, we may have a so-called logarithmic singularity, in which case the monodromy transformation for a loop near this point will have infinite-order. It may also be the case that the singular point is an *apparent* singular point, which, by definition, means that the corresponding monodromy transformation is trivial. That is, an apparent singularity is a singularity of the equation (2.1) that nonetheless admits a basis of single-valued (but possibly meromorphic) solutions

near the singularity.

We will also consider linear systems of differential equations of rank n . These are linear differential equations for the form

$$\frac{dy}{dx} = A(t)y, \quad (2.2)$$

where $y = (y_1, \dots, y_n)$ is a vector-valued function of t and $A(t)$ is a matrix. A matrix $Y(t)$ whose columns solve the Fuchsian system (2.2) is known as a fundamental matrix of solutions. Starting with the rank n Fuchsian differential equation (2.1) in the unknown y , then setting $y_i = \frac{d^{i-1}y}{dt^{i-1}}$, we can express equation (2.1) as a Fuchsian system.

Just like for Fuchsian differential equations, the system above is called Fuchsian if each singular point is regular. If $A(t)$ has at worst poles of order one, then the system is Fuchsian [26], but the converse is not true: there are Fuchsian systems that may have worse poles. While it will not be needed for us, there is an analogue of the Fröbenius method that tells us what the local solutions to the system (2.2) are. The analogue of the characteristic exponents are the eigenvalues of the residue matrices $\text{res}_{t=t_i} A(t)$ at the singular point $t = t_i$. If Y is a fundamental matrix for (2.2), then we can write

$$Y^\sigma = \rho(\sigma)Y,$$

where $\rho(\sigma) \in \text{GL}_n(\mathbf{C})$; this is what we mean when we say monodromy representation in the case of differential systems.

2.1.2 Local Systems and Parabolic Cohomology

Next we recall some of the theory of local systems, parabolic cohomology, and variations of local systems, following the treatment in [12]. We start with a connected and locally contractible topological space X , and let R be a commutative ring with unit; for all of our applications, we will take $R = \mathbf{Z}, \mathbf{Q}$ or \mathbf{C} .

Definition 1. A *local system* of R -modules on X is a locally constant sheaf \mathcal{V} on X , the stalks of which are free R -modules of finite rank p .

The stalk of \mathcal{V} at a point $x \in X$ will be denoted by \mathcal{V}_x . Once we fix a base point $x_0 \in X$, the fundamental group $\pi_1(X, x_0)$ acts on the stalk \mathcal{V}_{x_0} , which we will denote by V ; the following theorem of Deligne characterizes the structure of local systems in terms of this action:

Theorem ((2.5.2) in [11]). *The fundamental group $\pi_1(X, x_0)$ acts on the stalk \mathcal{V}_{x_0} , and the functor $\mathcal{V} \mapsto \mathcal{V}_{x_0}$ induces an equivalence of categories between local systems on X and representations of the fundamental group into $\text{GL}(V)$.*

Definition 2. The representation $\rho: \pi_1(X, x_0) \rightarrow \mathrm{GL}(V)$ associated to a local system will be called the *monodromy representation* associated to the local system.

Remark 1. We will use the convention that the fundamental group acts on V *on the right*. After picking a basis for V , we may represent elements of V as row vectors and the monodromy representation

$$\rho: \pi_1(X, x_0) \rightarrow \mathrm{GL}_p(R)$$

is given by right-multiplication:

$$v^\gamma = v \cdot \rho(\gamma).$$

These conventions are the same as those that appear in [12], and will allow us to most easily implement their algorithms.

Remark 2. We consider two representations ρ_1, ρ_2 to be isomorphic if they are related by a change of basis.

We now focus on the case where $X \cong \mathbf{P}_{\mathbb{C}}^1$ is the Riemann sphere. Let $D = \{x_1, \dots, x_r\} \subseteq X$ be a subset of r pairwise distinct points, and denote by U the compliment $U = X - D$. Then, one can choose simple loops $\gamma_i \in \pi_1(U, x_0)$ that go around x_i counter-clockwise in such a way that

$$\gamma_1 \cdots \gamma_r = 1.$$

This gives us a presentation of $\pi_1(U, x_0)$ as a free group on $r - 1$ generators. A local system of R -modules on U corresponds to a representation $\rho: \pi_1(U, x_0) \rightarrow \mathrm{GL}(V)$ which, in turn, corresponds to an r -tuple of transformations $g_i = \rho(\gamma_i)$ satisfying

$$g_1 \cdots g_r = 1.$$

Conversely, if we are given an r -tuple of transformations $\mathbf{g} = (g_1, \dots, g_r)$ whose product is trivial, then the categorical equivalence discussed above gives rise to a local system \mathcal{V} with this monodromy representation.

Let $j: U \rightarrow X$ denote the inclusion map.

Definition 3. The (first) *parabolic cohomology* of the local system \mathcal{V} is the sheaf cohomology of $j_*\mathcal{V}$ and will be denoted by

$$H_p^1(U, \mathcal{V}) := H^1(X, j_*\mathcal{V}).$$

According to [12], this cohomology group is a subgroup of $H^1(\pi_1(U, x_0), V)$, computed using group cohomology.

In concrete terms, a cocycle for $\pi_1(U, x_0)$ with values in V is a map $\delta: \pi_1(U, x_0) \rightarrow V$ satisfying $\delta(\alpha\beta) = \delta(\alpha) \cdot \rho(\beta) + \delta(\beta)$. If we set $v_i = \delta(\gamma_i)$, then since $\delta(1) = 0$, we find the following relation among the v_i :

$$v_1 \cdot g_2 \cdots g_r + v_2 \cdot g_3 \cdots g_r + \cdots + v_r = 0. \quad (2.3)$$

Conversely, if we have an r -tuple of vectors $(v_1, \dots, v_r) \in V^r$ that satisfy relation (2.3), then we obtain a unique cocycle by setting $\delta(\gamma_i) = v_i$ and extending to the rest of the fundamental group using the cocycle condition. The cocycle is a coboundary if and only if we can find a vector $v \in V$ for which $v_i = v \cdot (g_i - 1)$ holds for all i .

The parabolic cohomology group $H_p^1(U, \mathcal{V})$ is a subgroup of $H^1(U, \mathcal{V}) = H^1(\pi_1(U, x_0), V)$ and we call such cocycles *parabolic cocycles*. This subgroup is characterized by the following condition:

Lemma (Lemma 1.2 [12]). *The cocycle δ is a parabolic cocycle if and only if v_i lies in the image of $(g_i - 1)$ for all i .*

Define the following subspaces of V^r :

$$H_{\mathbf{g}} = \{(v_1, \dots, v_r) \mid v_i \in \text{image}(g_i - 1), \text{ and condition (2.3) holds}\}$$

and

$$E_{\mathbf{g}} = \{(v \cdot (g_1 - 1), \dots, v \cdot (g_r - 1)) \mid v \in V\}.$$

Then, the association $\delta \mapsto (v_1, \dots, v_r)$ is an isomorphism

$$H_p^1(U, \mathcal{V}) \cong W_{\mathbf{g}} := H_{\mathbf{g}}/E_{\mathbf{g}}$$

by the previous lemma.

If the stabilizer $V^{\pi_1(U,0)}$ is trivial, then this description of the parabolic cohomology group allows us to compute the rank in the case $R = K$ is a field:

$$\dim_K H_p^1(U, \mathcal{V}) = (r - 2) \cdot \dim_K V - \sum_{i=1}^r \dim_K \ker(g_i - 1). \quad (2.4)$$

The differential equations that we considered in the previous section give rise to complex local systems. Let \mathcal{V} be a quasi-coherent sheaf of \mathcal{O}_X -modules. A *connection* on \mathcal{V} is a \mathbf{C} -linear homomorphism

$$\nabla: \mathcal{V} \rightarrow \Omega_X^1 \otimes_{\mathcal{O}_X} \mathcal{V} := \Omega_X^1(\mathcal{V})$$

that satisfies the Leibniz identity:

$$\nabla(gs) = dg \otimes s + g\nabla s.$$

Given a connection $\nabla = \nabla_0: \mathcal{V} \rightarrow \Omega_X^1 \otimes \mathcal{V}$, it can be extended to a \mathbf{C} -linear map

$$\nabla_i: \Omega^i \otimes \mathcal{V} \rightarrow \Omega^{i+1} \otimes \mathcal{V}$$

via

$$\nabla_i(\omega \otimes s) := d\omega \otimes s + (-1)^i \omega \wedge \nabla_0(s).$$

The composition $R = \nabla_1 \nabla_0$ is called the *curvature* of the connection ∇ ; a connection ∇ is *flat*, or *integrable* if $R = 0$.

Suppose now that E is a complex local system on X , and let $\mathcal{E} = \mathcal{O}_X \otimes E$. Then we can give \mathcal{E} a natural connection ∇ for which $E = \ker \nabla$ by setting

$$\nabla(gs) = dgs,$$

where $g \in \mathcal{O}_X$ and $s \in E$. This connection is flat and known as the *Gauss-Manin connection* associated to the local system E . Conversely, we have the following theorem of Deligne:

Theorem (Deligne [11]). *Let ∇ be a connection on a locally free sheaf \mathcal{E} over a connected domain X . Set $E = \ker \nabla$. If ∇ is flat, then E is a local system on X and $\mathcal{E} = \mathcal{O}_X \otimes E$.*

2.1.3 Variations of Local Systems

In this section, we introduce the notion of a *variation of local systems*.

Definition 4. Let A be a connected complex manifold and $r \geq 3$. An *r -configuration* over A consists of a smooth and proper morphism $\bar{\pi}: X \rightarrow A$ of complex manifolds together with a smooth relative divisor $D \subseteq X$ for which the fibres X_a are isomorphic to $\mathbf{P}_{\mathbf{C}}^1$ and $D \cap X_a$ consists of r pairwise distinct points.

Fix an r -configuration (X, D) over A , let $U = X - D$, and denote by $j: U \rightarrow X$ the inclusion and $\pi: U \rightarrow A$ the projection. Choose a base point $a_0 \in A$ and set $X_0 = \bar{\pi}^{-1}(a_0)$, $D_0 = X_0 \cap D = \{x_1, \dots, x_r\}$, and $U_0 = X_0 - D_0$. Let $x_0 \in U_0$ be a base point. The fibration $\pi: U \rightarrow A$ gives rise to a short exact sequence of fundamental groups [12]:

$$1 \longrightarrow \pi_1(U_0, x_0) \longrightarrow \pi_1(U, x_0) \longrightarrow \pi_1(A, a_0) \longrightarrow 1. \quad (2.5)$$

Let \mathcal{V}_0 be a local system of R -modules on U_0 corresponding to a representation $\rho_0: \pi_1(U_0, x_0) \rightarrow \mathrm{GL}(V)$.

Definition 5. A *variation of the local system \mathcal{V}_0 over A* is a local system \mathcal{V} of R -modules on U whose restriction to U_0 is identified with \mathcal{V}_0 .

The *parabolic cohomology* of the variation \mathcal{V} is the higher direct image sheaf

$$\mathcal{W} = R^1\bar{\pi}_*(j_*\mathcal{V}).$$

By definition, the parabolic cohomology of the variation is a sheaf of R -modules on A . Locally on A , the configuration (X, D) is topologically trivial, and it follows that \mathcal{W} is locally constant with fibre

$$W = H_p^1(U_0, \mathcal{V}_0).$$

Therefore, \mathcal{W} is itself a local system of R -modules. Let $\eta: \pi_1(A, a_0) \rightarrow \mathrm{GL}(W)$ denote its corresponding monodromy representation. The following lemma describes the monodromy representation for this new local system:

Lemma (Lemma 2.2 [12]). *Let $\beta \in \pi_1(A)$ and $\delta: \pi_1(U_0) \rightarrow V$ be a parabolic cocycle, with $[\delta]$ the corresponding equivalence class. Let $\tilde{\beta} \in \pi_1(U)$ be a lift of β . Then $[\delta]^{\eta(\beta)} = [\delta']$, where $\delta': \pi_1(U_0) \rightarrow V$ is the cocycle*

$$\alpha \mapsto \delta(\tilde{\beta}\alpha\tilde{\beta}^{-1}) \cdot \rho(\tilde{\beta}), \quad \alpha \in \pi_1(U_0).$$

Remark 3. While it is not emphasized in [12], it should be noted that the sheaf \mathcal{W} may not, in general, be free—there may be torsion. We obtain a local system of R -modules, in the sense of [12], by dividing out by the torsion subgroup. The braid companion quotient $W_{\mathbf{g}}$ that one works with when implementing the algorithms in [12] is equal to the intersection of parabolic cohomology tensored with the field of fractions and the R -valued cohomology group, i.e., is identified with parabolic cohomology modulo torsion. This is not an issue for us because we divide out by the torsion anyway when working with Hodge structures, but we point it out because some of the parabolic cohomology groups we will work with are *not* torsion-free, as we will see in the next Chapter.

2.1.4 Computing the Monodromy Representation of Parabolic Cohomology

Given a variation of local systems \mathcal{V} , the monodromy representation η of the parabolic cohomology can be computed explicitly under some mild assumptions. In order to describe

the algorithm, we introduce a few more preliminaries.

Let

$$\mathcal{O}_{r-1} = \{D' \subseteq \mathbf{C} \mid |D'| = r - 1\} = \{D \subseteq \mathbf{P}_{\mathbf{C}}^1 \mid |D| = r, \infty \in D\}$$

be the configuration space of $r - 1$ points in the plane, or of r points on the Riemann sphere with one of the points at ∞ . The fundamental group $\pi_1(\mathcal{O}_{r-1}, D_0)$ is known as the *Artin* braid group on $r - 1$ strands. The braid group admits standard generators $\beta_1, \dots, \beta_{r-2}$ that exchange the position of x_i, x_{i+1} by rotating counterclockwise [2]. These generators satisfy the relations

$$\beta_i \beta_{i+1} \beta_i = \beta_{i+1} \beta_i \beta_{i+1}, \quad \beta_i \beta_j = \beta_j \beta_i \quad |i - j| > 1.$$

Let

$$\mathcal{E}_r(V) = \{\mathbf{g} = (g_1, \dots, g_r) \mid g_i \in \mathrm{GL}(V), g_1 \dots g_r = 1\}.$$

Then, A_{r-1} acts on $\mathcal{E}_r(V)$ from the right via

$$\mathbf{g}^{\beta_i} = (g_1, \dots, g_{i+1}, g_{i+1}^{-1} g_i g_{i+1}, \dots, g_r).$$

If $H_{\mathbf{g}}, E_{\mathbf{g}}$ denote the vector spaces introduced earlier, then we define an R -linear isomorphism

$$\Phi(\mathbf{g}, \beta): H_{\mathbf{g}} \rightarrow H_{\mathbf{g}^{\beta}},$$

by declaring

$$(v_1, \dots, v_r)^{\Phi(\mathbf{g}, \beta)} = (v_1, \dots, v_{i+1}, v_{i+1}(1 - g_{i+1}^{-1} g_i g_{i+1}) + v_i g_{i+1}, \dots, v_r), \quad (2.6)$$

and extending to all of the braid group using the ‘‘cocycle’’ rule:

$$\Phi(\mathbf{g}, \beta) \Phi(\mathbf{g}^{\beta}, \beta') = \Phi(\mathbf{g}, \beta \beta').$$

These maps act appropriately on the submodules $E_{\mathbf{g}}$ and therefore induce an isomorphism

$$\bar{\Phi}(\mathbf{g}, \beta): W_{\mathbf{g}} \rightarrow W_{\mathbf{g}^{\beta}}.$$

On the other hand, given $h \in \mathrm{GL}(V)$, we define isomorphisms

$$\Psi(\mathbf{g}, h) : \begin{cases} H_{\mathbf{g}^h} & \rightarrow & H_{\mathbf{g}} \\ (v_1, \dots, v_r) & \mapsto & (v_1 \cdot h, \dots, v_r \cdot h) \end{cases},$$

where $\mathbf{g}^h = (h^{-1}g_1h, \dots, h^{-1}g_rh)$. The maps $\Psi(\mathbf{g}, h)$ induce isomorphisms

$$\bar{\Psi}(\mathbf{g}, h): W_{\mathbf{g}^h} \rightarrow W_{\mathbf{g}}.$$

For the rest of this section, we make the following assumptions:

- $X = \mathbf{P}_A^1$ is the relative projective line over A ;
- the divisor D contains $\{\infty\} \times A \subseteq \mathbf{P}_A^1$;
- there exists a point $a_0 \in A$ such that D_0 is contained in the real-line.

Remark 4. These assumptions are only to make computations more feasible in [12]. As they will hold in all applications in this thesis, we choose to make these assumptions ourselves for clarity of exposition.

Since $\infty \times A \subseteq D$, we can use D_0 as a base point for the configuration space \mathcal{O}_{r-1} . The divisor $D \subseteq \mathbf{P}_A^1$ gives rise to a holomorphic map $A \rightarrow \mathcal{O}_{r-1}$ by sending each $a \in A$ to $D \cap X_a$. Let $A_{r-1} = \pi_1(\mathcal{O}_r, D_0)$ be the fundamental group—it is more commonly known as the *Artin braid group*.

Definition 6. Notation as above, let $\varphi: \pi_1(A, a_0) \rightarrow A_{r-1}$ be the corresponding push-forward homomorphism on fundamental groups. The map φ is called the *braiding map* induced by the configuration (X, D) .

The variation \mathcal{V} corresponds to a monodromy representation $\rho: \pi_1(U) \rightarrow \mathrm{GL}(V)$. Let $\rho_0: \pi_1(U_0) \rightarrow \mathrm{GL}(V)$ denote its restriction, via the exact sequence (2.5). As explained in [12], the short exact sequence is *split*, so that ρ is determined by ρ_0 and a representation $\chi: \pi_1(A) \rightarrow \mathrm{GL}(V)$. A loop $\gamma \in \pi_1(A)$ acts on the initial representation ρ_0 in two different ways. First, we can lift the loop γ to a loop in $\pi_1(U)$ and act by conjugation; this has the effect of conjugating the representation ρ_0 by $\chi(\gamma)^{-1}$. On the other hand, $\varphi(\gamma) \in A_{r-1}$ acts via the braid action defined above. These actions are compatible:

$$\mathbf{g}^{\varphi(\gamma)} = \mathbf{g}^{\chi(\gamma)^{-1}}.$$

We then have the following theorem proved in [12]:

Theorem (Theorem 2.5 [12]). *Let \mathcal{W} be the parabolic cohomology of \mathcal{V} and $\eta: \pi_1(A, a_0) \rightarrow \mathrm{GL}(W)$ the monodromy representation. For all $\gamma \in \pi_1(A, a_0)$, we have*

$$\eta(\gamma) = \bar{\Phi}(\mathbf{g}, \varphi(\gamma)) \cdot \bar{\Psi}(\mathbf{g}, \chi(\gamma)).$$

Remark 5. As is pointed out in [12], if R is a field and the local system is irreducible, then the homomorphism χ is determined up to scalar multiples by the braiding map because of Schur's lemma. It follows that the braiding map is enough to determine the projective monodromy representation. In many of the examples we discuss, we can use other knowledge of the parabolic cohomology local system, such as the Picard-Fuchs equation, to pin down the representation precisely.

This theorem, together with the preceding discussion, describes an algorithm to compute the monodromy representation of the parabolic cohomology of a variation of local systems, which we now summarize. Start with a variation of local systems defined on an r -configuration and fix a base point $a_0 \in A$, and the initial monodromy representation ρ^0 , which corresponds to an r -tuple of matrix \mathbf{g} . Further, suppose that $\gamma_1, \dots, \gamma_s$ are generators for $\pi_1(A, a_0)$. Then, the following steps compute the projective monodromy representation for the parabolic cohomology local system on A :

1. construct the spaces $H_{\mathbf{g}}, E_{\mathbf{g}}, W_{\mathbf{g}}$;
2. for each $i = 1, \dots, s$, find matrices $h_i \in \mathrm{GL}_r(\mathbf{C})$ for which

$$\mathbf{g}^{\varphi(\gamma_i)} = \mathbf{g}^{h_i^{-1}};$$

3. compute the transformations $\Phi(\mathbf{g}, \varphi(\gamma_i))$ and $\Psi(\mathbf{g}, h_i)$;
4. the projective monodromy is given by $\eta(\gamma_i) = \overline{\Phi}(\mathbf{g}, \varphi(\gamma_i)) \cdot \overline{\Psi}(\mathbf{g}, h_i)$

Thus, in order to compute the monodromy representation, we must know the braiding map φ and the representation χ . In practice, it is the description of the braiding map that is the most complicated part of the algorithm.

2.2 Variations of Hodge Structures

The local systems that will play the central role of this thesis are ones arising from geometry. Specifically, we will be studying *variations of Hodge structures*. We begin with some preliminaries on the subject, following the treatment found in the very-well written survey paper [44] and text [6].

2.2.1 Hodge structures

Definition 7. A (pure) Hodge structure of weight $n \in \mathbf{Z}$, denoted by $(H_{\mathbf{Z}}, H^{p,q})$ is a finitely generated abelian group $H_{\mathbf{Z}}$ together with a decomposition of the complexification:

$$H_{\mathbf{C}} = \bigoplus_{p+q=n} H^{p,q}$$

satisfying $H^{p,q} = \overline{H^{q,p}}$.

We will also be interested in rational Hodge structures, but we always want to be sensitive to the integral story in our work. Equivalent to the above Hodge decomposition is the Hodge filtration. This is a finite decreasing filtration $\{F^p\}$ of $H_{\mathbf{C}}$

$$H_{\mathbf{C}} \supset \cdots \supset F^p \supset F^{p+1} \supset \cdots,$$

such that

$$H_{\mathbf{C}} \cong F^p \oplus \overline{F^{n-p+1}}.$$

Given the hodge decomposition, we obtain the filtration by setting

$$F^p := \bigoplus_{i \geq p} H^{i, n-i},$$

given the filtration, we recover the decomposition by setting

$$H^{p,q} := F^p \cap \overline{F^q}.$$

The filtration perspective is a useful reformulation as it varies holomorphically in families [44].

Let us briefly recall the Hodge decomposition associate to a Kähler manifold. Start with an m -dimensional Riemannian manifold. Let \mathcal{A}_X^n be the sheaf of smooth n -forms and let $d: \mathcal{A} \rightarrow \mathcal{A}^{n+1}$ denote the exterior derivative. The laplacian is given by

$$\Delta_d = d\delta + \delta d,$$

where $\delta: \mathcal{A}^n \rightarrow \mathcal{A}^{n-1}$ is the *codifferential* given by $\delta = (-1)^{nm+m+1} * d*$ where $*$ is the Hodge star operator. Let $\mathcal{H}^n(X)$ denote the set of harmonic forms of degree n :

$$\mathcal{H}^n(X) := \{\alpha \in \mathcal{A}^n \mid \Delta\alpha = 0\}.$$

Then, Hodge's theorem states that

$$\mathcal{H}^n(X) \cong H^n(X, \mathbf{R}).$$

Now suppose X is a complex manifold with Hermitian metric. Then, the sheaf \mathcal{A}^n splits as a direct sum

$$\mathcal{A}_X^n = \bigoplus_{p+q=n} \mathcal{A}^{p,q},$$

where the sheaves on the right-hand side are the sheaves of (p, q) forms. The differential d decomposes as $d = \partial + \bar{\partial}$, the so-called Dolbeault operators. We have $\partial: \mathcal{A}^{p,q} \rightarrow \mathcal{A}^{p+1,q}$ and $\bar{\partial}: \mathcal{A}^{p,q} \rightarrow \mathcal{A}^{p,q+1}$. This allows to defined operators Δ_{∂} and $\Delta_{\bar{\partial}}$, which preserve the bidegree. Note that for an arbitrary complex manifold, these operators may not be related to the regular laplacian and the laplacian need not preserve bidgree.

This is why we restrict to Kähler manifolds, those for which the imaginary part ω of the hermitian metric (a $(1, 1)$ form) is closed. For such manifolds, we call ω the Kähler form. Under this assumption, we have

$$\Delta_d = 2\Delta_{\bar{\partial}} = 2\Delta_{\partial}.$$

This allows us to decompose

$$\mathcal{H}^n(X) = \bigoplus \mathcal{H}^{p,q}(X),$$

where $\mathcal{H}^{p,q}(X)$ is the space of harmonic forms of type (p, q) ; this decomposition satisfies the conjugacy conditions. If we further assume that X is compact, we have $\mathcal{H}^n(X) \cong H^n(X, \mathbf{C})$, and so we get a decomposition of complex cohomology. By Dolbeault's isomorphism, one can show that $H^{p,q} \cong H^q(X, \Omega_X^p)$, where Ω_X^p is the sheaf of holomorphic p -forms on X . Thus, to each Kähler manifold, we have an integral Hodge structure of weight n on $H^n(X, \mathbf{Z})/\text{torsion}$.

We will be interested in Hodge structures with an additional structure known as a *polarization*. Notation as above, consider the Hodge structure of weight n attached to the cohomology of a Kähler manifold X . The Kähler form ω allows us to define a non-degenerate bilinear form $Q: H_{\mathbf{Z}} \times H_{\mathbf{Z}} \rightarrow \mathbf{Z}$ by the formula

$$Q(\xi, \eta) := \int_X \xi \wedge \eta \wedge \omega^{\dim X - n}.$$

This form extends by \mathbf{C} -linearity to $H_{\mathbf{C}}$ on which it enjoys the following properties:

- Q is $(-1)^n$ -symmetric;
- $Q(\xi, \eta) = 0$ for $\xi \in H^{p,q}$ and $\eta \in H^{p',q'}$ with $p \neq q'$;

- $(-1)^{\frac{n(n-1)}{2}} i^{p-q} Q(\xi, \bar{\xi}) > 0$ for $\xi \neq 0 \in H^{p,q}$.

Definition 8. A polarized hodge structure of weight n consists of an (integral) hodge structure of weight n together with a non-degenerate bilinear form on $H_{\mathbf{Z}}$ which extends to $H_{\mathbf{C}}$ and enjoys the above properties.

2.2.2 Variation of Hodge Structure and Parabolic Cohomology

Given a *family* of Kähler manifolds, we now wish to consider the way in which the Hodge structures vary. More precisely, consider $f: \mathcal{X} \rightarrow \Delta$, a proper smooth surjective morphism onto a complex polydisc and assume that the fibres X_b are all compact Kähler manifolds. Further assume that there exists $\omega \in H^2(\mathcal{X}, \mathbf{Z})$ for which we have $\omega|_{X_b}$ is a Kähler class. We then have polarized hodge structures of weight n on each $H^n(X_b, \mathbf{Z})$ that varies with b . Under this set-up, there is a *unique* isomorphism $H^n(X_b, \mathbf{Z}) \cong H^n(X_{b'}, \mathbf{Z})$ for each $b, b' \in \Delta$ and so there is no ambiguity in us setting $H_{\mathbf{Z}} := H^n(X_b, \mathbf{Z})$ and $H_{\mathbf{C}} = H^n(X_b, \mathbf{C})$ since these don't depend on b . These isomorphisms do not preserve the Hodge decomposition as b varies, rather it varies in such a way that the hodge numbers are preserved.

Definition 9. Let \mathcal{D} be the set of collections of subspaces $\{H^{p,q}\}$ of $H_{\mathbf{C}}$ for which $H_{\mathbf{C}} = \bigoplus H^{p,q}$ and $\dim(H^{p,q}) = h^{p,q}$, on which Q satisfies the conditions we need. Alternatively, we may define \mathcal{D} to be the set of all filtrations $\{F^p\}$ for which $\dim F^p = h^{n,0} + \dots + h^{p,n-p}$ and Q satisfies the Hodge-Riemann relations.

The space \mathcal{D} is called the local period domain and is actually a real manifold. Moreover, we can enhance \mathcal{D} to a complex manifold. The point is that we obtain a map $\phi: \Delta \rightarrow \mathcal{D}$ defined by associating the Hodge-filtration to each point $b \in \Delta$; this is called the local period mapping.

In terms of the filtration, we find that the following two properties hold:

$$\frac{\partial F_b^p}{\partial b} \subseteq F_b^p$$

$$\frac{\partial F_b^p}{\partial b} \subseteq F_b^{p-1}.$$

The first is called holomorphicity and implies that ϕ is holomorphic and the second is known as Griffiths transversality.

Of course, we want to study families over non-contractible domains. In this case, the isomorphisms of the cohomology groups are no longer unique and we will have to quotient

out by monodromy. To this end, set

$$\mathrm{Aut}(H_{\mathbf{Z}}, Q) := \{g: H_{\mathbf{Z}} \rightarrow H_{\mathbf{Z}} \mid Q(\xi g, \eta g) = Q(\xi, \eta)\}.$$

This group acts on the period domain in the natural manner. Gluing isomorphisms $H^n(X_b, \mathbf{Z}) \cong H^n(X_{b'}, \mathbf{Z})$ for b, b' close together, we find that $H^n(X_b, \mathbf{Z})$ may not return itself when continued along a path. Instead, for each $\gamma \in \pi_1(B, b)$, there is an automorphism $\rho(\gamma) \in \mathrm{Aut}(H_{\mathbf{Z}}, Q)$ for which analytic continuation is given by multiplication-by- $\rho(\gamma)$. If Γ is a subgroup containing the image of this monodromy representation, then we obtain a well-defined period map

$$\phi: B \rightarrow \Gamma \backslash \mathcal{D},$$

which we call the *global* period mapping. The quotient is called the period domain.

Now let \mathcal{D} be a local period domain classifying Hodge structures of weight n on $H_{\mathbf{C}}$ polarized by Q , let $\Gamma \subseteq \mathrm{Aut}(H_{\mathbf{Z}}, Q)$ as above and B a complex manifold.

Definition 10. A map $\phi: B \rightarrow \Gamma \backslash \mathcal{D}$ defines a *polarized variation of Hodge structure of weight n on B* if

- for each $b \in B$, the map ϕ lifts a holomorphic map $\tilde{\phi}_b: \Delta \rightarrow \mathcal{D}$;
- the local lifts satisfy Griffiths transversality.

We can express this in the language of flat connections and local systems as follows. Let B be a complex manifold and let $\mathcal{E}_{\mathbf{Z}}$ be a locally constant system of finitely generated free \mathbf{Z} -modules on B . Set $\mathcal{E} := \mathcal{E}_{\mathbf{Z}} \otimes \mathcal{O}_B$. Then \mathcal{E} is a complex vector bundle and is equipped with the Gauss-Manin connection $\nabla: \mathcal{E} \rightarrow \mathcal{E} \otimes \Omega_B^1$ induced by $d: \mathcal{O}_B \rightarrow \Omega_B^1$. Let $\{\mathcal{F}^p\}$ be a filtration by subbundles.

Definition 11. The data $(\mathcal{E}_{\mathbf{Z}}, \mathcal{F})$ defines a variation of Hodge structure of weight n on B if

- $\{\mathcal{F}^p\}$ induces Hodge structures on weight n on the fibres of \mathcal{E} ;
- if s is a section of \mathcal{F}^p and ζ is a vector field of type $(1, 0)$, then $\nabla_{\zeta}s$ is a section of \mathcal{F}^{p-1} (Griffiths transversality).

Furthermore, if $\mathcal{E}_{\mathbf{Z}}$ carries a non-degenerate bilinear form $Q: \mathcal{E}_{\mathbf{Z}} \times \mathcal{E}_{\mathbf{Z}} \rightarrow \mathbf{Z}$, we have a polarized variation of hodge structures if

- Q defines a polarized Hodge structure on each fibre;

- Q is flat with respect to ∇ ; that is, we have

$$dQ(s, s') = Q(\nabla s, s') + Q(s, \nabla s').$$

In particular, a variation of Hodge structure is an integral local system; we may therefore consider the associated parabolic cohomology. Results of Zucker show that this group can be given a Hodge structure in the case where the base of the family is a curve. More precisely, he proves the following theorem

Theorem (Theorem 7.12 [45]). *Let S be a non-singular algebraic curve over \mathbf{C} , \bar{S} its smooth completion, $j: S \rightarrow \bar{S}$, and V a local system of complex vector spaces underlying a polarizable variation of Hodge structure of weight m . Then, there is a natural polarizable Hodge structure of weight $m + i$ on $H^i(\bar{S}, j_*V)$ associated to the variation of Hodge structure.*

As Zucker explains, when $V = R^m f_* \mathbf{C}$, j_*V is the sheaf of local invariant “cycles” and the Hodge structure is most interesting when $i = 1$. A Hodge structure can always be placed extrinsically on $H^1(\bar{S}, j_*R^m f_* \mathbf{C})$ using the Leray spectral sequence for \bar{f} ; one of the main results of [45] is that these two Hodge structures coincide:

Theorem (Theorem 15.5 [45]). *The Hodge structure on $H^1(S, R^i f_* \mathbf{C})$ is induced by that of $H^{i+1}(X)$.*

That is, there is an inclusion of $H^1(S, R^i f_* \mathbf{Q})$ inside $H^{i+1}(X, \mathbf{Q})$ for which the Hodge structure on $H^1(S, R^i f_* \mathbf{C})$ agrees with the one it inherits from the Hodge structure on $H^{i+1}(X, \mathbf{C})$.

2.2.3 Geometric Variations of Local Systems

Here, we combine the notions of variations of local systems and variations of Hodge structures and introduce the main subject of this thesis: *geometric variations of local systems*.

Let $\bar{\pi}: X \rightarrow A$ be an r -configuration. That is, we consider a proper morphism of complex manifolds $\bar{\pi}: X \rightarrow A$, together with a smooth relative divisor $D \subseteq X$ for which each fibre X_a is isomorphic to $\mathbf{P}_{\mathbf{C}}^1$, and $D_a = D \cap X_a$ consists of r pairwise-distinct points; let $U = X - D$ and set $U_a = X_a - D_a$ for each $a \in A$.

Theorem/Definition 1. *A geometric variation of local systems is a variation of local systems \mathcal{V} satisfying the following conditions:*

1. *the local system \mathcal{V} is a polarized variation of Hodge structures of weight n over A ;*

2. for each $a \in A$, the restriction \mathcal{V}_a is itself a polarized variation of Hodge structures of weight n over U_a ;
3. the parabolic cohomology \mathcal{W} is a polarized variation of Hodge structures of weight $n+1$.

Let $f: \mathcal{X} \rightarrow U \subseteq X$ be a family of Kähler manifolds, and let $\mathcal{V} = R^n f_* \mathbf{Z}$ be the polarized variation of Hodge structure of weight n on U corresponding to the n -th cohomology groups, equipped with the Gauss-Manin connection. For each $a \in A$, let $f_a: \mathcal{X}_a \rightarrow U_a$ be the restriction of f to the fibre \mathcal{X}_a over $a \in A$ of the composition $\pi \circ f$, and let \mathcal{V}_a, ∇_a denote the restrictions of \mathcal{V}, ∇ to the fibre $U_a \subseteq X_a \cong \mathbf{P}^1$. Then \mathcal{V} defines a geometric variation of local systems.

Remark 6. In the above definition, conditions (1) and (2) imply that each stalk \mathcal{W}_a carries a polarized Hodge structure by the results of Zucker [45]. The additional condition being imposed in this definition is that the Gauss-Manin connection on \mathcal{W} gives rise to a variation of Hodge structures. In practice, the only condition that needs checking is Griffiths transversality.

Proof. For each $a \in A$, the local system \mathcal{V}_a is equal to the local system $R^n_{f_a,*} \mathbf{Z}$ on $U_a \subseteq X_a \cong \mathbf{P}^1$, where $f_a: \mathcal{X}_a \rightarrow U_a$ is the restriction of f to the fibre over $a \in A$. The local system $\mathcal{W} := R^1 \pi_* j_* \mathcal{V}$ on A is the local system whose stalk at each $a \in A$ is the parabolic cohomology of \mathcal{V}_a . That is, $\mathcal{W}_a \cong R^1_{j_a,*} \mathcal{V}_a$. Each \mathcal{W}_a carries a Hodge structure of weight $n+1$ by [45]. On the other hand, the local system \mathcal{W} is contained in $R^{n+1}(\pi \circ f)_* \mathbf{Z}$, the local system whose stalks are the cohomology groups $H^{n+1}(\mathcal{X}_a, \mathbf{Z})$, and the Hodge structure on \mathcal{W}_a is the same as the one induced by this inclusion. Since $R^{n+1}(\pi \circ f)_* \mathbf{Z}$ is a variation of Hodge structure, its restriction to \mathcal{W} is also a variation of Hodge structure. Therefore, \mathcal{V} defines a geometric variation of local systems in the sense of Definition 1. \square

Chapter 3

Elliptic Fibrations

In this chapter we explore the geometric variations of local systems that come from families of elliptic fibrations. We start by reviewing some of the basic theory of elliptic surfaces and describing in some detail the structure of the parabolic cohomology groups. After discussing these foundations, we explore the geometric variations of local systems that arise from studying the moduli space of rational elliptic surfaces with four singular fibres that was completely described by Herfurtner [23]. The Herfurtner list was already examined by Doran in [15] with a view towards finding examples of geometric isomonodromic deformations. From this perspective, there are only five interesting examples that come from this moduli space. In contrast, we show that the seven “omitted” families of elliptic surfaces with four singular fibres do give rise to interesting geometric variations of local systems. For each of these variations, we determine the monodromy representation of the corresponding parabolic cohomology in Propositions 2, 3, and 4.

Next, we consider families of K3 surfaces that can be constructed out of the Herfurtner list by applying quadratic twists. By considering the most general quadratic twist (twisting two smooth points), we obtain two-parameter families of K3 surfaces from the thirty-eight rigid entries on Herfurtner’s list. Thus, *all* elliptic surfaces on this list give rise to geometric variations of local systems. Since the deformation spaces for the geometric variations of local systems that are obtained in this way are so simple, we are able to run the Dettweiler-Wewers algorithm to compute the monodromy of parabolic cohomology for all of these local systems. Propositions 5-11 summarize the computations that we performed and detail some of the interesting phenomena that occur. In particular, we are able to determine the Picard number for these families of K3 surfaces by proving that the corresponding parabolic cohomology local systems are irreducible.

3.1 Elliptic Surfaces and Parabolic Cohomology

We begin by reviewing some of the main features of elliptic surfaces and prove a structural theorem about their parabolic cohomology groups. Good references for the material here are the original papers by Kodaira [29, 30, 31], several of the papers by Stiller [42, 41], and the survey paper [40] by Schütt-Shioda [40], to name a few.

3.1.1 Geometry of Elliptic Surfaces

In this section we will briefly review the geometry of elliptic surfaces.

Definition 12. An *elliptic surface* E over S is a smooth projective surface E with an elliptic fibration over S , i.e., a surjective map

$$f: E \rightarrow S$$

for which

- all but finitely many fibres are smooth curves of genus 1;
- no fibre contains an exceptional curve of the first kind.

A *section* of an elliptic surface $f: E \rightarrow S$ is a morphism

$$\sigma: S \rightarrow E, \text{ for which } f \circ \sigma = \text{id}_S.$$

An elliptic surface with section will be called a *basic elliptic surface*.

Remark 7. All of the elliptic surfaces in this thesis will be assumed to have a section.

Since we are only dealing with complex basic elliptic surfaces, we can always choose a Weierstrass presentation of E :

$$y^2 = 4x^3 - g_2(t)x - g_3(t), \quad g_2, g_3 \in K(S). \quad (3.1)$$

The fibres of (3.1) are smooth elliptic curves as long as the discriminant $\Delta = g_2^3 - 27g_3^2$ does not vanish. For each $t \in S$ such that $\Delta(t) = 0$, the fibre is either a cuspidal or nodal rational curve, and the singular point of the curve may or may not be a surface singularity of (3.1). If the singular point of the fibre is a surface singularity, then we perform a sequence of blow-ups to resolve the singularity. Doing this for each singular fibre, we arrive at the Néron model, which is a smooth surface with elliptic fibration whose singular fibres are chains of rational curves.

In order to classify the kinds of chains of rational curves that occur, i.e., classify the kinds of singular fibres that can occur, Kodaira considered the following two invariants associated to an elliptic surface [29]:

Definition 13. Let $E \rightarrow S$ be an elliptic surface, Σ the support of the singular fibres, and $S_0 = S - \Sigma$. The functional invariant \mathcal{J} is the rational function on S whose value at $t \in S_0$ is the J -invariant of the fibre E_t at t . In terms of the Weierstrass form (3.1), we have

$$\mathcal{J} = \frac{g_2^3}{g_3^3 - 27g_2^2}.$$

The sheaf $\mathcal{G} := R^1 f_* \mathbf{Z}|_{S_0}$, which is the \mathbf{Z} -local system on S_0 whose stalks are given by the first cohomology groups $H^1(E_t, \mathbf{Z})$, is called the *homological invariant*; it is characterized by its monodromy representation

$$\rho: \pi_1(X_0) \rightarrow \mathrm{SL}_2(\mathbf{Z}),$$

and we will often refer to the representation as the homological invariant.

The dual local system \mathcal{G}^\vee , whose stalks are given by the homology groups $H_1(E_t, \mathbf{Z})$, is called the *geometric homological invariant* and its monodromy representation is called the *geometric monodromy representation*.

The classification of Kodaira is described in terms of the possible local geometric monodromy transformation around the singular fibre. In order to compute the type of singular fibre, we only need to know the order of vanishing of g_2, g_3 , and Δ at the singular fibre. The classification is tabulated in Table 3.1. Of the possible singular fibre types on an elliptic surface, those of type I_N are called *multiplicative* fibres, while all other singular fibre types are called *additive* (the terminology comes from the kind of singular curve obtained at this particular point).

Let us now consider the weight one integral variation of Hodge structure on the elliptic surface $f: E \rightarrow S$ associated to the homological invariant \mathcal{G} . The polarization on \mathcal{G} is induced by the cup-product and if we choose a basis $\alpha^*, \beta^* \in H^1(E_t, \mathbf{Z})$ that is Poincaré-dual to the standard cycles $\alpha, \beta \in H_1(E_t, \mathbf{Z})$, then the matrix of the polarization with respect to this basis is given by

$$\begin{pmatrix} 0 & 1 \\ -1 & 0 \end{pmatrix}. \tag{3.2}$$

The Hodge filtration on $H^1(E_t, \mathbf{C})$ is determined by a non-zero $\omega \in H^1(E_t, \mathbf{C})$ that spans the filtrant F^1 . If we write $\omega = z_1 \alpha^* + z_2 \beta^*$ in terms of the standard basis for $H^1(E_t, \mathbf{Z})$, then the Hodge-Riemann relations imply that $\frac{z_2}{z_1} \in \mathfrak{h}$, and conversely.

Type	$\nu(g_2)$	$\nu(g_3)$	$\nu(\Delta)$	Graph	Monodromy
I_0	$a \geq 0$	$b \geq 0$	0	—	$\begin{pmatrix} 1 & 0 \\ 0 & 1 \end{pmatrix}$
I_N	0	0	$N \geq 1$	\tilde{A}_N	$\begin{pmatrix} 1 & N \\ 0 & 1 \end{pmatrix}$
II	$a \geq 1$	1	2	—	$\begin{pmatrix} 1 & 1 \\ -1 & 0 \end{pmatrix}$
III	1	$b \geq 1$	3	\tilde{A}_1	$\begin{pmatrix} 0 & 1 \\ -1 & 0 \end{pmatrix}$
IV	$a \geq 2$	2	4	\tilde{A}_2	$\begin{pmatrix} 0 & 1 \\ -1 & -1 \end{pmatrix}$
I_0	$a \geq 2$	$b \geq 3$	6	\tilde{D}_4	$\begin{pmatrix} -1 & 0 \\ 0 & -1 \end{pmatrix}$
I_N^*	2	3	$N + 6 \geq 7$	\tilde{D}_{N+4}	$\begin{pmatrix} -1 & -N \\ 0 & -1 \end{pmatrix}$
IV^*	$a \geq 3$	4	8	\tilde{E}_6	$\begin{pmatrix} -1 & -1 \\ 1 & 0 \end{pmatrix}$
III^*	3	$b \geq 5$	9	\tilde{E}_7	$\begin{pmatrix} 0 & -1 \\ 1 & 0 \end{pmatrix}$
II^*	$a \geq 4$	5	10	\tilde{E}_8	$\begin{pmatrix} 0 & -1 \\ 1 & 1 \end{pmatrix}$

Table 3.1: Kodaira's Classification

One can associate to this variation of Hodge structure a Fuchsian differential equation known as the Picard-Fuchs equation as follows. Let $\omega = \frac{dx}{y}$ be the usual global holomorphic 1-form on the elliptic surface E , and let ∇ denote the Gauss-Manin connection on $\mathcal{G}_{\mathbf{C}}$. Since the rank of $\mathcal{G}_{\mathbf{C}}$ is equal to 2, there is a linear relation amongst $\omega, \nabla \frac{d}{dt} \omega, \nabla^2 \frac{d}{dt} \omega$ and so we may write:

$$a(t)\nabla^2 \frac{d}{dt} \omega + b(t)\nabla \frac{d}{dt} \omega + c(t)\omega = 0, \quad (3.3)$$

for rational functions a, b, c . If $\gamma \in H^1(E_t, \mathbf{Z})$ is a cycle, and $f_\gamma(t) := \int_\gamma \omega$, then the function $f_\gamma(t)$ satisfies the differential equation:

$$a(t)\frac{d^2 f}{dt^2} + b(t)\frac{df}{dt} + c(t)f(t) = 0, \quad (3.4)$$

which is known as the Picard-Fuchs equation. According to [22], this differential equation is a Fuchsian differential equation. As γ varies over all the cycles in \mathcal{G}^\vee , the 2-dimensional space of function $f_\gamma(t)$ spans the solution space to (3.4).

Remark 8. Given a cycle γ , the analytic continuation of $f_\gamma(t)$ along a loop $\sigma \in \pi_1(S_0)$ satisfies

$$f_\gamma^\sigma(t) = f_{\gamma\sigma}(t).$$

It follows that the monodromy representation for the Picard-Fuchs equation (3.4) can be identified with the geometric monodromy representation of the elliptic surface.

Remark 9. The formulation of Hodge structures is most natural for the cohomology groups because of the naturally defined cup-product on cohomology, which induces the polarization. However, in practice, one often works directly with the Picard-Fuchs equation and the geometric homological invariant. The reason for this stems from the *period map* associated to the variation of Hodge structure. In the setting of the elliptic surfaces, the period map is the map

$$\begin{aligned} \text{per}: S &\rightarrow \mathbf{P}(H_{\mathbf{C}}^1) \\ t &\mapsto \omega(t). \end{aligned} \quad (3.5)$$

If we fix the basis α^*, β^* of the homological invariant, then period map is given explicitly via

$$\text{per}(t) = f_\alpha(t)\alpha^* + f_\beta(t)\beta^*.$$

Thus, the variation of Hodge structure on the homological invariant is described, via the period map, in terms of properties of the geometric homological invariant. For this reason, we will often use the term homological invariant to describe the geometric homological invariant, as in the literature, and clarify when any confusion arises.

Given the Weierstrass form (3.1), there are a number of methods one can use to compute the Picard-Fuchs equations, such as the Griffiths-Dwork algorithm. This calculation was carried out in [7] for example, where it is shown that the Picard-Fuchs equation is

$$\frac{d^2 f}{dt^2} + P \frac{df}{dt} + Qf = 0, \quad (3.6)$$

where

$$P = \frac{\frac{dg_3}{dt}}{g_3} - \frac{\frac{dg_2}{dt}}{g_2} + \frac{d\mathcal{J}}{\mathcal{J}} - \frac{\frac{d^2 \mathcal{J}}{dt^2}}{\frac{d\mathcal{J}}{dt}},$$

$$Q = \frac{\left(\frac{d\mathcal{J}}{dt}\right)^2}{144\mathcal{J}(\mathcal{J}-1)} + \frac{\frac{d\Delta}{dt}}{12\Delta} \left(P + \frac{\frac{d^2 \Delta}{dt^2}}{\frac{d\Delta}{dt}} - \frac{13}{12} \frac{\frac{d\Delta}{dt}}{\Delta} \right).$$

More than just being a Fuchsian differential equation, the Picard-Fuchs equations arising from elliptic surfaces are K -equations, a term coined by Stiller [42].

Definition 14. A second order Fuchsian ODE is called a K -equation if it possesses two solutions ω_1, ω_2 which are holomorphic non-vanishing multivalued functions on a Zariski open subset $S_0 \subseteq S$ satisfying the following conditions:

- (i) ω_1, ω_2 form a basis of solutions;
- (ii) the monodromy representation of the differential equation with respect to this basis takes values in $\mathrm{SL}_2(\mathbf{Z})$;
- (iii) $\mathrm{im}\left(\frac{\omega_2}{\omega_1}\right) > 0$ on S_0 (positivity);
- (iv) the Wronskian lies in $K(S)$.

The pair ω_1, ω_2 is called a K -basis.

The solutions $\omega_1 = f_\alpha, \omega_2 = f_\beta$ to the Picard-Fuchs equation (3.4) form a K -basis thanks to the Hodge-Riemann relations. Therefore, the Picard-Fuchs equation of an elliptic surface is a K -equation. Conversely, as his article shows, every K -equation can be realized as the Picard-Fuchs equation associated to an elliptic surface [42][Theorem II.2.5].

Let us briefly go over some of the details of how this works. Stiller starts by considering the elliptic surface $E \rightarrow \mathbf{P}_t^1$ given by the Weierstrass presentation

$$y^2 = 4x^3 - \frac{27t}{t-1}x - \frac{27t}{t-1}. \quad (3.7)$$

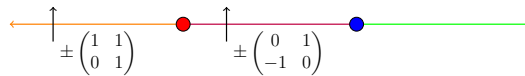


Figure 3.1: Branch cuts and transformations for Φ .

Then, the functional invariant in this case is $\mathcal{J} = t$. The Picard-Fuchs equation associated to this elliptic surface is given by

$$\frac{d^2 f}{dt^2} + \frac{1}{t} \frac{df}{dt} + \frac{\frac{31}{144}t - \frac{1}{36}}{t^2(t-1)^2} f = 0, \tag{3.8}$$

as can be computed using Equation (3.6), for example.

An explicit K -basis Φ_1, Φ_2 for (3.7) is constructed in [42]. The quotient of these solutions $\Phi = \frac{\Phi_1}{\Phi_2}$ induces a holomorphic multivalued map

$$\mathbf{P}_t^1 - \{0, 1, \infty\} \xrightarrow{\Phi} \mathfrak{h}, \tag{3.9}$$

because of the positivity condition of a K -basis. In fact, Φ is an inverse to the classical modular J -function. If one makes a branch cut on \mathbf{P}_t^1 joining ∞ to 0 along the negative real-axis and another branch cut along the interval $[0, 1]$, then one can choose a single-valued branch of Φ on the slit-sphere that takes values in the usual fundamental domain for the $\mathrm{SL}_2(\mathbf{Z})$ -action on \mathfrak{h} :

$$\{\tau \in \mathfrak{h} \mid -\frac{1}{2} < \mathrm{Re}(\tau) < \frac{1}{2}, |\tau| > 1\}.$$

Continuation along these slits in the directions indicated leads to monodromy transformations as shown in Figure 3.1 up to sign:

Choosing loops γ_0, γ_1 , based at i looping around 0 and 1 once, and setting $\gamma_\infty = (\gamma_0\gamma_1)^{-1}$, we can determine the monodromy transformations from these branch cuts up to sign. By analyzing the characteristic exponents of the differential equation (3.8), we can pin down the monodromy representation precisely. We find that

$$\begin{aligned} \gamma_0 &\mapsto \begin{pmatrix} 1 & 1 \\ -1 & 0 \end{pmatrix} \\ \gamma_1 &\mapsto \begin{pmatrix} 0 & -1 \\ 1 & 0 \end{pmatrix} \\ \gamma_\infty &\mapsto \begin{pmatrix} 1 & 1 \\ 0 & 1 \end{pmatrix}. \end{aligned} \tag{3.10}$$

In particular, we see that the elliptic surface defined by (3.7) has singular fibres of type III* at $t = 0$, II at $t = 1$ and I₁ at $t = \infty$ by consulting Table 3.1.

Next, suppose we have an arbitrary K -equation

$$\frac{d^2 f}{dt^2} + P \frac{df}{dt} Q + Rf = 0, \quad (3.11)$$

and let ω_1, ω_2 be a K -basis. Then, the ratio of these two solutions gives rise to a multivalued map to \mathfrak{h} and the composition $\mathcal{J} := J \circ \frac{\omega_2}{\omega_1}$ is a *rational* function from S_0 to \mathbf{P}^1 [42], called the *functional invariant* of the K -equation.

We then have the following structural results about K -equations:

Proposition. *[[42]] Given the K -equation (3.11), there exists an algebraic function λ satisfying $\lambda^2 \in K(S)$ for which the original K -equation is obtained by pulling back (3.8) by the functional invariant \mathcal{J} and then scaling by λ . Explicitly, we have*

$$P = \frac{\left(\frac{d\mathcal{J}}{dt}\right)^2 - \mathcal{J} \frac{d^2\mathcal{J}}{dt^2}}{\mathcal{J} \frac{d\mathcal{J}}{dt}} - \frac{d}{dt} \log \lambda^2,$$

$$Q = \frac{\left(\frac{d\mathcal{J}}{dt}\right)^2 \left(\frac{31}{144}\mathcal{J} - \frac{1}{36}\right)}{\mathcal{J}^2(\mathcal{J} - 1)^2} - \left(\frac{\left(\frac{d\mathcal{J}}{dt}\right)^2 - \mathcal{J} \frac{d^2\mathcal{J}}{dt^2}}{\mathcal{J} \frac{d\mathcal{J}}{dt}}\right) \frac{d}{dt} \log \lambda - \frac{d^2\lambda}{\lambda^2} + 2 \left(\frac{d\lambda}{\lambda}\right)^2,$$

In particular, the Picard-Fuchs equation of an arbitrary elliptic surface can be computed this way by taking $\lambda^2 = \frac{g_2}{g_3}$.

Finally, every K -equation is the Picard-Fuchs equation of an elliptic surface.

One the reasons why a result like Proposition 3.1.1 is so useful is that it helps us compute the homological invariant of an arbitrary elliptic surface in terms of the homological invariant of the well-understood elliptic surface given by (3.7), if we understand the functional invariant. Indeed, the monodromy representation of the Picard-Fuchs equation is obtained as follows. First, the functional invariant induces a push-forward map

$$\mathcal{J}_* : \pi_1(X_0) \rightarrow \pi_1(\mathbf{P}^1 - \{0, 1, \infty\}).$$

Composing this map with the monodromy representation (3.10), we obtain the monodromy representation for the pull back of (3.8) by \mathcal{J} . Scaling the solutions by $\lambda = \sqrt{\frac{g_2}{g_3}}$ has the effect of multiplying the monodromy transformations by -1 at the positions where λ has a pole or zero. Thus, if we understand the push-forward map \mathcal{J}_* , as well as where the poles and zeroes of λ lie, we can compute the homological invariant precisely.

3.1.2 The Structure of $H^2(E, \mathbf{Z})$ and Parabolic Cohomology

In this section, we will describe in some detail the lattice $H^2(E, \mathbf{Z})$ and its weight two integral Hodge structure. A good reference for this section is [citeschuettEllipticSurfaces2010](#). The Néron-Severi group, which is the group of divisors modulo algebraic equivalence, embeds in $H^2(E, \mathbf{Z})$ modulo via the *cycle-map* and is denoted $\text{NS}(E)$. If we assume the curve S is genus 0, as is the case for all examples in this thesis, then $\text{NS}(E)$ is torsion-free. The cup-product on $H^2(E, \mathbf{Z})$ coincides with the intersection pairing on $\text{NS}(E)$, and makes $\text{NS}(E)$ a sublattice; its rank is called the Picard number, which we denote $\rho(E)$. According to the Hodge index theorem, $\text{NS}(E)$ has signature $(1, \rho - 1)$. The orthogonal complement of $\text{NS}(E)$ in $H^2(E, \mathbf{Z})$ is called the *transcendental lattice* and is denoted by $T(E)$. The Hodge decomposition of $H^2(E, \mathbf{Z})$ induces weight 2 Hodge structures on both the Néron-Severi lattice and the transcendental lattice. However, by the Lefschetz $(1, 1)$ -theorem, we have

$$H^2(E, \mathbf{Z}) \cap H^{1,1} = \text{NS}(E), \quad (3.12)$$

from which it follows that the $h^{2,0}(\text{NS}(E)) = 0$. Typically, we are most interested in the Hodge structure on the transcendental lattice.

Each section σ of the elliptic surface $E \rightarrow S$ corresponds to a $K(S)$ -rational point on the generic fibre, making the generic fibre an elliptic curve over the function field $K(S)$. If we fix one section σ_0 as an origin, then the group law on the generic fibre induces a group law on the set of sections.

Definition 15. The group of sections of an elliptic surface $f: E \rightarrow S$ is called the *Mordell-Weil group* of $E \rightarrow S$ and is denoted $\text{MW}(E)$. The *narrow Mordell-Weil group*, denoted by $\text{MW}^0(E)$ is the subgroup of sections that meet the zero component of every fibre. The narrow Mordell-Weil group is torsion-free and has finite-index in the full Mordell-Weil group [citeschuettEllipticSurfaces2010](#).

Definition 16. The subgroup of $\text{NS}(E)$ generated by the zero section, general fibre, and the components of the bad fibres is called the *trivial lattice*, denoted by T .

The trivial lattice can be decomposed as follows. First, introduce the following notations:

- F is a general fibre;
- F_t is the fibre over t ;
- m_t is the number of components of F_t ;
- Σ is the set of singular points;

- $R \subseteq \Sigma$ is the subset of singular points lying under additive fibres;
- $\Theta_{t,0}$ is the component of F_t met by the zero section;
- $\Theta_{t,i}$ for $i = 1, \dots, m_t - 1$ are the other components;
- T_t is the lattice generated by the fibre components *not* meeting the zero-section;
- \mathcal{O} is the class of the zero-section.

Then we have:

$$T = \langle \mathcal{O}, F \rangle \oplus \bigoplus_{t \in R} T_t. \tag{3.13}$$

Thus, the rank of the trivial lattice is

$$\text{rank}(T) = 2 + \sum_{t \in R} (m_t - 1).$$

Since each section corresponds to a divisor on E , we obtain a map from the Mordell-Weil group to the Néron-Severi group. The induced map $P \mapsto P \bmod T$ induces an isomorphism

$$\text{MW}(E) \cong \text{NS}(E)/T. \tag{3.14}$$

This allows us to compute the rank of $\text{MW}(E)$:

$$\text{rank}(\text{MW}(E)) = \rho - 2 - \sum_{t \in R} (m_t - 1).$$

The trivial lattice does *not* embed primitively inside $\text{NS}(E)$, the cokernel is isomorphic to the torsion subgroup of $\text{MW}(E)$.

Definition 17. The *essential lattice* $L(E)$ is the orthogonal compliment of the trivial lattice inside $\text{NS}(E)$.

The essential lattice is even and negative-definite of rank equal to $r - 2 - \sum_x (m_x - 1)$, i.e., has rank equal to the Mordell-Weil group. Orthogonal projection with respect to the trivial lattice defines a map

$$\varphi: \text{NS}_{\mathbf{Q}}(E) \longrightarrow L(E)_{\mathbf{Q}}. \tag{3.15}$$

This map is characterized by the universal properties:

$$\varphi(D) \perp T(E)_{\mathbf{Q}}, \quad \varphi(D) \equiv D \bmod T(E)_{\mathbf{Q}}.$$

By restricting to $MW(E)$, we obtain a well-defined map from the Mordell-Weil group $MW(E) \rightarrow L(E)_{\mathbf{Q}}$, the kernel of which is the torsion subgroup. Thus, $MW(E)/\{\text{torsion}\}$ sits inside $L(E)_{\mathbf{Q}}$.

Remark 10. In general, if a section σ hits a non-zero fibre component, then its image in $L(E)_{\mathbf{Q}}$ will *not* lie in the integral part; that is, tensoring with \mathbf{Q} is necessary to define the above homomorphism.

This map can be used to give the Mordell-Weil group the structure of a *positive-definite* lattice by setting

$$\langle \sigma_1, \sigma_2 \rangle := -\varphi(\sigma_1) \cdot \varphi(\sigma_2).$$

Definition 18. The lattice $MW(E)/\{\text{torsion}\}$ is called the *Mordell-Weil lattice*. The sublattice $MW^0(E)$ is called the *narrow Mordell-Weil lattice*.

Remark 11. The lattice structure on $MW(E)$ was first discovered by Cox-Zucker in [46]; this is simply a more modern perspective on their approach.

Each torsion section must hit a non-zero fibre component [citeschuettEllipticSurfaces2010](#). It follows that the restriction of the orthogonal projection map to the narrow Mordell-Weil lattice is injective. The image of the the narrow Mordell-Weil group lies in the integral part, and if we flip the sign on the bilinear form on $L(E)$, then the essential lattice and narrow Mordell-Weil lattices are isomorphic [citeschuettEllipticSurfaces2010](#). The full Mordell-Weil lattice embeds in the dual of the essential lattice and is isomorphic to it if $NS(E)$ is unimodular.

Let us now consider the parabolic cohomology of the homological invariant $H^1(S, j_*\mathcal{G})$ and its Hodge structure. The torsion on $H^1(S, j_*\mathcal{G})$ is isomorphic to the torsions subgroup of the Mordell-Weil group, according to [46]. Modulo torsion, the parabolic cohomology group sits inside $H^2(E, \mathbf{Z})$, and its Hodge structure agrees with the one that is induced from this embedding, as discussed in Chapter 2. As described in [46], the parabolic cohomology group can be computed as follows. Consider the Leray filtration on $H^2(E, \mathbf{Z})$, given by

$$\begin{aligned} L^1 &= \ker(H^2(E, \mathbf{Z}) \rightarrow H^0(S, R^2f_*\mathbf{Z})) \\ L^1/L^2 &\cong H^1(S, j_*\mathcal{G}) \\ L^2 &= \text{image}(H^2(S, \mathbf{Z}) \rightarrow H^2(E, \mathbf{Z})) \cong \mathbf{Z}[F]. \end{aligned} \tag{3.16}$$

Using this, we can prove the following structural results:

Proposition 1. *The transcendental lattice $T(E)$ is contained in $H^1(S, j_*\mathcal{G})$. Over \mathbf{Q} , we have the following orthogonal decomposition of $H^1(S, j_*\mathcal{G})_{\mathbf{Q}}$:*

$$H^1(S, j_*\mathcal{G})_{\mathbf{Q}} = L(E)_{\mathbf{Q}} \oplus T(E)_{\mathbf{Q}}. \tag{3.17}$$

If the transcendental lattice is unimodular, then the above splitting holds over \mathbf{Z} .

Proof. The first statement follows from the fact that $L^1/L^2 \cong H^1(S, j_*\mathcal{G})$, that the transcendental lattice is contained in L^1 , and that the transcendental lattice has trivial intersection with $\mathbf{Z}[F]$. Tensoring with \mathbf{Q} , the kernel of the map $H^2(E, \mathbf{Q}) \rightarrow H^0(S, R^2f_*\mathbf{Q})$, which sends each divisor to its restriction to each fibre, is precisely

$$L(E)_{\mathbf{Q}} \oplus T(E)_{\mathbf{Q}} \oplus \mathbf{Q} \cdot [F].$$

Thus, the second result follows by taking the quotient by L^2 .

If the transcendental lattice is unimodular, we argue as follows. The discussion that preceded the proposition shows that the essential lattice is contained in parabolic cohomology. The discriminant of the essential lattice is equal to $\text{disc}(T)/n^2$ [39]. On the other hand, this is also the discriminant of the cup-product on parabolic cohomology, as was calculated in [46]. Thus, the quotient of parabolic cohomology by the transcendental lattice is a lattice of the same discriminant (by unimodularity), from which it follows that the quotient is equal to the essential lattice. Therefore, we have the splitting over \mathbf{Z} . \square

In particular, if E is a rational elliptic surface with homological invariant \mathcal{G} , then the group $H^1(E, j_*\mathcal{G})$, modulo torsion, is identified with the narrow Mordell-Weil group.

Remark 12. While all of the ingredients required to prove this result are in [46] and citeschuetttEllipticSurfaces2010, I have not seen this formulation in the literature.

Remark 13. From this decomposition, we see that the parabolic cohomology group over \mathbf{Q} breaks into one piece that does not depend on the fibration structure, the transcendental lattice, and another that *does*, the Mordell-Weil lattice. When we study these in families, the corresponding parabolic cohomology local systems therefore decompose into one “extrinsic” local system, capturing information about the transcendental data and one “intrinsic” local system, telling us information about the varying internal fibration structure.

3.2 Elliptic Surfaces with Four Singular Fibres

In this section, we consider the geometric variations of local systems coming from the moduli space of rational elliptic surfaces with four singular fibres that was studied in [23]. For rational elliptic surfaces, the transcendental lattices are trivial and the corresponding parabolic cohomology local systems are related to the Mordell-Weil group as described in the previous section. By applying a quadratic twist to the elliptic surfaces on Herfurtners list, we are able to produce families of K3 surfaces and compute the monodromy representations of the

corresponding parabolic cohomology local systems. We provide many examples for which we are able to determine that the monodromy representation is irreducible which, in turn, allows us to compute the Picard rank for these families of K3 surfaces.

3.2.1 Families of Rational Elliptic Surfaces

In his article [23], Herfurtnner classified the all elliptic surfaces with four singular fibres and tabulated them in what is known as *Herfurtnner's list*. The classification consists of twelve one-parameter families of elliptic surfaces and thirty-eight isolated, rigid, elliptic surfaces. Of the twelve families, seven of them posses I_0^* fibres and this means, in particular, that the corresponding family of Picard-Fuchs equations are all projectively equivalent to each other. For this reason, these seven families were considered uninteresting to Doran in [15] for the purpose of finding solutions to the sixth Painlevé equation.

We begin our exploration of Herfurtnner's list by considering the five families that Doran studied in [15]. The Weierstrass invariants and singular fibre types are indicated in Table 3.2. In each case, we have a one-parameter family of rational elliptic surfaces with four singular fibres parameterized by $a \in A = \mathbf{P}^1 - \Sigma$, where Σ is the finite set of points that corresponds to the collision of these singular fibres. Let $X = \mathbf{P}_t^1 \times A$, $D \subseteq X$ be the divisor that cuts out the four singular points, and $U = X - D$. We consider the local system \mathcal{V} on U whose stalk at each (t, a) is the first cohomology group

$$\mathcal{V}_{(t,a)} = H^1(E_{t,a}, \mathbf{Z}).$$

If we fix a base point $a_0 \in A$, the restricted local system \mathcal{V}_0 is the local system on $\mathbf{P}_t^1 - D_0$ that corresponds to the elliptic surface \mathcal{E}_{a_0} .

The local system \mathcal{V} satisfies the conditions of Theorem/Definition 1, so we have a geometric variation local systems \mathcal{V} over A and (X, D) is a 4-configuration that satisfies the computational assumptions described in Chapter 2. Thus, we can use the Dettweiler-Wewers algorithm described earlier to compute the monodromy representation of the parabolic cohomology. By our earlier structural result, we know that the parabolic cohomology local system for each of these rational elliptic surface can be identified with the narrow Mordell-Weil group.

Since these local systems are irreducible, the rank formula (2.4) allows us to compute the ranks of the integral parabolic cohomology. For singular fibres of type I_b , $b > 0$, the monodromy matrices have one-dimensional stabilizers. All other kinds of singular fibres have trivial stabilizers. It follows that the parabolic cohomology of the variation of local system in family 1 is a rank two local system, while the other four families have rank one parabolic

Family	Sing. Fibre Types	Weierstrass Presentation
1	I_1, I_1, II, IV^* $(0, \infty, 1, a^2)$	$g_2(t, a) = 3(t-1)(t-a^2)^3$ $g_3(t, a) = (t-1)(t-a^2)^4(t+a)$
2	I_1, I_1, I_2, I_2^* $(\omega_1, \omega_2, \infty, 0)$	$g_2(t, a) = 12t^2(t^2 + at + 1)$ $g_3(t, a) = 4t^3(2t^3 + 3at^2 + 3at + 2)$
3	I_1, I_1, I_1, I_3^* $(\omega_1, \omega_2, \infty, 0)$	$g_2(t, a) = 12t^2(t^2 + 2at + 1)$ $g_3(t, a) = 4t^3(2t^3 + 3(a^2 + 1)t^2 + 6at + 2)$
4	I_1, I_1, I_1, III^* $(\omega_1, \omega_1, \infty, 0)$	$g_2(t, a) = 3t^3(t+1)$ $g_3(t, a) = t^5(t+1)$
5	I_1, I_1, I_2, IV^* $(\omega_1, \omega_2, \infty, 0)$	$g_2(t, a) = 3t^3(t+2a)$ $g_3(t, a) = t^4(t^2 + 3at + 1)$

Table 3.2: The five families.

cohomologies. We now compute the monodromy representations of these local systems.

Family 1: For this family of elliptic surface, the functional invariant is

$$\mathcal{J}(t, a) = \frac{1}{(a+1)^2} \frac{(t-1)(a^2-t)}{t}.$$

This allows us to determine the global monodromy representation for the elliptic surface \mathcal{E}_a for any a . To do this, we draw a figure that describes the cover $\mathcal{J}(t, a)$. This is done by drawing a graph on \mathbf{P}^1 with red vertices corresponding to the pre-images of 0, blue vertices corresponding to the pre-images of 1, yellow vertices corresponding to the pre-images of ∞ , and brown vertices that correspond to ramification points other than $\{0, 1, \infty\}$. Further, we draw coloured arcs for the fibres between vertices: purple arcs map to $[0, 1]$, green arcs map to $[1, \infty]$, and orange arcs to $[-\infty, 0]$. By drawing loops on such graphs that correspond to the generators of the relevant fundamental group, it is possible to determine the images under the push-forward. For this family of covers, we obtain the graph in Figure 3.2.

As long as $a \notin \{0, \pm 1, \infty\}$, the elliptic surface has four singular fibres as shown in Table 3.2. Let us choose $a = -2$ as a base point on $A = \mathbf{P}_a^1 - \{-1, 0, 1, \infty\}$. The corresponding elliptic surface has singular fibres at $t = \{0, 1, 4, \infty\}$ and if we choose a basis of loops $\gamma_1, \dots, \gamma_4$ as indicated above, then \mathcal{E}_{-2} has the following monodromy representation:

$$g_1 = \begin{pmatrix} 1 & 1 \\ 0 & 1 \end{pmatrix}, g_2 = \begin{pmatrix} 1 & 1 \\ -1 & 0 \end{pmatrix}, g_3 = \begin{pmatrix} 0 & -1 \\ 1 & -1 \end{pmatrix}, g_4 = \begin{pmatrix} 1 & 1 \\ 0 & 1 \end{pmatrix}.$$

Next, we must determine the braiding map $\varphi: \pi_1(A, -2) \rightarrow A_3$. Choose standard generators $\sigma_1, \sigma_2, \sigma_3$ for $\pi_1(A, -2)$ around $-1, 0, 1$ respectively, as depicted in Figure 3.3. As a moves around σ_1 , the point a^2 starts at 4 and moves around 1 in a counter clockwise

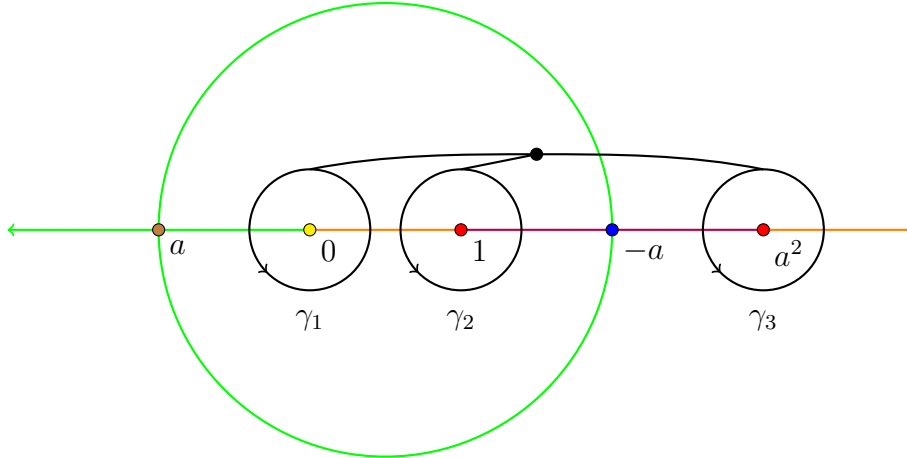


Figure 3.2: Initial configuration for Family 1.

fashion, returning to its starting point; we see that

$$\varphi(\sigma_1) = \beta_2^2.$$

By considering the motions of the poles carefully, which is depicted in Figure 3.3, we find that

$$\varphi(\sigma_2) = \beta_2^{-1} \beta_1^4 \beta_2, \quad \varphi(\sigma_3) = \beta_2^{-1} \beta_1^{-2} \beta_2^2 \beta_1^2 \beta_2.$$

One computes the following:

$$\left(\left(\begin{pmatrix} 1 & 1 \\ 0 & -1 \end{pmatrix}, \begin{pmatrix} 1 & 1 \\ -1 & 0 \end{pmatrix}, \begin{pmatrix} 0 & -1 \\ 1 & -1 \end{pmatrix}, \begin{pmatrix} 1 & 1 \\ 0 & 1 \end{pmatrix} \right)^{\varphi(\sigma_1)} = \left(\begin{pmatrix} 1 & 1 \\ 0 & -1 \end{pmatrix}, \begin{pmatrix} -1 & 3 \\ -1 & 2 \end{pmatrix}, \begin{pmatrix} 2 & -7 \\ 1 & -3 \end{pmatrix}, \begin{pmatrix} 1 & 1 \\ 0 & 1 \end{pmatrix} \right).$$

Next, we check that this is also equal to $\mathbf{g}^{h^{-1}}$, where

$$h = \begin{pmatrix} 1 & 2 \\ 0 & 1 \end{pmatrix}.$$

It follows that $\chi(\sigma_1)$, is determined up to scalars, where $\chi: \pi_1(A, -2) \rightarrow \mathrm{SL}_2(\mathbf{C})$ is the auxiliary monodromy representation as described in the Dettweiler-Wewers algorithm in Chapter 2. Since we are working integral local systems, we have thus determined $\chi(\sigma_1)$ up to multiplication by ± 1 . The braids $\varphi(\sigma_2)$ and $\varphi(\sigma_3)$ act trivially on \mathbf{g} and so $\chi(\sigma_2), \chi(\sigma_3)$ are equal to ± 1 ; $\chi(\sigma_4)$ is determined by the other three since $\sigma_1 \sigma_2 \sigma_3 \sigma_4 = 1$.

We have now determined the braid map and the representation χ . Computing the monodromy representation is now simply a matter of running the algorithm outlined in the previous section. In this example, a convenient computational basis for the parabolic co-

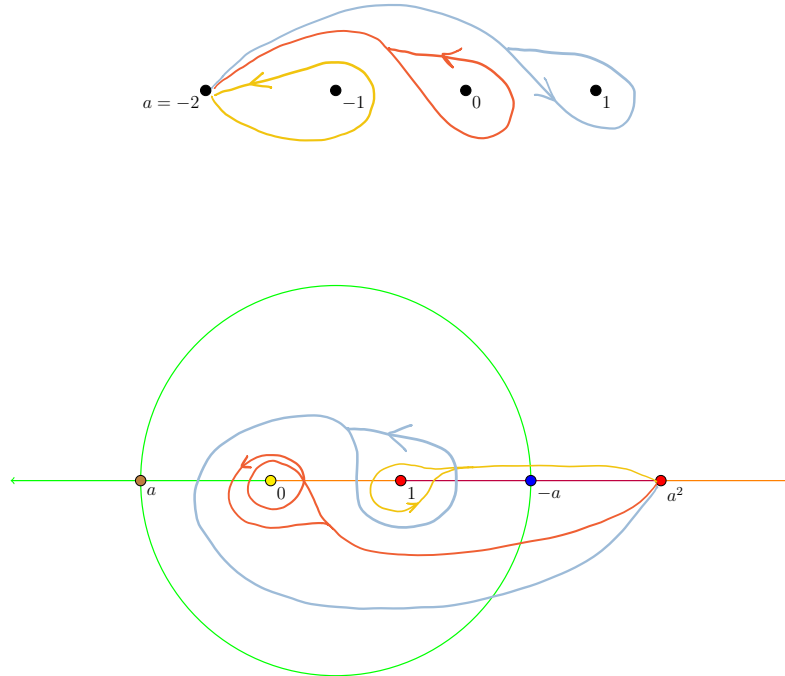


Figure 3.3: The braiding action for Family 1.

homology group is obtained by taking the “characteristic” vectors associated to the two unipotent monodromy transformations g_2 and g_4 ; that is, let v_2 be a basis for $\text{image}(g_2 - 1)$ and similarly, let v_4 be a basis for $\text{image}(g_4 - 1)$. Then let

$$\mathbf{v}_2 = (0, v_2, *, 0), \quad \mathbf{v}_4 = (0, 0, *, v_4),$$

where the third entry is determined by relation (2.3). The results of running the Dettweiler-Wewers algorithm are summarized below.

Proposition 2. *With respect to the basis $\bar{\mathbf{v}}_2, \bar{\mathbf{v}}_4$, the monodromy of the parabolic cohomology local system is given as follows:*

$$\eta(\sigma_1) = \begin{pmatrix} 1 & 0 \\ 0 & 1 \end{pmatrix}, \quad \eta(\sigma_2) = \begin{pmatrix} -1 & 0 \\ 1 & 1 \end{pmatrix}, \quad \eta(\sigma_3) = \begin{pmatrix} 1 & 1 \\ -1 & 0 \end{pmatrix}, \quad \eta(\sigma_4) = \begin{pmatrix} -1 & -1 \\ 0 & 1 \end{pmatrix}.$$

We have the following relations:

$$\eta(\sigma_2)^2 = 1, \quad \eta(\sigma_3)^3 = -1, \quad \eta(\sigma_2)\eta(\sigma_3)\eta(\sigma_2)^{-1} = \eta(\sigma_3)^{-1}.$$

Thus, the projective monodromy group is isomorphic to the dihedral group of order 6.

Since we are working with rational elliptic surfaces, the fact that the parabolic cohomol-

ogy has rank 2 implies that the Mordell-Weil rank is equal to 2. With a little bit of algebraic manipulations, one can find the following infinite order sections on this family of elliptic surfaces:

$$x = C(t - a^2)^2, \quad y = \frac{1}{2\sqrt{A}}(t - a^2)^2(2At + B)$$

where C is root of

$$\delta = 16a(a - 1)C^3 + 9(a - 1)^2C^2 - 6(a - 1)C + 1,$$

$$A = (C - 1)(2C + 1)^2, \quad B = -8a^2C^3 + 3a^2C - a + 3C + 1.$$

Since each elliptic surface in the family has a fibre of type II, there is no torsion in the Mordell-Weil group

citeschuetttEllipticSurfaces2010. A basis for the Mordell-Weil group can be chosen by taking two sections of the above form corresponding to two different choices of roots C of δ . By examining these sections closely, the results of our monodromy computation are not surprising—these sections can be defined over an algebraic extension of the function field of degree 6.

Remark 14. We will be examining many different kinds of covers in this thesis and often represent them by drawing graphs such as the one in Figure 3.2. We will consistently use red dots to denote points above 0, blue dots to denote points above 1, and yellow dots above ∞ (when considered thrice-punctured spheres whose punctures are at $0, p, \infty$ for $p \neq 1$, the fibre over p will also be coloured blue). Similarly, green arcs denote pre-images of the line segment joining the blue and yellow dot, purple arcs join red and blue dots, and orange arcs join red and yellow dots. Black dots will denote base points and another coloured point will denote a point of excess ramification—a ramified point not lying over one of the three punctures.

Families 2-5: For the other families considered in [15], three of the monodromy transformations are unipotent and the remaining transformation has no fixed vectors. It follows that the corresponding parabolic cohomology groups are rank 1 and the associated monodromy representations will correspond to characters $\chi: \pi_1(A) \rightarrow \{\pm 1\}$. Thus, each projective monodromy representation is trivial in this case and applying the Dettweiler-Wewers algorithm in these four cases would be uninteresting. Rather, to close the discussion of these five families for the time being, we compute the Mordell-Weil group for the remaining cases.

Proposition 3. *The Mordell-Weil group for the elliptic surfaces in Families 3,4,5 in Table 3.2 are free of rank 1. The Mordell-Weil group for the surfaces in Family 2 have rank 1 and*

Family	x -coordinate	y -coordinate
2	$t(2 - t)$	$6i\sqrt{a + 1} \cdot t^2$
3	$-t(at + 1)$	$\sqrt{-4a^3 + 12a - 8} \cdot t^3$
4	$-\frac{t^2}{3a}$	$i\frac{3a-2}{3a}\sqrt{\frac{3a+1}{3a}} \cdot t^3$
5	$\frac{4-9a^2}{4} \cdot t^2$	$-\frac{i}{4}t^2(9a(3a^2 - 2)t - 4)$

Table 3.3: Generating sections for Mordell-Weil of Families 2-4.

torsion subgroup isomorphic to $\mathbf{Z}/2\mathbf{Z}$. Moreover, the x -coordinate of each of the sections that generate the free part of the Mordell-Weil group are rational functions of t and a .

Proof. We have already remarked that the Mordell-Weil rank is equal to 1. It therefore remains to find a generating section of the free part and to determine the torsion subgroups.

Generating sections for the free part are tabulated in Table 3.3. We can determine the torsion subgroup with the help of [39] in which the complete structure of the Mordell-Weil group for rational elliptic surfaces is determined.

We find that Family 2 has torsion subgroup isomorphic to $\mathbf{Z}/2\mathbf{Z}$, and the other families have no non-trivial torsion sections. The 2-torsion section on the elliptic surfaces in Family 2 is given by

$$(x, y) = (-t(t + 1), 0).$$

□

We can see by looking at the sections that there is non-trivial monodromy as a varies in A . So, even though the *projective monodromy* representations associated to the parabolic cohomology local systems were trivial, this allows us to see that the “honest” monodromy representation are not.

Despite the fact that the seven families with I_0^* singular fibres were not useful to Doran in [15], they still provide interesting examples of geometric variations of local systems. The seven I_0^* families and their Weierstrass presentations are tabulated in Table 3.4. Note that the functional invariants for each of these families do *not* depend on a , which shows that the projective normal forms of the Picard-Fuchs equations are also independent of a .

We can examine the parabolic cohomology local system attached to these families in a uniform manner. Let $A = \mathbf{P}_a^1 - \{0, 1, \infty\}$, $X = \mathbf{P}_t^1 \times A$, $D = \{(0, a), (1, a), (\infty, a), (a, a) \mid a \in A\}$ and $U = X - D$. Use $a = -1$ as a base point and let $U_{-1} = X_{-1} \cap D = \mathbf{P}^1 - \{-1, 0, 1, \infty\}$. Using similar methods to what we did in the five families calculation, we can easily write down the global monodromy representations for these examples. We do this with respect to

Name	Sing. Fibre Types	Weierstrass Presentation
1	I_4, I_1, I_1, I_0^* $(1, \infty, 0, a)$	$g_2(t, a) = 3(t - a)^2(t^2 + 14t + 1)$ $g_3(t, a) = (t - a)^3(t^3 - 33t^2 - 33t + 1)$
2	I_2, I_2, I_2, I_0^* $(1, \infty, 0, a)$	$g_2(t, a) = 12(t - a)^2(t^2 - t + 1)$ $g_3(t, a) = 4(t - a)^3(2t^3 - 3t^2 - 3t + 2)$
3	I_3, I_1, II, I_0^* $(0, \infty, 1, a)$	$g_2(t, a) = 3(t - a)^2(t - 1)(t - 9)$ $g_3(t, a) = (t - a)^3(t - 1)(t^2 + 18t - 27)$
4	I_2, I_1, III, I_0^* $(0, \infty, 1, a)$	$g_2(t, a) = 3(t - a)^2(t - 1)(t - 4)$ $g_3(t, a) = (t - a)^3(t - 1)^2(t + 8)$
5	I_1, I_1, IV, I_0^* $(0, \infty, 1, a)$	$g_2(t, a) = 3(t - a)^2(t - 1)^2$ $g_3(t, a) = (t - a)^3(t - 1)^2(t + 1)$
6	I_1, II, III, I_0^* $(\infty, 0, 1, a)$	$g_2(t, a) = 3t(t - a)^2(t - 1)$ $g_3(t, a) = t(t - a)^3(t - 1)^2$
7	I_2, II, II, I_0^* $(\infty, 0, 1, a)$	$g_2(t, a) = 12t(t - a)^2(t - 1)$ $g_3(t, a) = 4t(t - a)^3(t - 1)(2t - 1)$

Table 3.4: The seven families with I_0^* fibres.

loops $\gamma_1, \gamma_2, \gamma_3, \gamma_4$ around $-1, 0, 1, \infty$ respectively. The rank of the parabolic cohomology is easily calculated using (2.4).

In order to compute the monodromy representation of the parabolic cohomology local system, we need to determine the braiding map $\varphi: \pi_1(A, -1) \rightarrow A_3$. Let σ_0, σ_1 be loops based at $a = -1$ wrapping once around 0 and 1 respectively in the upper half-plane. Then we have

$$\varphi(\sigma_0) = \beta_1^2, \quad \varphi(\sigma_1) = \beta_1^{-1}\beta_2^2\beta_1.$$

We now apply the Dettweiler-Wewers algorithm to compute the monodromy representations of the parabolic cohomology groups.

Proposition 4. *For each of the seven families in Table 3.4, the parabolic cohomology local system on $\mathbf{P}^1 - \{0, 1, \infty\}$ is irreducible and has finite monodromy group.*

Proof. The monodromy representations are tabulated in Table 3.5. For each representation, we check that the group generated by $\eta(\sigma_0)$ and $\eta(\sigma_1)$ is finite of the indicated order. It is straight forward to check that in each case, the matrices $\eta(\sigma_0)$ and $\eta(\sigma_1)$ do not have a common eigenvector, which establishes irreducibility. \square

Thus, we see that even though these seven families were not interesting from the perspective of [15], we see that there is non-trivial information captured by the corresponding variations of local systems. In these examples, the local system on the base $\mathbf{P}^1 - \{0, 1, \infty\}$ is describing how the narrow Mordell-Weil group varies with the deformation parameter.

Name	$\eta(\sigma_0)$	$\eta(\sigma_1)$	Size
1	-1	-1	2
2	-1	-1	2
3	$\begin{pmatrix} -1 & 3 \\ 0 & 1 \end{pmatrix}$	$\begin{pmatrix} 1 & -3 \\ 1 & -2 \end{pmatrix}$	6
4	$\begin{pmatrix} -1 & 2 \\ 0 & 1 \end{pmatrix}$	$\begin{pmatrix} 1 & -2 \\ 1 & -1 \end{pmatrix}$	8
5	$\begin{pmatrix} -1 & 3 \\ 0 & 1 \end{pmatrix}$	$\begin{pmatrix} 2 & -3 \\ 1 & -1 \end{pmatrix}$	12
6	$\begin{pmatrix} -1 & -1 & 0 \\ -1 & 0 & 1 \\ -4 & -2 & 1 \end{pmatrix}$	$\begin{pmatrix} -2 & -1 & 1 \\ 3 & 2 & -1 \\ -2 & 0 & 1 \end{pmatrix}$	24
7	$\begin{pmatrix} 1 & 1 & 1 \\ -1 & -2 & -1 \\ 2 & 4 & 1 \end{pmatrix}$	$\begin{pmatrix} -2 & -3 & -1 \\ 1 & 1 & 0 \\ 0 & 0 & 1 \end{pmatrix}$	12

Table 3.5: Monodromies for the seven I_0^* families.

3.2.2 Families of K3 Surfaces from Herfurtner's List

In this section we consider some families of K3 surfaces that can be constructed from Herfurtner's list and study their associated variations of homological invariants. Given any of the rational elliptic surfaces on Herfurtner's list, we construct a K3 surface by performing a quadratic twist at the points $t = a_1, t = a_2$, for smooth points a_1, a_2 . This results in a two-parameter family of K3 surfaces with six singular fibres. In particular, we can do this for the thirty-eight isolated cases to produce geometric variations of local systems.

Proposition 5. *Let E be an elliptic surface with four singular fibres, $A = \{(a_1, a_2) \in \mathcal{O}^2 \mid a_1, a_2 \notin \Sigma\}$, and $\mathcal{E} \rightarrow A$ be the family of elliptic K3 surfaces obtained by applying a quadratic twist at the points $t = a_1$ and $t = a_2$. Let $\nu = \nu(E)$ denote the number of I_b -fibres in E with $b > 0$. The rank of the parabolic cohomology local system on A is*

$$r_E = 8 - \nu.$$

As E varies over Herfurtner's list, the rank r_E takes on the values $\{4, 5, 6, 7\}$.

Proof. This follows from the rank formula (2.4). Each K3 surface in the family is an elliptic surface with six singular fibres. The only types of singular fibres that unipotent monodromy are the I_b fibres; every other kind of singular fibre has no fixed-vectors. It follows that

$$r_E = (6 - 2) \cdot 2 - \nu = 8 - \nu.$$

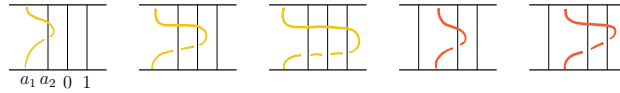


Figure 3.4: The loops $\gamma_1, \dots, \gamma_5$.

By inspection, as E varies in Herfurtner’s list, ν takes on the values $\{1, 2, 3, 4\}$. □

We can use the Dettweiler-Wewers algorithm to compute the monodromy representation of the corresponding two-parameter local system of parabolic cohomology groups. Let us normalize the singular fibres to be located at $t = a_1, a_2, 0, 1, \infty$, so that we can identify the relevant subspace of the configuration space with $A = \{(a_1, a_2) \in \mathbf{C}^2 \mid a_1 \neq a_2, a_i \notin \Sigma\}$, and choose $(a_1, a_2) = (-2, -1)$ as a base point for A . As explained in [12], the fundamental group of A is generated by five elements $\gamma_1, \gamma_2, \gamma_3, \gamma_4, \gamma_5$ as depicted in Figure 3.4. Their images under the braiding map $\varphi: \pi_1(A, (-2, -1)) \rightarrow A_5$ are as follows:

$$\begin{aligned} \varphi(\gamma_1) &= \beta_1^2 \\ \varphi(\gamma_2) &= \beta_1^{-1} \beta_2^2 \beta_1 \\ \varphi(\gamma_3) &= \beta_1^{-1} \beta_2^{-1} \beta_3^2 \\ \varphi(\gamma_4) &= \beta_2^2 \\ \varphi(\gamma_5) &= \beta_2^{-1} \beta_3^2 \beta_2. \end{aligned}$$

Once we determine the initial homological invariant, we can then run the Dettweiler-Wewers algorithm to compute the monodromy representation for the parabolic cohomology groups.

To demonstrate the technique, let us examine the eleven isolated examples on Herfurtner’s list for which there is exactly one additive fibre. These are tabulated in Table 3.6. By examining the functional invariants in each case, we can determine the homological invariant for each of the eleven examples. The homological invariants for the twists are obtained by adding -1 monodromies at $t = a_1, a_2$. Let

$$\frac{d^2 f}{dt^2} + P \frac{df}{dt} + Qf = 0$$

be the Picard-Fuchs equation for one of these elliptic surfaces. The quadratic twist is obtained by setting $\lambda = (t - a_1)(t - a_2)$ and scaling g_2 by λ^2 and g_3 by λ^3 . The a -dependent family

Name	Sing. Fibre Type	Weierstrass Presentation
1	I_1, I_1, I_8, II $(\delta^+, \delta^-, \infty, 0)$	$g_2(t) = 12t(t^3 - 6t^2 + 15t - 12)$ $g_3(t) = 4t(2t^5 - 18t^4 + 72t^3 - 144t^2 + 135t - 27)$
2	I_1, I_2, I_7, II $(\frac{-9}{4}, \frac{-8}{9}, \infty, 0)$	$g_2(t) = 12t(9t^3 + 36t^2 + 42t + 14)$ $g_3(t) = 12t(18t^5 + 108t^4 + 234t^3 + 222t^2 + 87t + 8)$
3	I_1, I_4, I_5, II $(-10, 0, \infty, \frac{1}{8})$	$g_2(t) = 3(8t - 1)(8t^3 + 87t^2 + 96t - 64)$ $g_3(t) = (8t - 1)(64t^5 + 2^4 \cdot 5 \cdot 13t^4 + 5^2 \cdot 157t^3 + 100t^2 + 2^7 \cdot 5^2t - 2^9)$
4	I_2, I_3, I_5, II $(\frac{-5}{9}, 0, \infty, 3)$	$g_2(t) = 3(t - 3)(81t^3 - 9t^2 - 53t - 27)$ $g_3(t) = (t - 3)(3^6t^5 - 3^55t^4 - 23^35^2t^3 - 350t^2 - 3^35^2t - 243)$
5	I_1, I_1, I_7, III $(\omega_1, \omega_2, \infty, 0)$	$g_2(t) = 12t(t^3 + 4t^2 + 10t + 6)$ $g_3(t) = 4t^2(2t^4 + 12t^3 + 42t^2 + 70t + 63)$
6	I_1, I_2, I_6, III $(4, 1, \infty, 0)$	$g_2(t) = 12t(t^3 - 6t^2 + 9t - 3)$ $g_3(t) = 4t^2(2t^4 - 18t^3 + 54t^2 - 63t + 27)$
7	I_1, I_3, I_5, III $(\frac{-25}{3}, 0, \infty, \frac{1}{5})$	$g_2(t) = 75(5t - 1)(5t^3 + 45t^2 + 39t - 25)$ $g_3(t) = 25(5t - 1)^2(25t^4 + 340t^3 + 2 * 3 * 181t^2 + 100t + 5^4)$
8	I_2, I_3, I_4, III $(\frac{-1}{3}, 0, \infty, 1)$	$g_2(t) = 3(t - 1)(16t^3 - 3t - 1)$ $g_3(t) = (t - 1)^2(64t^4 + 32t^3 + 6t^2 + 5t + 1)$
9	I_1, I_1, I_6, IV $(1, -1, \infty, 0)$	$g_2(t) = 3t^2(9t^2 - 8)$ $g_3(t) = s^2(27s^4 - 36s^2 + 8)$
10	I_1, I_2, I_5, IV $(\frac{-27}{4}, \frac{-1}{2}, \infty, 0)$	$g_2(t) = 12t^2(t^2 + 8t + 10)$ $g_3(t) = 4s^2(2t^4 + 24t^3 + 78t^2 + 56t + 27)$
11	I_3, I_3, I_2, IV $(\infty, 0, -1, 1)$	$g_2(t) = 3(t - 1)^2(9t^2 + 14t + 9)$ $g_3(t) = (t - 1)^2(27t^4 + 36t^3 + 2t^2 + 36t + 27)$

Table 3.6: The 11 examples with one additive fibre.

of Picard-Fuchs equations for the twists is therefore

$$\frac{d^2f}{dt^2} + \left(P + \frac{2t - a_1 - a_2}{(t - a_1)(t - a_2)} \right) \frac{df}{dt} + \left(Q + P \cdot \frac{2t - a_1 - a_2}{2(t - a_1)(t - a_2)} - \frac{(a_1 - a_2)^2}{4(t - a_1)^2(t - a_2)^2} \right) f = 0. \quad (3.18)$$

Proposition 6. *Let $\mathcal{E} \rightarrow A$ be the two-parameter family of K3 surfaces obtained by starting with an elliptic surface in Table 3.6 and applying a quadratic twist at $t = a_1, a_2$. Then, the monodromy representation for the parabolic cohomology local system is irreducible. The family $\mathcal{E} \rightarrow A$ is a family of Picard-rank seventeen K3 surfaces.*

Proof. One applies the Dettweiler-Wewers algorithm in each case to compute the monodromy representation for the parabolic cohomology local system. Since each of these families originates from a rigid elliptic surface with one additive fibre, the rank of parabolic cohomology is equal to five. These monodromy representations are tabulated in Table B.1, located in

the appendix.

Irreducibility is argued as follows. For each of the eleven monodromy representations, at least one the transformations is diagonalizable; call this transformation T . It follows that any subspace that is left invariant by all monodromy transformations is a direct sum of the eigenspaces T . One then checks by brute force that for each subspace W constructed as the direct sum of eigenspaces of T that some other monodromy transformation does not leave W invariant. Thus, the monodromy representation is irreducible.

On the other hand, the parabolic cohomology local system always contains the transcendental lattice local system and so these two are equal by irreducibility. It follows that the Mordell-Weil rank is equal to zero for these surfaces and, therefore, the Picard-rank is equal to seventeen. \square

Rather than consider the most general kind of quadratic twist, we can instead consider quadratic twists in which we twist one mobile smooth fibre $t = a$ and one of the fixed singular fibres $t = s$ for some $s \in \Sigma$. This produces a one-parameter family of elliptic K3 surfaces with five singular fibres, and we can compute the ranks of the parabolic cohomology group in the same manner as earlier, taking into account a “correction” factor depending on whether we twist at an additive or multiplicative fibre.

Proposition 7. *Let E be an elliptic surface with four singular fibres, one of which is at ∞ , $A = \mathbf{P}^1 - \Sigma$, and $\mathcal{E} \rightarrow A$ be the family of elliptic K3 surfaces obtained by performing a quadratic twist at a and the singular fibre $t = s$. Let ν denote the number of I_b -fibres in E with $b > 0$. Let $\delta_s = 0$ if s is an additive fibre, and let $\delta_s = 1$ if s is an I_b fibre. Then, the rank of the parabolic cohomology local system on A is*

$$r_E = 6 - \nu + \delta_s.$$

The a -dependent family of Picard-Fuchs equations are obtained from (3.18) by setting $a_1 = s, a_2 = a$ where $s \in \Sigma$ is the fixed singular fibre we are twisting. By choosing $a = -1$ as a base point, the braiding map used in the Dettweiler-Wewers algorithm is determined by

$$\varphi(\sigma_1) = \beta_1^2, \quad \varphi(\sigma_2) = \beta_1^{-1}\beta_2^2\beta_1, \quad \varphi(\sigma_3) = \beta_1^{-1}\beta_2^{-1}\beta_3^2\beta_2^{-1}\beta_1^{-1}.$$

Applying the algorithm to the eleven examples in Table 3.6 where the unique additive fibre is twisted, we obtain the following results:

Proposition 8. *Let $\mathcal{E} \rightarrow A$ be the one-parameter family of K3 surfaces obtained by starting with an elliptic surface in Table 3.6 and applying a quadratic twist at the unique additive fibre*

and at $t = a$ for $a \notin \Sigma$. Then, the monodromy representation for the parabolic cohomology local system is irreducible. The family $\mathcal{E} \rightarrow A$ is a family of Picard-rank nineteen K3 surfaces.

Proof. By our rank formula, we know parabolic cohomology will be rank three. The monodromy representations are tabulated in Table 3.7. Since we have a *family* of K3 surfaces, we know that the smallest the rank of the transcendental lattice can be is three, and so we are guaranteed the fact that the parabolic cohomology local system and transcendental lattice local system agree. Irreducibility follows, as does the fact that these K3 surfaces have Picard-rank nineteen. \square

Remark 15. These eleven one-parameter family of K3 surfaces were considered by Besser-Livné in [1] in which they show that these families are closely related to certain Shimura curves. In their work, they compute the Picard-Fuchs equations for these eleven families. Therefore, the monodromy representations in Table 3.7 are the monodromy representations for the eleven Picard-Fuchs equations computed in [1]. The connection to the kinds of Shimura curves considered in [1] explains the orders of the monodromy transformations computed above.

Note that we may of course apply this quadratic twist construction to the families of solutions on Herfurtner's list as well. If we start with the seven I_0^* families in Table 3.4, and apply the general quadratic twist at $t = a_1, a_2$ for $a_i \notin \{0, 1, a, \infty\}$, then we obtain a three-parameter family of K3 surfaces with six singular fibres. Here, we have a three-parameter variation of local systems with deformation space equal to

$$A = \{(a_1, a_2, a_3) \in \mathbf{C}^3 \mid a_i \neq a_j, a_i \notin \{0, 1, \infty\}\}.$$

As earlier, the fundamental group is generated by nine elements γ_i and the braiding map is

Name	$\eta(\sigma_1)$	$\eta(\sigma_2)$	$\eta(\sigma_3)$	Orders
1	$\begin{pmatrix} 1 & 3 & -2 \\ -3 & -8 & 5 \\ -8 & -16 & 9 \end{pmatrix}$	$\begin{pmatrix} -1 & -3 & 2 \\ 0 & 1 & 0 \\ 0 & 0 & 1 \end{pmatrix}$	$\begin{pmatrix} 1 & 0 & 0 \\ -3 & -1 & 1 \\ 0 & 0 & 1 \end{pmatrix}$	(6, 2, 2, 2)
2	$\begin{pmatrix} -1 & -2 & 1 \\ 0 & 1 & 0 \\ 0 & 0 & 1 \end{pmatrix}$	$\begin{pmatrix} 1 & 0 & 0 \\ -4 & -1 & 2 \\ 0 & 0 & 1 \end{pmatrix}$	$\begin{pmatrix} -6 & -5 & 1 \\ 10 & 7 & -2 \\ -7 & -7 & 1 \end{pmatrix}$	(2, 2, 6, 2)
3	$\begin{pmatrix} -1 & -2 & 1 \\ 0 & 1 & 0 \\ 0 & 0 & 1 \end{pmatrix}$	$\begin{pmatrix} 1 & 0 & 0 \\ -8 & -1 & 4 \\ 0 & 0 & 1 \end{pmatrix}$	$\begin{pmatrix} -4 & -3 & 1 \\ 12 & 5 & -4 \\ -5 & -5 & 1 \end{pmatrix}$	(2, 2, 6, 2)
4	$\begin{pmatrix} 1 & 3 & -3 \\ -2 & -5 & 4 \\ -5 & -10 & 6 \end{pmatrix}$	$\begin{pmatrix} -1 & -3 & 3 \\ 0 & 1 & 0 \\ 0 & 0 & 1 \end{pmatrix}$	$\begin{pmatrix} 1 & 0 & 0 \\ -2 & -1 & 2 \\ 0 & 0 & 1 \end{pmatrix}$	(6, 2, 2, 2)
5	$\begin{pmatrix} -1 & -3 & 1 \\ 0 & 1 & 0 \\ 0 & 0 & 1 \end{pmatrix}$	$\begin{pmatrix} 1 & 0 & 0 \\ -3 & -1 & 2 \\ 0 & 0 & 1 \end{pmatrix}$	$\begin{pmatrix} -6 & -11 & 1 \\ 4 & 6 & -1 \\ -7 & -14 & 1 \end{pmatrix}$	(2, 2, 4, 2)
6	$\begin{pmatrix} -1 & -2 & 1 \\ 0 & 1 & 0 \\ 0 & 0 & 1 \end{pmatrix}$	$\begin{pmatrix} 1 & 0 & 0 \\ -4 & -1 & 2 \\ 0 & 0 & 1 \end{pmatrix}$	$\begin{pmatrix} -5 & -4 & 1 \\ 8 & 5 & -2 \\ -6 & -6 & 1 \end{pmatrix}$	(2, 2, 4, 2)
7	$\begin{pmatrix} -1 & -2 & 1 \\ 0 & 1 & 0 \\ 0 & 0 & 1 \end{pmatrix}$	$\begin{pmatrix} 1 & 0 & 0 \\ -6 & -1 & 3 \\ 0 & 0 & 1 \end{pmatrix}$	$\begin{pmatrix} -4 & -3 & 1 \\ 9 & 4 & -3 \\ -5 & -5 & 1 \end{pmatrix}$	(2, 2, 4, 2)
8	$\begin{pmatrix} -1 & -2 & 2 \\ 0 & 1 & 0 \\ 0 & 0 & 1 \end{pmatrix}$	$\begin{pmatrix} 1 & 0 & 0 \\ -3 & -1 & 3 \\ 0 & 0 & 1 \end{pmatrix}$	$\begin{pmatrix} -7 & -6 & 2 \\ 9 & 7 & -3 \\ -4 & -4 & 1 \end{pmatrix}$	(2, 2, 4, 2)
9	$\begin{pmatrix} -1 & -3 & 1 \\ 0 & 1 & 0 \\ 0 & 0 & 1 \end{pmatrix}$	$\begin{pmatrix} 4 & 3 & -2 \\ 3 & 1 & -1 \\ 12 & 6 & -5 \end{pmatrix}$	$\begin{pmatrix} 1 & 0 & 0 \\ -3 & -1 & 1 \\ 0 & 0 & 1 \end{pmatrix}$	(2, 3, 2, 2)
10	$\begin{pmatrix} 1 & 4 & -2 \\ -2 & -7 & 3 \\ -5 & -15 & 6 \end{pmatrix}$	$\begin{pmatrix} -1 & -4 & 2 \\ 0 & 1 & 0 \\ 0 & 0 & 1 \end{pmatrix}$	$\begin{pmatrix} 1 & 0 & 0 \\ -2 & -1 & 1 \\ 0 & 0 & 1 \end{pmatrix}$	(3, 2, 2, 2)
11	$\begin{pmatrix} 1 & 3 & -3 \\ -2 & -5 & 4 \\ -3 & -6 & 4 \end{pmatrix}$	$\begin{pmatrix} -1 & -3 & 3 \\ 0 & 1 & 0 \\ 0 & 0 & 1 \end{pmatrix}$	$\begin{pmatrix} 1 & 0 & 0 \\ -2 & -1 & 2 \\ 0 & 0 & 1 \end{pmatrix}$	(3, 2, 2, 2)

Table 3.7: Monodromy representations associated to examples in Table 3.6

determined by

$$\begin{aligned}
\varphi(\gamma_1) &= \beta_1^2 \\
\varphi(\gamma_2) &= \beta_1^{-1}\beta_2^2\beta_1 \\
\varphi(\gamma_3) &= \beta_1^{-1}\beta_2^{-1}\beta_3^2\beta_2\beta_1 \\
\varphi(\gamma_4) &= \beta_1^{-1}\beta_2^{-1}\beta_3^{-1}\beta_4^2\beta_3\beta_2\beta_1 \\
\varphi(\gamma_5) &= \beta_2^2 \\
\varphi(\gamma_6) &= \beta_2^{-1}\beta_3^2\beta_2 \\
\varphi(\gamma_7) &= \beta_2^{-1}\beta_3^{-1}\beta_4^2\beta_3\beta_2 \\
\varphi(\gamma_8) &= \beta_3^2 \\
\varphi(\gamma_9) &= \beta_3^{-1}\beta_4^2\beta_3,
\end{aligned}$$

and we can then apply the Dettweiler-Wewers algorithm to compute the monodromy representations for the parabolic cohomology groups.

Proposition 9. *Let $\mathcal{E} \rightarrow A$ be a three-parameter family of K3 surfaces with six singular fibres obtained by starting with an elliptic surface E in Table 3.4 and applying a quadratic twist at $t = a_2, a_3 \notin \{0, 1, a_1, \infty\}$. Then, the monodromy representation for the parabolic cohomology local system is irreducible. The family $\mathcal{E} \rightarrow A$ is a family of Picard-rank $22 - r_E$ K3 surfaces where r_E is computed as in Proposition 5.*

Proof. This is argued similarly to the previous propositions. We apply the Dettweiler-Wewers algorithm to compute the monodromy representations. These are tabulated in Table B.3 in the appendix. For each representation, at least one of the monodromy transformations is diagonalizable and a case-by-case analysis tells us that each monodromy representation is irreducible. \square

For the twelve families of surfaces in Hefurtner's classification, we can also produce one-parameter families of K3 surfaces by taking quadratic twists at two of the singular fibres not of type I_0^* . We summarize the results of these computations below, starting with the five families studied by Doran.

Proposition 10. *Let E_1 be the first elliptic surface in Table 3.2. A K3 surface is produced by quadratic twisting two singular fibres if and only if we twist both the I_1 fibres or twist one I_1 fibre and the type II fibre. In the first case, the corresponding one-parameter family of K3 surfaces has Picard rank eighteen; in the second case, the corresponding one-parameter family of K3 surfaces has Picard rank nineteen.*

If E is any other elliptic surface in Table 3.2, then a K3 surface is produced by quadratic twisting two singular fibres if and only if we do not twist the unique additive fibre. The resulting family of K3 surfaces has Picard rank nineteen.

Proof. Whether or not we obtain we obtain K3 surfaces is determined by the euler characteristics of the singular fibres, as described in [37]. A case-by-case analysis shows us that the only possibilities are as stated above.

If we take E_1 and twist at the two I_1 fibres, then the rank of the parabolic cohomology local system is equal to four. Applying the Dettweiler-Wewers algorithm to compute the monodromy representation of the parabolic cohomology, we see that it is irreducible, which shows that the K3 surfaces has Picard-rank eighteen. In all other cases, parabolic cohomology is of rank three, and so irreducibility and the statement about the Picard follows from the fact that the K3 surfaces are not rigid.

$$\begin{aligned} \gamma_1 &\mapsto \begin{pmatrix} 1 & 2 & 0 & 0 \\ 0 & 1 & 0 & 0 \\ 0 & 2 & 1 & 0 \\ -2 & -3 & 0 & 1 \end{pmatrix} & \gamma_2 &\mapsto \begin{pmatrix} -9 & -10 & 1 & 4 \\ 4 & 3 & -1 & -2 \\ -8 & -4 & 3 & 4 \\ -8 & -14 & -1 & 3 \end{pmatrix} \\ \gamma_3 &\mapsto \begin{pmatrix} 3 & 9 & 4 & 0 \\ -4 & -5 & -1 & 2 \\ 10 & 9 & 0 & -6 \\ -4 & 6 & 6 & 5 \end{pmatrix} & \gamma_4 &\mapsto \begin{pmatrix} 3 & 2 & 0 & -2 \\ -2 & 0 & 1 & 2 \\ 2 & -1 & -2 & -2 \\ 2 & 3 & 1 & -1 \end{pmatrix} \end{aligned} \tag{3.19}$$

□

Next, we summarize the results for the seven I_0^* families.

Proposition 11. *For each family of elliptic surface in Table 3.4, quadratic twisting any two singular fibres not of type I_0^* produce a one-parameter family of K3 surfaces whose transcendental lattices have rank equal to three or four depending on the number of surviving multiplicative fibres.*

Proof. One applies the Dettweiler-Wewers algorithm to compute the monodromy representations. The only thing left to check is that the cases for which parabolic cohomology has rank four have irreducible representations and this is checked the same way as before. The monodromy representation are located in Table B.4 in the appendix. □

Remark 16. Completely mapping out the families of K3 surfaces that can be constructed from Herfurtner’s list constitutes work in progress. The above illustrates both the method and some interesting phenomena.

Remark 17. In general, it is not an easy problem to determine the Picard-rank of a K3 surface, or, equivalently, the Mordell-Weil rank. Stiller was able to find an interesting series of examples in which he could compute these ranks by taking advantage of automorphisms of fibration [43] and their induced action on the parabolic cohomology groups. However, these kinds of useful automorphisms rarely occur in families and would not help us here.

In contrast, our ability to use the Dettweiler-Wewers algorithm to compute the monodromy representation of parabolic cohomology allows us to make statements about the Picard-rank of K3 surfaces moving in families by analyzing the representations.

Remark 18. Note that the number of parameters for these families of K3 surfaces does not always agree with the dimension of the corresponding moduli space as lattice-polarized K3 surfaces. For example, if we twist the two I_1 -fibres in the first family considered by Doran, we obtain a one-parameter family of rank eighteen K3 surfaces, from which it follows that the corresponding period map is not surjective. One may therefore reasonably ask: are we getting *interesting* sub-loci when this happens. This is analogous to the situation of M -polarized K3 surfaces, whose moduli space is two-dimensional, but possesses a one-dimensional sub-locus (the $\sigma = 1$ locus that we will discuss in detail shortly) on which the Picard-rank of each K3 surfaces cannot jump to twenty. Investigating the special properties of the families that we are obtaining in this, such as the Picard-rank jumping, is another direction of future research.

Chapter 4

K3 Surface Fibrations

In this section, we study some interesting geometric variations of local systems coming from families of K3 surfaces—that is, we are moving up a dimension. We begin by studying a certain family of K3 surfaces for which the Néron-Severi group is isomorphic to the rank eighteen lattice $H \oplus E_8 \oplus E_8$. The moduli space of M -polarized K3 surfaces \mathcal{M}_M was described in [8]. It is a two-dimensional variety for which the generic K3 surface admits exactly two elliptic fibration structures. We show that each of these fibration structures leads to a geometric variation of local systems parameterized by \mathcal{M}_M whose parabolic cohomology is the rank four transcendental lattice local system on \mathcal{M}_M . By restricting to a particularly interesting one-dimensional sub-loci, the so-called $\sigma = 1$ locus, we are able to apply the Dettweiler-Wewers algorithm to compute the corresponding monodromy representation. That is, we compute the monodromy representation for the Picard-Fuchs differential equation describing the periods of the K3 surfaces in this locus, and we are able to do this for each of the two fibration structures.

In [9], the “fourteenth case” of integral variations of Hodge structures of weight three underlying the thrice-punctured sphere, classified in [20], was constructed by considering a particular one-parameter family of Calabi-Yau threefolds admitting an M -polarization. We show that this local system is realized as the parabolic cohomology associated to the geometric variation of local systems induced by the M -polarized K3 surface fibration. This is done by explicitly writing out the variation of local systems and applying the Dettweiler-Wewers algorithm.

We then discuss M_n -polarized K3 surfaces and threefolds admitting fibrations by such surfaces. It is observed that the Picard-Fuchs equations that govern M_n -polarized K3 surfaces share much of the same structure as Stiller’s K -equations, which describe the kinds of differential equations that occur as Picard-Fuchs equations for elliptic surfaces.

Finally, we consider two examples of interesting geometric variations of local systems

that arise naturally from M_n -polarized K3 surfaces. One example is the Dwork-pencil of mirror hypersurfaces. Starting with the family of mirror cubic elliptic curves, we construct a geometric of variation of local systems whose parabolic cohomology corresponds to the variation of Hodge structure on the mirror quartic family of K3 surfaces. In turn, we construct a geometric variation of local systems whose parabolic cohomology corresponds to the variation of Hodge structure on the quintic mirror family of Calabi-Yau threefolds. We also discuss an interesting example found in [38] that showcases some of the subtleties of the subject.

4.1 The 14th Case VHS of Doran-Morgan

4.1.1 M -polarized K3-surfaces

In this section, we review the necessary details of the theory of M -polarized K3-surfaces, where M denotes the rank-eighteen even lattice

$$M = H \oplus E_8 \oplus E_8,$$

with H being the standard rank-two hyperbolic lattice and E_8 is the unique even, negative-definite, unimodular lattice of rank of eight. More generally, we start by considering L -polarized K3 surfaces where L is an even lattice of signature $(1, r)$, $r \geq 0$. We follow the treatment found in [16].

Consider a family of K3 surfaces, which we will take to mean a variety \mathcal{X} together with a flat and surjective morphism $\pi: \mathcal{X} \rightarrow U$ onto a smooth, irreducible, quasiprojective variety U for which each fibre X_p is a smooth K3 surface. It is also assumed that there is a line bundle \mathcal{L} for which the restriction to each fibre is ample and primitive in $\text{Pic}(X_p)$ for each $p \in U$. We consider the integral local system $R^2\pi_*\mathbf{Z}$, whose fibres above p are isomorphic to the second cohomology group $H^2(X_p, \mathbf{Z})$, together with the Gauss-Manin connection ∇ . The cup-product pairing on the stalks extend to produce a bilinear pairing of sheaves

$$R^2\pi_*\mathbf{Z} \times R^2\pi_*\mathbf{Z} \rightarrow R^4\pi_*\mathbf{Z} \cong \mathbf{Z}. \quad (4.1)$$

Now consider the Hodge filtration on $R^2\pi_*\mathbf{Z} \otimes \mathcal{O}_U$. Since each fibre is a K3-surface, the filtrant $\mathcal{F}^2 = F^2(R^2\pi_*\mathbf{Z} \otimes \mathcal{O}_U)$ is given by a rank one local subsystem of $R^2\pi_*\mathbf{C}$. Let $\omega_{\mathcal{X}}$ be a flat local section of \mathcal{F}^2 . Since the pairing is \mathbf{Z} -linear and $\omega_{\mathcal{X}}$ is flat, the orthogonal compliment $\omega_{\mathcal{X}}^{\perp}$ is well-defined on U ; we call this local system $\mathcal{NS}(\mathcal{X})$. Note that $\mathcal{NS}(\mathcal{X})_p \cong \text{NS}(X_p)$ for each fibre. Let $\mathcal{T}(X)$ be the integral orthogonal compliment of $\mathcal{NS}(X)$. Then, we have an

orthogonal decomposition of the \mathbf{Q} -local system:

$$R^2\pi_*\mathbf{Q} = (\mathcal{T}(\mathcal{X}) \oplus \mathcal{NS}(\mathcal{X})) \otimes_{\mathbf{Z}} \mathbf{Q}.$$

Let \mathcal{N} be a local subsystem of $\mathcal{NS}(\mathcal{X})$ for which the restriction of the bilinear form to the fibre \mathcal{N}_p gives \mathcal{N}_p the structure of a non-degenerate integral lattice of signature $(1, n-1)$, which is isomorphic to a lattice N , embedded in $H^2(X_p, \mathbf{Z})$.

Definition 19. The family \mathcal{X} is N -polarized if the local system \mathcal{N} is a trivial local system.

Now suppose $\mathcal{X} \rightarrow U$ is an M -polarized family of K3 surfaces in this sense. The corresponding transcendental lattice is isomorphic to the rank-four lattice $H \oplus H$. Let $\{x_1, x_2, y_1, y_2\}$ be a basis of the local system $\mathcal{T}(\mathcal{X})$ for which the intersection matrix is

$$\begin{pmatrix} 0 & 0 & 1 & 0 \\ 0 & 0 & 0 & 1 \\ 1 & 0 & 0 & 0 \\ 0 & 1 & 0 & 0 \end{pmatrix}.$$

Then, the section $\omega_{\mathcal{X}}$ can be expressed as

$$\omega_{\mathcal{X}} = f_1(p)x_1 + f_2(p)x_2 + g_1(p)y_1 + g_2(p)y_2,$$

where the f_i , and g_i are the periods of ω , the integrals being defined on the 2-cycles dual to the x_i and y_i via Poincaré duality. The filtrant \mathcal{F}^2 is determined by ω up to non-zero scaling, and we see that the corresponding period map can be realized as the map

$$\begin{aligned} U &\rightarrow \mathbf{P}(H \oplus H) \\ p &\mapsto f_1(p)x_1 + f_2(p)x_2 + g_1(p)y_1 + g_2(p)y_2 \end{aligned} \quad (4.2)$$

Remark 19. Similar to elliptic surfaces, we see that the period map can be concretely realized, after fixing the basis $\{x_1, x_2, y_1, y_2\}$, in terms of the *dual* local system $(R^2\pi_*\mathbf{C})^\vee$. This local system is identified with the solution sheaf of rank four differential operator on U known as the Picard-Fuchs operator. The monodromy of $(R^2\pi_*\mathbf{Z})^\vee$ is identified with the monodromy of the associated Picard-Fuchs equation, and we often work with this local system, rather than $R^2\pi_*\mathbf{Z}$. This will be the case for the examples considered in this thesis.

The Hodge-Riemann relations imply that we may normalize the image of the period map as follows:

$$\tau x_1 + x_2 + uy_1 + (-\tau u)y_2,$$

where τ, u are uniquely defined elements of \mathfrak{h} (that depend on the basis we started with)[8].

Definition 20. The *modular invariants* of the M -polarized K3 surface X are

$$\begin{aligned}\sigma &= J(\tau) + J(u) \\ \pi &= J(\tau) \cdot J(u),\end{aligned}$$

where J is the classical modular function.

It follows that the classifying space of these Hodge structures can be identified with

$$\mathcal{H}_1 = G \backslash \mathfrak{h} \times \mathfrak{h},$$

where

$$G = (\mathrm{PSL}_2(\mathbf{Z}) \times \mathrm{PSL}_2(\mathbf{Z})) \rtimes \mathbf{Z}/2\mathbf{Z}.$$

Here, $\mathrm{PSL}_2(\mathbf{Z})$ acts on each factor of \mathfrak{h} in the standard way, while the $\mathbf{Z}/2\mathbf{Z}$ factor exchanges the two copies; the invariants σ, π are natural coordinates on the space \mathcal{H}_1 . The space \mathcal{H}_1 also classifies Hodge structures corresponding to products of elliptic curves. A precise relationship between M -polarized K3 surfaces and products elliptic curves by way of a canonical *Shioda-Inose* structure is described further in [8].

A complete classification of M -polarized K3 surfaces was presented by Clingher-Doran in [8]. We summarize some of the important features.

Proposition. *Let X be an M -polarized K3 surface. Then, there is a triple $(a, b, d) \in \mathbf{C}^3$ with $d \neq 0$ such that X is isomorphic to the minimal resolution of the quartic surface:*

$$Q_{a,b,d} : y^2zw - 4x^3z + 3axzw^2 + bw^3 - \frac{1}{2}(dz^2w^2 + w^4) = 0. \quad (4.3)$$

Two quartics Q_{a_1,b_1,d_1} and Q_{a_2,b_2,d_2} correspond to isomorphic M -polarized K3 surfaces if and only if

$$(a_2, b_2, d_2) = (\lambda^2 a_1, \lambda^3 b_1, \lambda^6 d_1),$$

for some $\lambda \in \mathbf{C}^\times$.

A coarse moduli space for M -polarized K3 surfaces is thus given by an open sub-variety of weighted projective space:

$$\mathcal{M}_M = \{[a : b : d] \in \mathbf{WP}(2, 3, 6) \mid d \neq 0\},$$

and the following invariants are known as the *fundamental \mathcal{W} -invariants*:

$$\mathcal{W}_1 = \frac{a^3}{d}, \quad \mathcal{W}_2 = \frac{b^2}{d}.$$

The inverse of the period map $\text{per}^{-1}: \mathcal{H}_1 \rightarrow \mathcal{M}_M$ is given by

$$\text{per}^{-1} = \left[\pi^{\frac{1}{3}}, (\pi - \sigma + 1)^{\frac{1}{2}}, 1 \right];$$

that is, we have

$$\mathcal{W}_1 = \pi, \quad \mathcal{W}_2 = \pi - \sigma + 1.$$

Let $\mathcal{X} \rightarrow \mathcal{M}_M$ denote the M -polarized family of K3 surfaces described above. As described earlier, the rank four local system $\mathcal{T}(\mathcal{X})$ is determined by the Picard-Fuchs differential system on the space \mathcal{M}_M . By applying the Griffiths-Dwork algorithm to the family of quartic surfaces (4.3), the associated Picard-Fuchs system was computed in [7]. In the affine chart corresponding to $a = 1$, the result is the following rank-four differential system in b, d :

$$\begin{aligned} \frac{\partial^2 f}{\partial b^2} - 4 \left(d \frac{\partial^2 f}{\partial d^2} + \frac{\partial f}{\partial d} \right) &= 0 \\ (b^2 + d - 1) \frac{\partial^2 f}{\partial b^2} + 2b \frac{\partial f}{\partial b} + 4bd \frac{\partial^2 f}{\partial b d} + 2d \frac{\partial f}{\partial d} + \frac{5}{36} f &= 0. \end{aligned} \tag{4.4}$$

The local system $\mathcal{T}(\mathcal{X})$ arises as the parabolic cohomology local system associated to elliptic fibrations in two different ways. Generically, an M -polarized K3 surface admits exactly two elliptic fibrations [8]. As $[a : b : d] \in \mathcal{M}_M$ varies we obtain a variation of local systems parameterized by a Zariski-open subset of \mathcal{M}_M , namely, the variation of homological invariants of the elliptic fibrations. By our consideration in section Chapter 2, the local system of parabolic cohomology groups will be contained in the local system $R^2\pi_*\mathbf{Z}$ and carries a weight two integral Hodge structure that agrees with the one inherited by the embedding in $R^2\pi_*\mathbf{Z}$. Moreover, \mathcal{V} will necessarily contain the local system $\mathcal{T}(\mathcal{X})$ by Proposition 1.

Let us make this explicit for each of the two fibration structures. First consider the so-called standard fibration on an M -polarized K3 surface X , given by the vanishing of

$$Q_{a,b,d} = y^2zw - 4x^3z + 3axzw^2 + b zw^3 - \frac{1}{2}(dz^2w^2 + w^4).$$

This is obtained by noting that for each fixed w , the resulting curve is an elliptic curve. Since we have typically been using t to denote the fibration parameter on an elliptic surface, we will rename variables $t = w$. Scaling variables via $(x, y) \mapsto (tx, ty)$, and considering the

affine piece $z = 1$, we obtain the model

$$\tilde{Q}_{a,b,d} = y^2 - 4x^3 + 3ax + b - \frac{1}{2t}(d + t^2).$$

This is a Weierstrass equation of the sort we are used to, but it is not minimal at $t = \infty$; we scale $(x, y) \mapsto (t^{-2}x, t^{-3}y)$ to produce the following minimal model:

$$Q_{a,b,d}^{\text{standard}} = y^2 - 4x^3 + 3at^4x - \frac{1}{2}t^5(t^2 - 2bt + d). \quad (4.5)$$

The standard fibration on the M -polarized K3 surface is then described by the following Weierstrass presentation:

$$g_2(t; a, b, d) = 3aw^4, \quad g_3(t; a, b, d) = -\frac{1}{2}t^5(t^2 - 2bt + d).$$

The discriminant is

$$\Delta(t; a, b, d) = -\frac{27}{4} \cdot t^{10} \cdot (t^4 - 4bt^3 + (-4a^3 + 4b^2 + 2d)t^2 - 4bdt + d^2).$$

From this, we see that there are singular fibres of type II^* at $t = 0, \infty$ and four I_1 fibres located at the four roots of the quartic polynomial appearing in the discriminant. The discriminant of this quartic is

$$\delta = 2^{12}a^6d^2 \cdot (a^6 - 2a^3b^2 + b^4 - 2a^3d - 2b^2d + d^2). \quad (4.6)$$

The functional invariant is

$$\mathcal{J} = -4a^3 \frac{t^2}{t^4 - 4bt^3 + (-4a^3 + 4b^2 + 2d)t^2 - 4bdt + d^2}.$$

We see that \mathcal{J} is a degree-four cover of the projective line. The fibre over 0 is $t = 0, \infty$, which corresponds to the two II^* -fibres; the fibre over ∞ consists of the four I_1 -fibres; the fibre over 1 consists of the two roots of $t^2 - 2bt + d$, each ramified to order two. From the Weierstrass presentation above, we can compute the internal Picard-Fuchs equation for the elliptic fibrations; we compute the following expressions for $[a : b : d]$ -dependant family of Picard-Fuchs equations:

$$\frac{d^2 f}{dt^2} + P_{\text{standard}} \frac{df}{dt} + Q_{\text{standard}} f = 0, \quad (4.7)$$

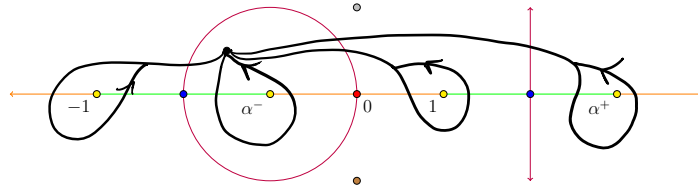


Figure 4.1: The standard fibration when $[a : b : d] = [1 : 1 : -1]$.

where

$$\begin{aligned} P_{\text{standard}} &= 2 \frac{2t^6 - 6bt^5 + (-4a^3 + 4b^2 - d)t^4 + 8bdt^3 + (8a^3d - 8b^2d - 4d^2)t^2 + 6bd^2t - d^3}{t(t^2 - d)(t^4 - 4bt^3 + (-4a^3 + 4b^2 + 2d)t^2 - 4bdt + d^2)} \\ Q_{\text{standard}} &= \frac{77t^6 - 144bt^5 - 159dt^4 + 576bdt^3 + (288a^3d - 288b^2d - 201d^2)t^2 + 144bd^2t - 5d^3}{36t^2(t^2 - d)(t^4 - 4bt^3 + (-4a^3 + 4b^2 + 2d)t^2 - 4bdt + d^2)} \end{aligned} \quad (4.8)$$

Note that the singular points $t^2 = d$ are apparent singularities of this family of Picard-Fuchs equations and do not correspond to singular fibres, but rather points at which the functional invariant \mathcal{J} is ramified over points other than $\{0, 1, \infty\}$.

We now choose $[a : b : d] = [1 : 1 : -1]$ as a base point and determine the homological invariant of the corresponding local system. The functional invariant simplifies to

$$\mathcal{J} = -4 \frac{t^2}{(t^2 - 1)(t^2 - 4t - 1)},$$

and the I_1 -fibres are located at $t = -1, 1$ and $t = 2 \pm \sqrt{5}$. The Picard-Fuchs equation for this fibration is

$$\begin{aligned} \frac{d^2 f}{dt^2} + \frac{4t^6 - 12t^5 + 2t^4 - 16t^3 - 8t^2 + 12t + 2}{t(t^2 - 1)(t^2 + 1)(t^2 - 4t - 1)} \frac{df}{dt} + \\ \frac{77t^6 - 144t^5 + 159t^4 - 576t^3 - 201t^2 + 144t + 5}{36t^2(t^2 - 1)(t^2 + 1)(t^2 - 4t - 1)} f = 0 \end{aligned} \quad (4.9)$$

Note that the singularities of the Picard-Fuchs equation above at $t = \pm i$ are the apparent singularities. We draw the graph on \mathbf{P}^1 that represents this cover and use it to help write down the functional invariant; see Figure 4.1.

We label the points

$$(t_1, t_2, t_3, t_4, t_5, t_6) = (-1, \alpha^-, 0, 1, \alpha^+, \infty),$$

and choose loops $\gamma_1, \dots, \gamma_6$ as indicated. The resulting monodromy representation is

$$\begin{aligned} M_1 &= \begin{pmatrix} 1 & 0 \\ -1 & 1 \end{pmatrix} & M_2 &= \begin{pmatrix} 1 & 1 \\ 0 & 1 \end{pmatrix} & M_3 &= \begin{pmatrix} 0 & -1 \\ 1 & 1 \end{pmatrix} \\ M_4 &= \begin{pmatrix} 1 & 0 \\ -1 & 1 \end{pmatrix} & M_5 &= \begin{pmatrix} 1 & 1 \\ 0 & 1 \end{pmatrix} & M_6 &= \begin{pmatrix} 0 & -1 \\ 1 & 1 \end{pmatrix}. \end{aligned} \quad (4.10)$$

As $[a : b : d]$ varies in $\mathcal{M}_M^0 := \mathcal{M} - \{\delta = 0\}$, we obtain a two-parameter variation of local systems. The rank of the parabolic cohomology local system \mathcal{V} on A can be easily computed using our formula (2.4). We have six singular points in total, four of which are unipotent and so we conclude that the rank of \mathcal{V} is four. On the other hand, we know that the transcendental lattices of the generic member of this family have rank four, and so we conclude that \mathcal{V} is equal to transcendental lattice local system, i.e., the Mordell-Weil rank is equal to zero.

Next we consider the ‘‘alternate fibration’’ structure. This fibration is obtained by considering the projection map from the quartic surface model (4.3) to $\mathbf{P}_{[x:w]}^1$. The fibre over a point $[t : 1] = [tw : w]$ is

$$y^2 zw - 4t^3 zw^3 + 3atzw^3 + bztw^3 - \frac{1}{2}(dz^2w^2 + w^4). \quad (4.11)$$

Set $p(t; a, b, d) = 4t^3 - 3at - b$. Then, after making a change of variable of the form $z \mapsto z - \frac{2p}{3d}$, one derives the following Weierstrass presentation for the alternate fibration:

$$\begin{aligned} y^2 &= 4z^3 - g_2(t; a, b, d)z - g_3(t; a, b, d) \\ g_2(t; a, b, d) &= \frac{4(4p^2 - 3d)}{3d^2} \\ g_3(t; a, b, d) &= -\frac{8p(8p^2 - 9d)}{27d^3}. \end{aligned} \quad (4.12)$$

The discriminant and functional invariant take the following form:

$$\begin{aligned} \Delta &= \frac{64(p^2 - d)}{d^4} \\ \mathcal{J} &= \frac{(4p^2 - 3d)^3}{27d^2(p^2 - d)} \\ \mathcal{J} - 1 &= \frac{p^2(8p^2 - 9d)^2}{27d^2(p^2 - d)}. \end{aligned} \quad (4.13)$$

By consulting Table 3.1, we see that the six roots of $p^2 - d$ are I_1 singular fibres and that ∞ is a type I_{12}^* fibre. By computing the discriminant of $p^2 - d$, one sees that that collisions of singular fibres occur if and only if $[a : b : d] \in \{\delta = 0\}$, where δ is given by (4.6). While one can compute the family of internal Picard-Fuchs equations for this family in the exact same manner as we did earlier, the equation is quite complicated and hard to display. Note

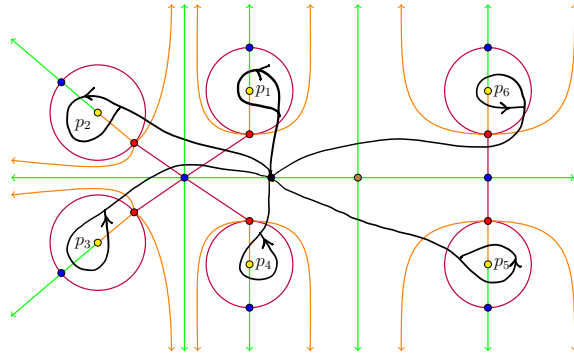


Figure 4.2: The alternate fibration when $[a : b : d] = [1 : 1 : -1]$.

that the degree of the functional invariant in this case is eighteen, rather than four for the standard fibration.

Using $[a : b : d] = [1 : 1 : -1]$ as a base point (the same base point we considered for the standard fibration), the six I_1 fibres are located at the roots of $p^2 + 1 = (4x^3 - 3x - 1)^2 + 1$. The Picard-Fuchs equation corresponding to this fibration is

$$\frac{d^2 f}{dt^2} + \frac{2(128t^7 - 144t^5 - 16t^4 + 48t^3 - 17t - 3)}{(16t^6 - 24t^4 - 8t^3 + 9t^2 + 6t + 2)(4t^2 - 1)} f + \frac{9(4t^2 - 1)^2}{4(16t^6 - 24t^4 - 8t^3 + 9t^2 + 6t + 2)} f = 0 \quad (4.14)$$

The singular points $t = \pm \frac{1}{2}$ of this equation are apparent singularities and once again correspond to excess ramification of the functional invariant.

In figure 4.2, we have marked these poles and drawn the graph that describes the corresponding cover. We take 0 as a base point for the initial local system and choose loops γ_i around the p_i as indicated. This allows to determine the initial monodromy representation:

$$\begin{aligned} \gamma_1 &\mapsto \begin{pmatrix} 2 & 1 \\ -1 & 0 \end{pmatrix} & \gamma_2 &\mapsto \begin{pmatrix} 0 & 1 \\ -1 & 2 \end{pmatrix} & \gamma_3 &\mapsto \begin{pmatrix} 2 & 1 \\ -1 & 0 \end{pmatrix} \\ \gamma_4 &\mapsto \begin{pmatrix} 0 & 1 \\ -1 & 2 \end{pmatrix} & \gamma_5 &\mapsto \begin{pmatrix} 2 & 1 \\ -1 & 0 \end{pmatrix} & \gamma_6 &\mapsto \begin{pmatrix} 0 & 1 \\ -1 & 2 \end{pmatrix} \\ & & \gamma_7 &\mapsto \begin{pmatrix} -1 & -12 \\ 0 & -1 \end{pmatrix} \end{aligned} \quad (4.15)$$

The first six monodromy transformations are unipotent and the the last does not have any fixed vectors. It follows from our rank formula (2.4) that the parabolic cohomology

group corresponding to this representation has rank given by:

$$(7 - 2) \cdot 2 - (1 + 1 + 1 + 1 + 1 + 1) = 4,$$

from which it follows that the parabolic cohomology local system is identified with the transcendental lattice local system on \mathcal{M}_M .

Proposition 12. *Let $\mathcal{M}_M^0 \subseteq \mathcal{M}_M$ be the compliment of $\{\delta = 0\}$ where δ is as in (4.6). Both the standard and alternate fibration structures on the K3 surfaces parameterized by \mathcal{M}_M^0 , as described in [8], give rise to geometric variations of local systems whose local system of parabolic cohomology groups agree with the rank four local system of transcendental lattices.*

Remark 20. The significance of the above example is that we are able to access information about the local system $\mathcal{T}(\mathcal{X})$ in two different ways, corresponding to the two different fibration structures. The fibration structures are quite different from each other: the number of singular fibres is different in each fibration, in addition to certain types of fibres only being found in one fibration. Nonetheless, the parabolic cohomology local system corresponding to the two different fibrations agree with each other in this case.

In general, this need not happen. While the transcendental lattice local system will always be contained as an irreducible piece of the parabolic cohomology local system, it is possible that two different fibration structures will have different Mordell-Weil lattices, which will correspond to different parabolic cohomologies.

Remark 21. In principle, if we had a good understanding of the fundamental group of $A = \mathcal{M}_M - \{\delta = 0\}$, then we could apply the Dettweiler-Wewers algorithm to compute the corresponding monodromy matrices. In the next section, we will look a certain sub-locus on which we will be able to implement the algorithm.

4.1.2 The $\sigma = 1$ Locus

In this section, we consider the sub-locus of the M -polarized moduli space cut out by setting $\sigma = 1$. In the affine chart defined by $a = 1$, this corresponds to setting $[a : b : d] = [1, 1, \frac{1}{\pi}]$; the K3-surfaces in this family are the minimal resolutions of the surfaces cut out by

$$Q_{a,b,d} : y^2zw - 4x^3z + 3xzw^2 + zw^3 - \frac{1}{2\pi}(z^2w^2 + \pi w^4) = 0. \quad (4.16)$$

We start by computing the “external” Picard-Fuchs equation—the π -dependent Picard-Fuchs equation that corresponds to the periods of the K3 surfaces in this family. Applying the Griffiths-Dwork algorithm to the family of hypersurfaces defined in (4.18), we obtain the

following Picard-Fuchs equation:

$$\frac{d^4 f}{d\pi^4} + \frac{\frac{13}{2}\pi - 1}{\pi(\pi - \frac{1}{4})} \frac{d^3 f}{d\pi^3} + \frac{\frac{17}{2}\pi - \frac{167}{288}}{\pi^2(\pi - \frac{1}{4})} \frac{d^2 f}{d\pi^2} + \frac{\frac{3}{2}}{\pi^2(\pi - \frac{1}{4})} \frac{df}{d\pi} - \frac{\frac{385}{82944}}{\pi^4(\pi - \frac{1}{4})} f = 0 \quad (4.17)$$

On the other hand, we also have two internal fibration structures coming from the standard and alternate fibrations. We first consider the standard fibration for the K3 surfaces in this sub-locus given by the Weierstrass presentation:

$$y^2 = 4x^3 - 3t^4x + \frac{1}{2\pi}t^5(\pi t^2 - 2\pi^3t + 1) \quad (4.18)$$

The corresponding π -dependent family of Picard-Fuchs equations is

$$\frac{d^2 f}{dt^2} + 2 \frac{2\pi^3t^6 - 6\pi^3t^5 - \pi^2t^4 + 8\pi^2t^3 - 4\pi t^2 + 6\pi t - 1}{t(\pi t^2 - 1)(\pi t^2 + 1)(\pi t^2 - 4\pi t + 1)} \frac{df}{dt} \quad (4.19)$$

$$+ \frac{77\pi^3t^6 - 144\pi^3t^5 - 159\pi^2t^4 + 576\pi^2t^3 - 201\pi t^2 + 144\pi t - 5}{36t^2(\pi t^2 - 1)(\pi t^2 + 1)(\pi t^2 - 4\pi t + 1)} f = 0 \quad (4.20)$$

Note that the singularities located at the roots of $\pi t^2 + 1$ are apparent singularities, while the poles correspond to the I_1 singular fibres.

The discriminant of this fibration is

$$\Delta = -\frac{27}{4\pi^2}t^{10}(\pi t^2 + 1)(\pi t^2 - 4\pi t + 1),$$

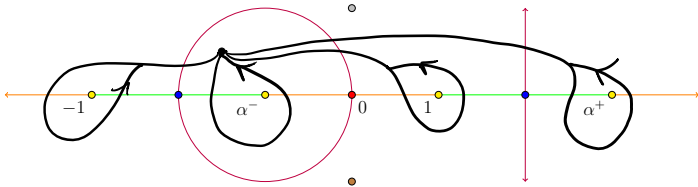
and the discriminant of the right-most quadratic term is equal to $\frac{4}{\pi}(4\pi - 1)$. Identifying the $\sigma = 1$ locus with \mathbf{P}_π^1 , it follows that the standard fibration gives rise to a variation of local systems over $\mathbf{P}_\pi^1 - \{0, \frac{1}{4}, \infty\}$. Using $\pi = -1$ as a base point, the initial local system is exactly the one we used as a base point when we studied the full M -polarized locus; the monodromy representation is therefore given by (4.10).

Let $\sigma_0, \sigma_{\frac{1}{4}}$ denote the loops around 0 and $\frac{1}{4}$ based at $\pi = -1$ as indicated in Figure 4.3. By carefully analyzing the motion of the singular points as π moves in these loops, we can determine the braiding map $\varphi: \pi_1(\mathbf{P}_\pi^1 - \{0, \frac{1}{4}, \infty\}, -1) \rightarrow A_5$:

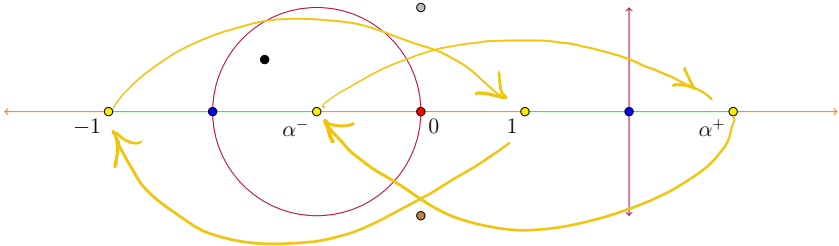
$$\begin{aligned} \varphi(\sigma_0) &= \beta_2^{-1}\beta_1^{-1}\beta_3^{-1}\beta_2^{-1}\beta_1^{-1}\beta_4^{-1}\beta_3^{-1}\beta_2^{-1} \\ \varphi(\sigma_{\frac{1}{4}}) &= \beta_2^{-1}\beta_3^{-1}\beta_4\beta_3\beta_2. \end{aligned} \quad (4.21)$$

We now apply the Dettweiler-Wewers algorithm to compute the monodromy representation of the corresponding parabolic cohomology local system.

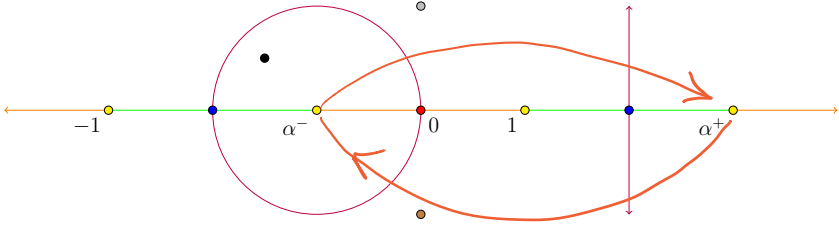
Proposition 13. *The monodromy representation of the parabolic cohomology local system*



(a) The standard fibration when $\pi = -1$.



(b) The braid $\varphi(\sigma_0)$.



(c) The braid $\varphi(\sigma_{\frac{1}{4}})$.

Figure 4.3: The standard fibration variation.

associated to the standard fibration over the $\sigma = 1$ locus is given by the matrices:

$$\eta(\sigma_0) = \begin{pmatrix} -1 & 1 & 0 & -1 \\ -1 & 0 & 1 & 0 \\ 0 & 1 & 0 & -1 \\ -1 & 0 & 1 & 1 \end{pmatrix}, \quad \eta(\sigma_{\frac{1}{4}}) = \begin{pmatrix} 1 & 0 & 0 & 0 \\ 1 & -1 & 1 & 1 \\ 0 & 0 & 1 & 0 \\ 0 & 0 & 0 & 1 \end{pmatrix}, \quad \eta(\sigma_\infty) = \begin{pmatrix} -1 & 0 & 1 & 0 \\ -2 & 1 & 1 & 0 \\ -1 & 1 & 1 & 0 \\ 0 & -1 & 0 & 1 \end{pmatrix}.$$

Their Jordan canonical forms are as follows:

$$J_0 = \begin{pmatrix} \omega & 0 & 0 & 0 \\ 0 & \omega^5 & 0 & 0 \\ 0 & 0 & \omega^7 & 0 \\ 0 & 0 & 0 & \omega^{11} \end{pmatrix}, \quad J_{\frac{1}{4}} = \begin{pmatrix} -1 & 0 & 0 & 0 \\ 0 & 1 & 0 & 0 \\ 0 & 0 & 1 & 0 \\ 0 & 0 & 0 & 1 \end{pmatrix}, \quad J_\infty = \begin{pmatrix} -1 & 0 & 0 & 0 \\ 0 & 1 & 1 & 0 \\ 0 & 0 & 1 & 1 \\ 0 & 0 & 0 & 1 \end{pmatrix}.$$

Proof. The matrices above are obtained by applying the Dettweiler-Wewers algorithm with the initial monodromy representation (4.10) with the braiding map determined as above. These monodromy matrices are equal to the monodromy matrices of the parabolic cohomology local system up to a sign ambiguity. To eliminate the ambiguity, we can compute the Picard-Fuchs differential equation for this family of K3 surfaces.

The characteristic exponents of the Picard-Fuchs equation (4.17) at $\pi = \frac{1}{4}$ are $0, \frac{1}{2}, 1, 2$, which means that the corresponding monodromy transformation has 1 and -1 for eigenvalues, with -1 appearing with algebraic multiplicity one. The characteristic exponents at $\pi = \infty$ are 0 , with multiplicity three, and $\frac{1}{2}$ with multiplicity one, which means that the corresponding monodromy transformation has 1 as an eigenvalue with algebraic multiplicity three, and eigenvalue -1 with multiplicity one. Since the monodromy matrices written above have the correct multiplicities of eigenvalues, we have resolved the sign ambiguity. \square

We now perform the same computation using the alternate fibration. The π -dependent family of Picard-Fuchs equations corresponding to the alternate fibration is by

$$\frac{d^2 f}{dt^2} + 2 \frac{128\pi t^7 - 144\pi t^5 - 16\pi t^4 + 48\pi t^3 - 13\pi t - 3\pi + 4t}{(4t^2 - 1)(\pi p^2 - 1)} \frac{df}{dt} + \frac{9(4t^2 - 1)^2}{4(\pi p^2 - 1)}. \quad (4.22)$$

Using $\pi = -1$ as a base point, the initial homological invariant was computed earlier in (4.15). If $\sigma_0, \sigma_{\frac{1}{4}}$ are the same loops from the earlier, then Figure 4.4 describe the motion of the singular points and allow us to determine the braiding morphism. We determine that

$$\begin{aligned} \varphi(\sigma_0) &= \beta_1^{-1} \beta_2^{-1} \beta_3^{-1} \beta_4^{-1} \beta_5^{-1} \\ \varphi(\sigma_{\frac{1}{4}}) &= \beta_5 \beta_4 \beta_5^{-1}. \end{aligned} \quad (4.23)$$

Using these braids, we run the Dettweiler-Wewers algorithm to compute the monodromy representation, using the structure of the external Picard-Fuchs equation to eliminate the sign ambiguity.

4.1.3 A New Perspective on the 14th Case

In this section, we demonstrate how the fourteenth case of integral variation of Hodge structure constructed in [9] arises from geometric variations local systems. This variation of Hodge structure corresponds to a one-parameter family \mathcal{Y} of Calabi-Yau threefolds admitting fibrations by M -polarized K3 surfaces lying in the $\sigma = 1$ locus. As described in [9], the fibration is described by a map $\alpha: \mathcal{Y} \rightarrow C \cong \mathbf{P}_t^1$, and each fibre $\alpha^{-1}(t)$ is an M -polarized K3-surface [9]. The M -polarization structure is described in terms of its modular invariants as follows:

$$\pi_{\mathcal{Y}} = \frac{1}{12^6 \xi} \cdot \frac{t}{(t+1)^2} \quad (4.24)$$

$$\sigma_{\mathcal{Y}} = 1, \quad (4.25)$$

where $\xi \in \mathbf{C}$ denotes the parameter for the family \mathcal{Y} . The ξ -dependent family of degree-two covers of \mathbf{P}_{π}^1 defined above are generalized functional invariant maps to the $\sigma = 1$ locus that determine the internal M -polarized K3 surface-fibration on each \mathcal{Y}_{ξ} .

Let \mathcal{V} denote the rank-four local system of transcendental lattices on the $\sigma = 1$ locus whose monodromy was computed in Proposition 13. Then, the family of pull-back local systems $p_{\xi}^* \mathcal{V}$ defines a variation of local systems that describe the internal M -polarized K3 surface-fibration structure. For each $\xi \notin \{0, \infty\}$, we have

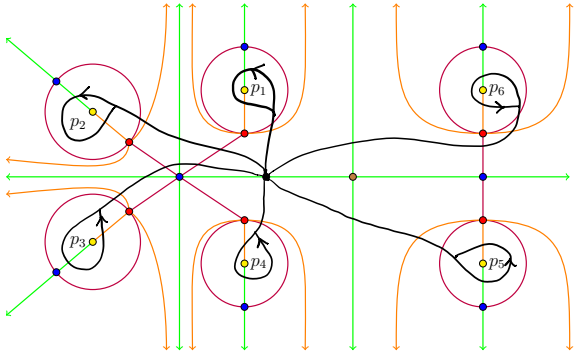
$$p_{\xi}^{-1}(0) = \{0, \infty\}, \quad p_{\xi}^{-1}(\infty) = \{-1\}, \quad p_{\xi}^{-1}\left(\frac{1}{4}\right) := \{\alpha^+, \alpha^-\}.$$

The map p_{ξ} is ramified at $t = 1$, which lies over $\frac{1}{4 \cdot 12^6 \xi}$; this branch point is equal to $\frac{1}{4}$ only if $\xi = \frac{1}{12^6}$. Therefore, the local systems $p_{\xi}^* \mathcal{V}$ form a variation of local systems parameterized by $\mathbf{P}_{\xi}^1 - \{0, \frac{1}{12^6}, \infty\}$.

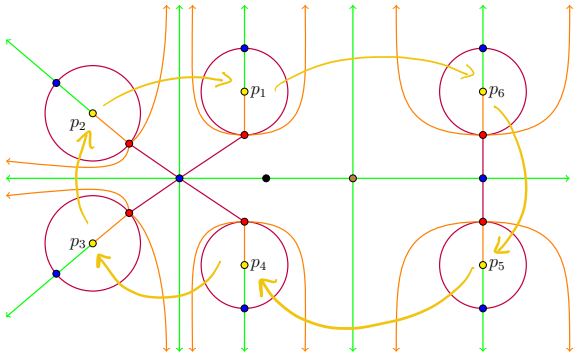
Remark 22. When $\xi = \frac{1}{12^6}$, the threefold $\mathcal{Y}_{\frac{1}{12^6}}^1$ is still fibred by M -polarized K3 surfaces, but the number of singular points in the corresponding local system is less than the generic one. This is why, from the perspective of variations of local systems, we omit $\xi = \frac{1}{12^6}$.

The ξ -dependent family of Picard-Fuchs equation is given by

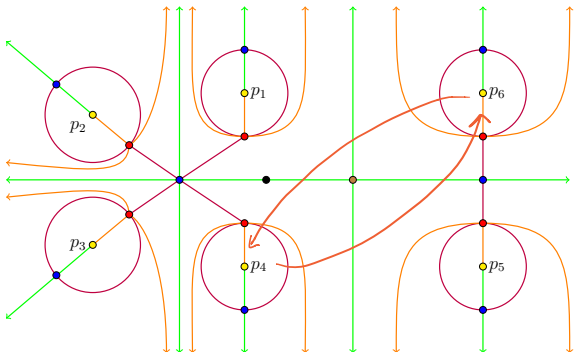
$$\frac{d^4 f}{dt^4} + P_{\xi} \frac{d^3 f}{dt^3} + Q_{\xi} \frac{d^2 f}{dt^2} + R_{\xi} \frac{df}{dt} + S_{\xi} f = 0, \quad (4.26)$$



(a) The alternate fibration when $\pi = -1$.



(b) The braid $\varphi(\sigma_0)$.



(c) The braid $\varphi(\sigma_{\frac{1}{4}})$.

Figure 4.4: The alternate fibration variation.

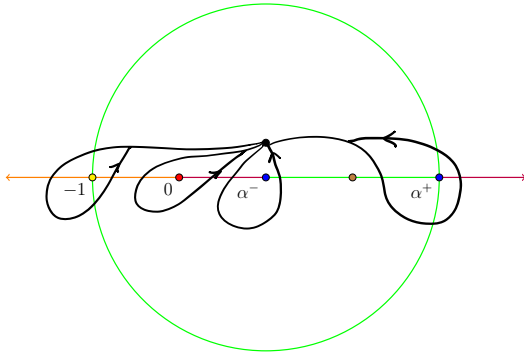
where

$$\begin{aligned}
P_\xi &= 6 \frac{\xi t^4 - \frac{7}{8957952} t^3 + (-4\xi + \frac{7}{4478976}) t^2 + (-4\xi + \frac{17}{8957952}) t - \xi}{\xi t(t^2-1)(t^2 + (2 - \frac{4}{12^6 \xi}) t + 1)} \\
Q_\xi &= \frac{491(\xi t^6 + (-2\xi - \frac{7}{20362752}) t^5 + (-\frac{1355}{491} \xi + \frac{7}{5090688}) t^4 + (\frac{5420}{491} \xi - \frac{1}{377088}) t^3 + (\frac{9013}{491} \xi - \frac{35}{5090688}) t^2 + (\frac{4202}{491} \xi - \frac{67}{20362752}) t + \xi)}{72\xi t^2(t^2-1)^2(t^2 + (2 - \frac{4}{12^6 \xi}) t + 1)} \\
R_\xi &= 59 \frac{\xi t^8 + (-4\xi + \frac{1}{4893696}) t^7 + (2\xi - \frac{1}{815616}) t^6 + (-\frac{1256}{59} \xi + \frac{67}{4893696}) t^5}{72\xi t^3(t^2-1)^3(t^2 + (2 - \frac{4}{12^6 \xi}) t + 1)} \\
&\quad + 59 \frac{(-\frac{9112}{59} \xi + \frac{17}{407808}) t^4 + (-\frac{14060}{59} \xi + \frac{47}{543744}) t^3 + (-\frac{8286}{59} \xi + \frac{109}{2446848}) t^2 + (-\frac{1728}{59} \xi + \frac{53}{4893696}) t - \xi}{72\xi t^3(t^2-1)^3(t^2 + (2 - \frac{4}{12^6 \xi}) t + 1)} \\
S_\xi &= \frac{25(\xi t^2 + (2\xi - \frac{1}{7200}) t + \xi)}{20736\xi t^4(t^2-1)^4(t^2 + (2 - \frac{4}{12^6 \xi}) t + 1)}
\end{aligned} \tag{4.27}$$

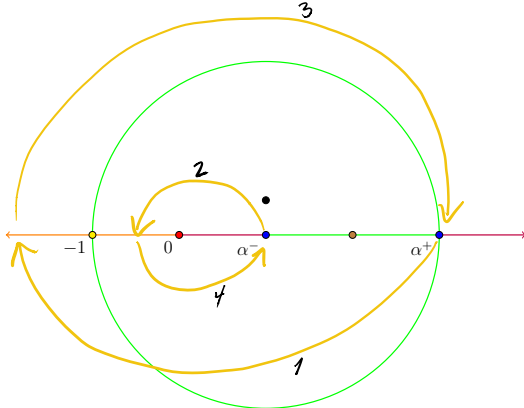
Note that $t = 1$ is an apparent singularity of these equations, corresponding to the excess ramification of the degree-two covers.

The monodromy representation for each $p_\xi^* \mathcal{V}$ is determined in the usual manner by examining the push-forward homomorphism, using the monodromy representation for \mathcal{V} that was computed in 13. Choosing $\xi = \frac{1}{2 \cdot 12^6}$ as a base point on, we determine the monodromy representation of the pull-back by drawing the graph in Figure 4.5. Let $\tau_1, \tau_2, \tau_3, \tau_4, \tau_5$ be the loops indicated in the figure. Then, we determine their images under the push-forward map $p_{\frac{1}{2 \cdot 12^6}, *}$ as follows:

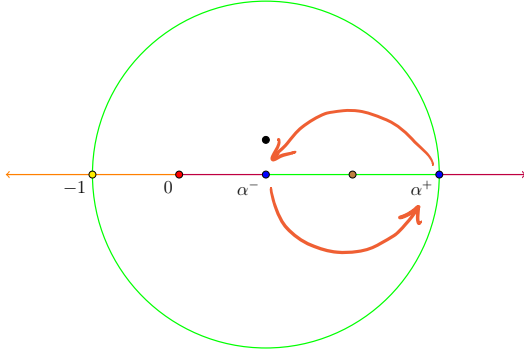
$$\begin{aligned}
\tau_1 &\mapsto \sigma_\infty^2 \\
\tau_2 &\mapsto \sigma_0 \\
\tau_3 &\mapsto \sigma_1 \\
\tau_4 &\mapsto \sigma_1 \\
\tau_5 &\mapsto \sigma_1^{-2} \sigma_0^{-1} \sigma_\infty^{-2}.
\end{aligned} \tag{4.28}$$



(a) The degree-two cover when $\xi = \frac{1}{2 \cdot 12^6}$.



(b) The braid $\varphi(\sigma_0)$. The numbers indicated the order in which the corresponding motion happens.



(c) The braid $\varphi(\sigma_{\frac{1}{12^6}})$.

Figure 4.5: The M -polarized fibration variation.

It follows that the monodromy representation of $p^*_{\frac{1}{2 \cdot 12^6}} \mathcal{V}$ is given by

$$\begin{aligned}
 \tau_1 &\mapsto \begin{pmatrix} 0 & 1 & 0 & 0 \\ -1 & 2 & 0 & 0 \\ -2 & 2 & 1 & 0 \\ 2 & -2 & -1 & 1 \end{pmatrix} & \tau_2 &\mapsto \begin{pmatrix} -1 & 1 & 0 & -1 \\ -1 & 0 & 1 & 0 \\ 0 & 1 & 0 & -1 \\ -1 & 0 & 1 & 1 \end{pmatrix} \\
 \tau_3 &\mapsto \begin{pmatrix} 1 & 0 & 0 & 0 \\ 1 & -1 & 1 & 1 \\ 0 & 0 & 1 & 0 \\ 0 & 0 & 0 & 1 \end{pmatrix} & \tau_4 &\mapsto \begin{pmatrix} 1 & 0 & 0 & 0 \\ 1 & -1 & 1 & 1 \\ 0 & 0 & 1 & 0 \\ 0 & 0 & 0 & 1 \end{pmatrix} \\
 \tau_5 &\mapsto \begin{pmatrix} 0 & -1 & 1 & 0 \\ 1 & -2 & 2 & 1 \\ 1 & -1 & 1 & 0 \\ -1 & 0 & 1 & 1 \end{pmatrix}
 \end{aligned} \tag{4.29}$$

Let $\sigma_0, \sigma_{\frac{1}{12^6}}, \sigma_\infty$ be the usual generators of $\mathbf{P}_\xi^1 - \{0, \frac{1}{12^6}, \infty\}$ based at $\frac{1}{2 \cdot 12^6}$. Then, the braiding map φ is determined by

$$\varphi(\sigma_0) = \beta_3^{-1} \beta_2^{-1} \beta_1^{-1} \beta_3 \beta_1^{-1} \beta_2^{-1} \beta_3^{-1} \beta_2, \quad \varphi(\sigma_{\frac{1}{12^6}}) = \beta_3. \tag{4.30}$$

Applying the Dettweiler-Wewers algorithm, we compute the monodromy representation for the parabolic cohomology local system \mathcal{W} on $\mathbf{P}_\xi^1 - \{0, \frac{1}{12^6}, \infty\}$.

Proposition 14. *The local system \mathcal{W} has the following monodromy representation:*

$$\sigma_0 \mapsto \begin{pmatrix} -2 & 1 & -1 & 1 \\ -4 & 2 & -1 & 1 \\ -5 & 1 & -1 & 2 \\ -10 & 3 & -4 & 5 \end{pmatrix}, \quad \sigma_{\frac{1}{12^6}} \mapsto \begin{pmatrix} 1 & 0 & 0 & 0 \\ 0 & 1 & 0 & 0 \\ 0 & 0 & 1 & 0 \\ -3 & 1 & -1 & 1 \end{pmatrix}, \quad \sigma_\infty \mapsto \begin{pmatrix} 4 & -1 & 1 & -1 \\ 7 & -1 & 2 & -2 \\ 9 & -2 & 4 & -3 \\ 25 & -7 & 9 & -7 \end{pmatrix}. \tag{4.31}$$

This is exactly the representation corresponding the 14th case in the Doran-Morgan classification of variations of integral Hodge structures corresponding to one-parameter families of Calabi-Yau threefold over thrice-punctured spheres.

Proof. The monodromy matrices above are found by applying the Dettweiler-Wewers algorithm with braiding map determined as above. We can verify that we have computed the correct representation by using the fact the 14th case monodromy representation is uniquely characterized by the the fact that the monodromy at 0 is maximally unipotent, and that the

characteristic polynomial of the monodromy at ∞ is $x^4 - x^2 + 1$ [20]. \square

The Picard-Fuchs equation for the family \mathcal{Y}_ξ is equal to the generalized hypergeometric equation ${}_4F_3\left(\frac{1}{12}, \frac{5}{12}, \frac{7}{12}, \frac{11}{12}\right)$, after the change of variable $t = 12^6\xi$, which can be written as

$$\theta^4 f - \left(\theta + \frac{1}{12}\right) \left(\theta + \frac{5}{12}\right) \left(\theta + \frac{7}{12}\right) \left(\theta + \frac{11}{12}\right) f = 0, \quad (4.32)$$

where θ denotes the differential operator $t \frac{d}{dt}$.

4.2 M_n -Polarized K3 Surface-Fibrations

In this section, we will examine M_n -polarized K3 surface-fibrations, where M_n is the rank nineteen lattice

$$M_n = H \oplus E_8 \oplus E_8 \oplus \langle -2n \rangle,$$

for $n \geq 2$.

4.2.1 General Theory

We begin by describing the moduli space \mathcal{M}_n of M_n -polarized K3 surfaces. Since each M_n -polarized K3 surface is M -polarized, there is a morphism $\mathcal{M}_n \rightarrow \mathcal{M}_M$. The image of this map consists of the pairs $\tau, u \in \mathfrak{h}^2$ for which the elliptic curves E_τ and E_u are joined by a cyclic n -isogeny. Thus, the image of \mathcal{M}_n inside \mathcal{M} is identified with the modular curve $X_0(n)^+$, which is the quotient of the upper half-plane \mathfrak{h} by the group

$$\Gamma_0(n)^+ = \Gamma_0(N) \cup \tau_n \Gamma_0(N), \quad \tau_n = \begin{pmatrix} 0 & -\frac{1}{\sqrt{n}} \\ \sqrt{n} & 0 \end{pmatrix}.$$

In fact, the map $\mathcal{M}_n \rightarrow \mathcal{M}$ is an isomorphism onto its image [17].

Now suppose $\pi: \mathcal{X} \rightarrow U$ is an M_n -polarized family in the sense of Definition 19.

Definition 21. The *generalized functional invariant* of $\mathcal{X} \rightarrow U$ is the map $g: U \rightarrow \mathcal{M}_n$ defined by sending each fibre X_p to its corresponding point in moduli.

For families of M_n -polarized K3 surfaces, the functional invariant is enough to characterize the family up to isomorphism:

Theorem. [Theorem 2.2 [17]] *The family $\pi: \mathcal{X} \rightarrow U$ is uniquely determined by its functional invariant $g: U \rightarrow \mathcal{M}_n$.*

It follows that any M_n -polarized family of K3 surfaces $\pi: \mathcal{X} \rightarrow U$ is the pull-back of a fundamental modular family $\mathcal{X}_n \rightarrow \mathcal{M}_n$ by the functional invariant. In general, computing explicit models for the families \mathcal{X}_n is difficult, but for low values of n , models are tabulated in [17]. As an example, the modular family \mathcal{X}_2 is given by

$$\lambda w^4 + xyz(x + y + z - w) = 0, \tag{4.33}$$

where λ is the coordinate on $X_0(2)^+$ for which the orbifold points of orders $(2, 4, \infty)$ are located at $\lambda = \frac{1}{4^4}, \infty, 0$ respectively.

We are interested in the variation of Hodge structure on U given by the local system $\mathcal{T}(\mathcal{X})$; we begin by describing the period domain, following the treatment of Dolgachev [13]. Start by choosing a basis (e, f, g) for $M_n^\perp = H \oplus \langle 2n \rangle$, where e is a generator of $2n$, and (f, g) is a standard basis for H . The period domain \mathcal{D}_n is defined as

$$\mathcal{D}_n = \{z \in \mathbf{P}(M_n^\perp \otimes \mathbf{C}) \mid \langle z, z \rangle = 0, \langle z, \bar{z} \rangle > 0\}.$$

The group $O(M_n^\perp)^*$, defined to be the kernel of the morphism $O(M_n^\perp) \rightarrow \text{Aut}(A_{M_n^\perp})$, where $A_{M_n^\perp}$ is the discriminant lattice, acts on the space \mathcal{D}_n , and is generated by $SO(M_n^\perp)^* := O(M_n^\perp)^* \cap SO(M_n^\perp)$ and the involution

$$\iota = \begin{pmatrix} 0 & 0 & 1 \\ 0 & 1 & 0 \\ 1 & 0 & 0 \end{pmatrix}.$$

Dolgachev shows that there is an isomorphism between the compactification of the quotient $\mathcal{D}_n/O(M_n^\perp)^*$ and the moduli space \mathcal{M}_n .

As explained in [17], we can construct Hodge structures on the quotients as follows. Let \mathcal{F}_2 be the line bundle $\mathcal{O}_{\mathbf{P}^2}(-1)$ restricted to \mathcal{D}_n , which is a sub-bundle of $\mathcal{F}^0 := (\mathcal{M}_n^\perp \otimes \mathcal{O}_{\mathbf{P}^2})|_{\mathcal{D}_n}$ on \mathcal{D}_n . This defines a weight two integral variation of Hodge structure which descends to Hodge structures \mathbf{V}_n and \mathbf{V}_n^+ on the quotients $\mathcal{D}_n/SO(M_n^\perp)^*$ and $\mathcal{D}_n/O(M_n^\perp)^*$. The local system \mathbf{V}_n is the pull-back of \mathbf{V}_n^+ via the double cover $\mathcal{D}_n/SO(M_n^\perp)^* \rightarrow \mathcal{D}_n/O(M_n^\perp)^*$. Moreover, the Hodge-theoretic analogue of Theorem 4.2.1 holds:

Proposition (Proposition 2.6 [17]). *The variation of Hodge structure $\mathcal{T}(\mathcal{X})$ is the pull-back of \mathbf{V}_n^+ by the functional invariant.*

Thus, from the perspective of local systems and variations of Hodge structures, we are reduced to studying the local systems that arise by pulling back \mathbf{V}_n^+ along rational functions. This is not dissimilar to the situation of elliptic surfaces in which Stiller showed, among

other things, that the Picard-Fuchs equation of an elliptic surface is projectively equivalent to the pull-back differential equation of a specific hypergeometric function via the functional invariant. Following the ideas of Stiller, we can attempt to categorize the types of differential equations that can occur in this setting and prove similar structural results.

To motivate the next definition, suppose that $\pi: \mathcal{X} \rightarrow U$ is an M_n -polarized family of K3 surfaces, and fix a choice of holomorphic non-vanishing section $\omega_{\mathcal{X}}$ that generates the filtrant \mathcal{F}^2 . Choosing a basis (f, e, g) for M_n^\perp for which the pairing is given by

$$\begin{bmatrix} 0 & 0 & 1 \\ 0 & 2n & 0 \\ 1 & 0 & 0 \end{bmatrix},$$

we may write $\omega_{\mathcal{X}} = \eta e + \zeta f + \xi g$, for holomorphic functions η, ζ, ξ on U . The functions η, ζ, ξ are the periods of $\omega_{\mathcal{X}}$ and satisfy the corresponding rank three Picard-Fuchs differential equation. The condition that $\langle \omega, \omega \rangle = 0$ implies that

$$n\eta^2 + \zeta\xi = 0.$$

Scaling ω by η , and using $\xi = -\zeta/n$, we find that

$$Q(\omega, \bar{\omega}) = 2 - (w + \bar{w}),$$

where $w = \frac{\zeta}{\eta}$. This quantity is always non-negative and is equal to 0 precisely when $\zeta \in \mathbf{R}$. It follows that the period domain \mathcal{D}_n splits into two connected components, each isomorphic to the upper half-plane, say \mathcal{D}_n^\pm and $\frac{\zeta}{\eta}$ will stay in one component. By changing basis to $(-\eta, -\zeta, \xi)$ if needed, we will assume that $\frac{\zeta}{\eta} \in \mathfrak{h}$. Finally, the monodromy representation of the Picard-Fuchs equation with respect to the basis (η, ζ, ξ) will take values in $O(M_n^\perp)^+$, the subgroup that fixes the component \mathcal{D}_n^+ .

This prompts the following definition:

Definition 22. A rank three K -equation for $O(M_n^\perp)^*$ is a Fuchsian differential equation of the form

$$\Lambda f = \frac{d^3 f}{du^3} + P \frac{d^2 f}{du^2} + Q \frac{df}{du} + Rf = 0,$$

where $P, Q, R \in K(U)$, together with three non-vanishing holomorphic, multivalued solutions η, ζ, ξ satisfying:

1. $n\eta^2 + \zeta\xi = 0$;
2. $\text{im}(\frac{\zeta}{\eta}) > 0$;

3. the monodromy representation takes values in $O(M_n^\perp)^*$;
4. the Wronskian $W = e^{-\int P dx} \in K(U)$

Given a rank 3 K -equation for $O(M_n^\perp)^*$ as above, it follows that we have a multi-valued map

$$U_0 \rightrightarrows \mathcal{D}_n^+,$$

defined on a Zariski-open subset of U . Composing this map with the map

$$\mathcal{D}_n^+ \rightarrow O(M_n^\perp)^+ \setminus \mathcal{D}_n^+ \cong X_0(n)^+,$$

we obtain a single-valued function $\mathcal{G}: U \rightarrow X_0(n)^+$; the fact that we have a Fuchsian equation and properties of the quotient map above imply that \mathcal{G} is meromorphic, much in the same as is argued in [21].

Definition 23. Given a K equation as above, the rational function $\mathcal{G}: U \rightarrow X_0(n)^+$ is called the *functional invariant of the K -equation*.

Proposition 15. For each n , the Picard-Fuchs equation for the family $\mathcal{X}_n \rightarrow X_0(n)^+$ is a K -equation for $O(M_n^\perp)^+$. We denote this equation by \mathcal{K}_n .

Proof. This is just by definition of K -equations. The K -basis is given, after fixing the form $\omega_{\mathcal{X}_n}$, by the periods of ω along the cycles that are Poincaré dual to e, f, g . \square

Remark 23. Note that for the equation \mathcal{K}_n , the map $u \mapsto \eta(u)e + \zeta(u)f + \xi(u)g$ from $X_0(n)^+$ to \mathcal{D}_n^+ is a local single-valued inverse to the quotient map $\mathcal{D}_n^+ \rightarrow X_0(n)^+$, the same way that the K -basis for the Picard-Fuchs equation corresponding to $\mathcal{J} = t$ defines a local inverse to the modular J -map. In particular, the functional invariant for each \mathcal{K}_n is the identity map.

By using the Griffiths-Dwork algorithm to the family \mathcal{X}_2 in (4.33), we find that \mathcal{K}_2 is equal to

$$\frac{d^3 f}{d\lambda^3} + \frac{\frac{9}{2}\lambda - \frac{3}{256}}{\lambda(\lambda - \frac{1}{256})} \frac{d^2 f}{d\lambda^2} + \frac{\frac{51}{16}\lambda - \frac{1}{256}}{\lambda^2(\lambda - \frac{1}{256})} \frac{df}{d\lambda} + \frac{\frac{3}{32}}{\lambda^2(\lambda - \frac{1}{256})} f = 0. \quad (4.34)$$

After changing variables $t = 4^4\lambda$, this equation is the generalized hypergeometric equation ${}_3F_2(\frac{1}{4}, \frac{1}{2}, \frac{3}{4})$.

Proposition 16. Each K -equation for $O(M_n^\perp)^+$ is projectively equivalent to the pull-back of \mathcal{K}_n by the functional invariant \mathcal{G} . More precisely, let

$$\frac{d^3 f}{du^3} + P \frac{d^2 f}{du^2} + Q \frac{df}{du} + Rf = 0$$

be the K -equation \mathcal{K}_n . Then any other K -equation is obtained by pulling back by the functional invariant \mathcal{G} and then scaling the solutions by some algebraic function μ satisfying $\mu^3 \in K(U)$.

Proof. Let $\mathcal{G}: U \rightarrow X_0(n)^+$ be the functional invariant for \mathcal{K} and let $\lambda_n: \mathcal{D}_n^+ \rightarrow X_0(n)^+$ be the quotient map. The period-map associated to \mathcal{K} is the multi-valued map $\lambda_n^{-1} \circ \mathcal{G}$. On the other hand, this is also the period-map associated to $\mathcal{G}^*\mathcal{K}_n$, the pull-back of \mathcal{K}_n of by \mathcal{G} with respect to the pull-back K -basis. Since the two period maps agree, we deduce that there is an overall scaling function μ that relates the differential equations, i.e., they are projectively equivalent. One sees by expanding the resulting formulae that μ^3 must be a rational function for the Wronskian of the scaled equation to be rational. \square

Given a K -basis for the K -equation \mathcal{K} , we can construct a variation of Hodge structure over U by setting $\omega = \eta(u)e + \zeta(u)f + \xi(u)g$, which determines a Hodge structure. Scaling ω by a function $\lambda(u)$ will not change the Hodge structure, but it will scale each of the period functions η, ζ, ξ . Thus, the projective equivalence class of the K -equation is completely determined by the functional invariant \mathcal{G} , and fixing a choice of section $\omega_{\mathcal{K}}$ corresponds to fixing a particular K -equation in the equivalence class.

4.2.2 The Dwork Pencil

In this section, we will consider the Dwork pencil of Calabi-Yau manifolds given in affine coordinates by

$$x_1 \cdots x_n (x_1 + \cdots + x_n + 1) + \frac{(-1)^{n+1} t_{n-1}}{(n+1)^{n+1}} = 0. \quad (4.35)$$

For each n , this defines a smooth family of $n - 1$ -dimensional Calabi-Yau hypersurfaces $Y_{t_{n-1}}^{(n-1)}$. As described in [19], the family $Y_{t_{n-1}}^{(n-1)}$ admits a fibration by hypersurfaces $Y_{t_{n-2}}^{(n-2)}$. We consider this family for $n = 2, 3, 4$.

When $n = 2$, the pencil (4.35) defines a family of 1-dimensional Calabi-Yau manifolds, i.e., defines an elliptic surface, known as the *cubic mirror family* of hypersurfaces. This fibration can be described in terms of our usual Weierstrass invariants by setting

$$g_2 = \frac{16}{3} - 4t, \quad g_3 = -\frac{64}{27} + \frac{8}{3}t; \quad (4.36)$$

one computes that the functional invariant is $\mathcal{J} = \frac{1}{27} \frac{(3t-4)^3}{t^2(t-1)}$. There are singular fibres of type I_2 at $t = 0$, type I_1 at $t = 1$, and type III^* at $t = \infty$. The rational map \mathcal{J} is described in Figure 4.6 and we determine the homological invariant to be

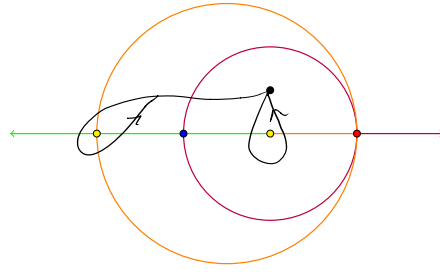


Figure 4.6: The graph representing the functional invariant for the elliptic fibration (4.36).

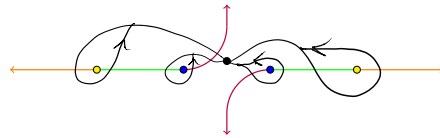


Figure 4.7: The graph representing the initial elliptic fibration (4.38) on the quartic mirror family.

$$\begin{pmatrix} 1 & 0 \\ -2 & 1 \end{pmatrix}, \begin{pmatrix} 1 & 1 \\ 0 & 1 \end{pmatrix}, \begin{pmatrix} -1 & -1 \\ 2 & 1 \end{pmatrix}. \quad (4.37)$$

When $n = 3$, the Dwork pencil (4.35) is the family of K3 surfaces cut out by

$$x_1x_2x_3(x + y + z + 1) + \frac{t_2}{4^4} = 0,$$

which is exactly the family \mathcal{X}_2 described above in (4.33) if we look at the affine chart $w = -1$ and set $\lambda = \frac{t}{4^4}$. The pencil $Y_{t_2}^2$ admits a fibration by cubic mirror elliptic curves. In fact, for each t_2 , the fibration is the pull-back of (4.36) by the rational function

$$g(t; t_2): u \mapsto \frac{-t_2}{4t(t+1)}.$$

Thus, the fibration of the quartic mirror family gives rise to a variation of local systems corresponding to the varying elliptic curve fibrations.

If $t_2 \notin \{0, 1, \infty\}$, the rational function $g(t; t_2)$ satisfies

$$\begin{aligned} g(t; t_2)^{-1}(0) &= \{t = \infty\}, & g(t; t_2)^{-1}(\infty) &= \{t = 0, t = -1\}, \\ g(t; t_2)^{-1}(1) &= \{t = -\frac{1}{2} \pm \frac{\sqrt{1-t_2}}{2}\}. \end{aligned} \quad (4.38)$$

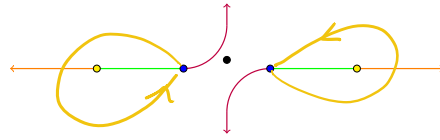


Figure 4.8: The braid $\varphi(\sigma_0)$.

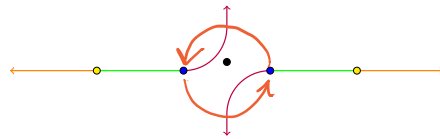


Figure 4.9: The braid $\varphi(\sigma_1)$.

It follows that for each $t_2 \notin \{0, 1, \infty\}$, the corresponding elliptic fibration has two III*-fibres at $t = 0, -1$, one I_4 -fibre at $t = \infty$, and two I_1 -fibres at $t = -\frac{1}{2} \pm \frac{\sqrt{1-t}}{2}$. Choosing $t_2 = \frac{1}{2}$ as a base point, the degree two cover $g(t; \frac{1}{2})$ can be represented by the graph in Figure 4.7, from which we compute the homological invariant for $t_2 = \frac{1}{2}$ to be

$$\begin{aligned} \gamma_1 &\mapsto \begin{pmatrix} 1 & -1 \\ 2 & -1 \end{pmatrix} & \gamma_2 &\mapsto \begin{pmatrix} 1 & 1 \\ 0 & 1 \end{pmatrix} & \gamma_3 &\mapsto \begin{pmatrix} 1 & 1 \\ 0 & 1 \end{pmatrix} \\ \gamma_4 &\mapsto \begin{pmatrix} -1 & -1 \\ 2 & 1 \end{pmatrix} & \gamma_5 &\mapsto \begin{pmatrix} 1 & 0 \\ -4 & 1 \end{pmatrix}, \end{aligned} \tag{4.39}$$

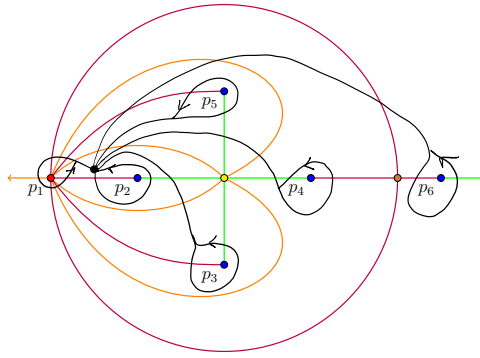
for the loops indicated in the figure.

Let σ_0, σ_1 be the loops based at $t_2 = \frac{1}{2}$ around 0 and 1 in the usual manner. Then, the braiding map $\varphi: \pi_1(\mathbf{P}_t^1 - \{0, 1, \infty\}) \rightarrow A_4$ is determined by the motion of the poles, as indicated in Figures 4.9. We see that the braiding map is given as follows:

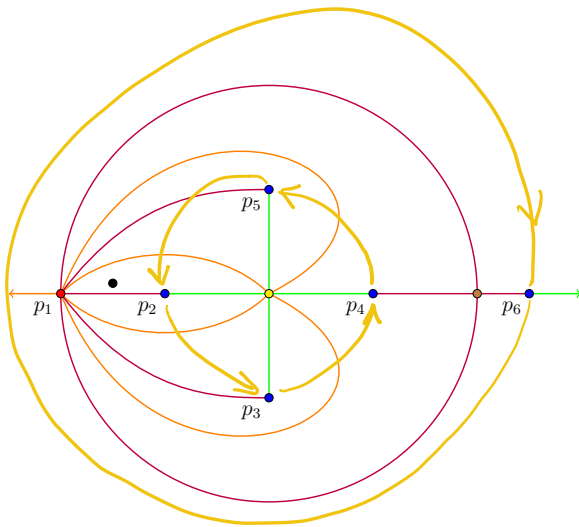
$$\begin{aligned} \varphi(\sigma_0) &= \beta_1^2 \beta_3^2 \\ \varphi(\sigma_1) &= \beta_2. \end{aligned} \tag{4.40}$$

Applying the Dettweiler-Wewers algorithm with the above input produces the following monodromy representation for the rank three parabolic cohomology:

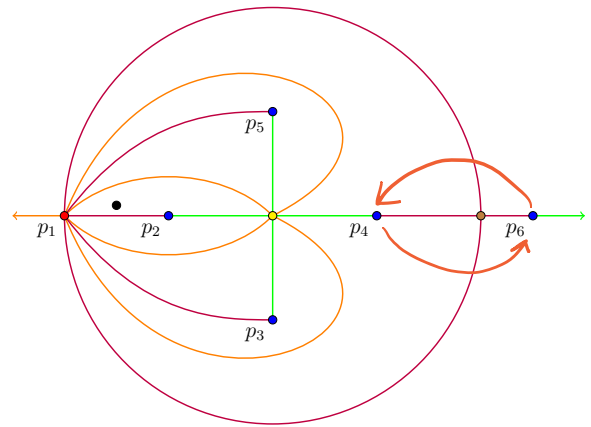
$$\sigma_0 \mapsto \begin{pmatrix} -3 & 1 & 3 \\ -4 & 1 & 4 \\ -4 & 0 & 5 \end{pmatrix}, \sigma_1 \mapsto \begin{pmatrix} 1 & 0 & 0 \\ 0 & 1 & 0 \\ -2 & 3 & -1 \end{pmatrix}, \sigma_\infty \mapsto \begin{pmatrix} 5 & -5 & 1 \\ 4 & -3 & 0 \\ -2 & 5 & -3 \end{pmatrix} \tag{4.41}$$



(a) The initial K3 surface-fibration for the quintic mirror family.



(b) The braid $\varphi(\sigma_{\frac{1}{5^5}})$.



(c) The braid $\varphi(\sigma_1)$.

Figure 4.10: The quintic mirror fibration

The corresponding Jordan normal forms of these matrices are

$$\begin{pmatrix} 1 & 1 & 0 \\ 0 & 1 & 1 \\ 0 & 0 & 1 \end{pmatrix}, \begin{pmatrix} -1 & 0 & 0 \\ 0 & 1 & 0 \\ 0 & 0 & 1 \end{pmatrix}, \begin{pmatrix} -1 & 0 & 0 \\ 0 & i & 0 \\ 0 & 0 & -i \end{pmatrix}. \quad (4.42)$$

We have thus computed the monodromy representation for the Picard-Fuchs equation of the family \mathcal{X}_2 , once we change the variables $\lambda = \frac{t}{4^4}$.

When $n = 4$, the Dwork pencil is given by

$$x_1 x_2 x_3 x_4 (x_1 + x_2 + x_3 + x_4 + 1) - \frac{t_3}{5^5} = 0. \quad (4.43)$$

This is a family of Calabi-Yau manifolds known in the literature as the *quintic mirror family*.

As described in [14], the quintic mirror family (4.43) is fibred by quartic mirror K3 surfaces, i.e, M_2 -polarized K3-surfaces. This fibration is induced by a family of rational functions from \mathbf{P}^1 to $X_0(2)^+$, so that each quintic mirror surface is an M_2 -polarized family of K3 surfaces in the sense of the previous section. The family of functional invariants that produces this fibration structure is, according to [14]:

$$t_2 = g(t; t_3) = \frac{4^4}{5^5} t_3 \frac{t^5}{(t-1)^4}. \quad (4.44)$$

For $t_3 \notin \{0, 1, \infty\}$, the maps $g(t; t_3)$ are totally ramified (to degree 5) at $t = 0$, unramified over $t_3 = 1$, and have one simple pole at $t = \infty$, and an order four pole at $t = 1$. The maps $g(t; t_3)$ are ramified at $t = 5$ which lies over $t_2 = t_3$. The fibre over $t_3 = 1$ consists of the five roots of the following quintic polynomial:

$$w(t; t_3) = 256t_3t^5 - 3125t^4 + 12500t^3 - 18750t^2 + 12500t - 3125. \quad (4.45)$$

The discriminant of $w(t; t_3)$ is $2^{32}5^{25}t_3^3(t_3 - 1)$.

The t_3 -dependent family of Picard-Fuchs equations that describes the internal fibration structures is obtained by pulling back the hypergeometric equation ${}_3F_2(\frac{1}{4}, \frac{1}{2}, \frac{3}{4})$ along the family of rational maps $g(t; t_3)$. We compute the following expressions:

$$\frac{d^3 f}{dt^3} + P_{t_3} \frac{d^2 f}{dt^2} + Q_{t_3} \frac{df}{dt} + R_{t_3} f = 0,$$

where

$$\begin{aligned} P_{t_3} &= \frac{1152t_3t^7 + (-11520t_3 - 9375)t^6 + (13440t_3 + 131250)t^5 - 478125t^4}{t(t-1)(t-5)w(t; t_3)} \\ &+ \frac{787500t^3 - 665625t^2 + 281250t - 46875}{t(t-1)(t-5)w(t; t_3)} \\ Q_{t_3} &= \frac{816t_3t^9 + (-16320t_3 - 3125)t^8 + (114720t_3 + 75000)t^7 + (-239040t_3 - 737500)t^6}{t^2(t-1)^2(t-5)^2w(t; t_3)} \\ &+ \frac{(164400t_3 + 2700000)t^5 - 4893750t^4 + 4875000t^3 - 2687500t^2 + 750000t - 78125}{t^2(t-1)^2(t-5)^2w(t; t_3)} \\ R_{t_3} &= \frac{24t_3t^2(t-5)^3}{(t-1)^3w(t; t_3)} \end{aligned}$$

The monodromy representation for each of these Picard-Fuchs equations is obtained by analyzing the push-forward map induced by $g(t; t_3)$ and using the monodromy representation

we computed earlier. Since the original local system on $\mathbf{P}_{t_2}^1$ has order four monodromy at $t_2 = \infty$, the pull-back local system will have trivial monodromy at $t = 1$, the order-four pole. Therefore, the points $t = 1$ and $t = 5$ are apparent singularities and we have non-identity monodromy transformations at the five roots of $w(t; t_3)$, $t = 0$ and $t = \infty$. By choosing a $t_3 = \frac{1}{2}$ as a base point, we can describe the degree five cover graphically and then compute the corresponding monodromy representation; see Figure 4.10.

If we label the singular points p_1, \dots, p_7 as indicated in Figure 4.10, we can work out the braiding map by keeping track of the motion of these points as t_3 moves through the usual loops σ_0, σ_1 around 0 and 1. These motions are described in Figure 4.10, and we find that the braiding map is determined by

$$\begin{aligned} \varphi(\sigma_0) &= \beta_5^{-1} \beta_4^{-1} \beta_3^{-1} \beta_2^{-1} \beta_1^{-1} \beta_5 \beta_4 \beta_3 \beta_1^{-1} \beta_2^{-1} \beta_3^{-1} \beta_4^{-1} \beta_5^{-1} \\ \varphi(\sigma_{\frac{1}{5^5}}) &= \beta_4 \beta_5 \beta_4^{-1}. \end{aligned} \tag{4.46}$$

With the braiding action determined, we now run the Dettweiler-Wewers algorithm to compute the monodromy representation of the parabolic cohomology local system. By choosing bases appropriately, we can conjugate the representation to the following:

$$\begin{aligned} \sigma_0 &\mapsto \begin{pmatrix} 1 & 1 & 0 & 0 \\ 0 & 1 & 5 & 0 \\ 0 & 0 & 1 & 1 \\ 0 & 0 & 0 & 1 \end{pmatrix} & \sigma_1 &\mapsto \begin{pmatrix} 1 & 0 & 0 & 0 \\ -5 & 1 & 0 & 0 \\ -1 & 0 & 1 & 0 \\ -1 & 0 & 0 & 1 \end{pmatrix} \\ \sigma_\infty &\mapsto \begin{pmatrix} 1 & -1 & 5 & -5 \\ 5 & -4 & 20 & -20 \\ 1 & -1 & 6 & -6 \\ 1 & -1 & 5 & -4 \end{pmatrix} \end{aligned} \tag{4.47}$$

The Picard-Fuchs equation for the quintic mirror is the generalized hypergeometric equation ${}_4F_3(\frac{1}{5}, \frac{2}{5}, \frac{3}{5}, \frac{4}{5})$; thus, we have computed the monodromy representation for this differential equation with respect to an integral basis.

4.2.3 An Interesting Example

We close this chapter by examining an example closely related to the quartic mirror family that was previously studied by Narumiya-Shiga in [38]. This example illuminates a number of the subtleties of the subject and showcases how we can use the variation of local systems and parabolic cohomology to capture many interesting phenomena.

Let $V(a)$ denote the following elliptic surface over \mathbf{P}_t^1 :

$$V(t) : y^2 = x(x^2 + (t + \frac{1}{t} + a)x + 1). \quad (4.48)$$

As is shown in [38], for $a \notin \{0, \pm 4, \infty\}$, the elliptic fibration (4.48) has six singular fibres: there are four fibres of type I_1 located at

$$t_{1,2} = \frac{1}{2} \left(2 - a \pm \sqrt{a^2 - 4a} \right), \quad t_{4,5} = \frac{1}{2} \left(-2 - a \pm \sqrt{a^2 + 4a} \right),$$

and two fibres of type I_4^* at $t_3 = 0$ and $t_6 = \infty$. Based on the singular fibre types, it follows that each $V(a)$ is an elliptic K3 surface and that the trivial lattice has rank eighteen.

The authors proceed to compute monodromy matrices for the rank-four local system obtained by taking the orthogonal complement of the trivial lattice in $H^2(V(a), \mathbf{Z})$. This is done by choosing a basis of cycles for the complement and analyzing how they deform as a varies in loops. Of course, this is very closely related to variations of local systems and parabolic cohomology even though the authors do not make use of these notions. After they compute their 4×4 monodromy matrices, they observe that the representation is reducible: there is a one-dimensional invariant submodule that corresponds to a section of the fibration (4.48). It follows that each $V(a)$ is in fact a rank nineteen K3 surface and the authors show further that $V(a)$ is an M_2 -polarized K3 surface. We will reproduce these matrices and make some important comments using the variations of local systems framework developed in this thesis.

Choosing $a = 2$ as a base point for the deformation parameter and $t = -1$ as a base point on \mathbf{P}_t^1 , the authors of [38] pin down precisely the homological invariant with respect to the basis of loops indicated in Figure 4.11. We have

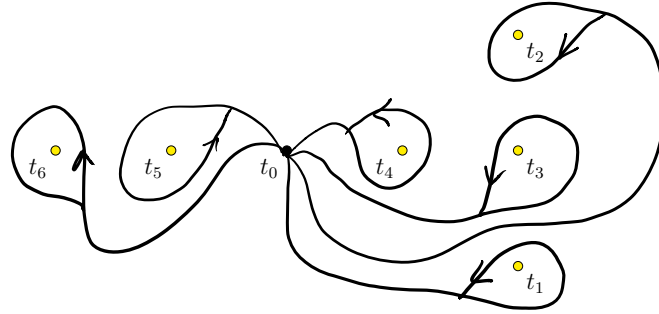
$$\gamma_1, \gamma_2 \mapsto \begin{pmatrix} 0 & -1 \\ 1 & 2 \end{pmatrix}, \quad \gamma_3 \mapsto \begin{pmatrix} -1 & 4 \\ 0 & -1 \end{pmatrix}, \quad \gamma_4, \gamma_5 \mapsto \begin{pmatrix} 2 & -1 \\ 1 & 0 \end{pmatrix}, \quad \gamma_6 \mapsto \begin{pmatrix} -1 & 0 \\ -4 & -1 \end{pmatrix}. \quad (4.49)$$

As a varies in $\mathbf{P}_a^1 - \{0, \pm 4, \infty\}$, we consider the corresponding variation of this local system. Using the loops $\delta_1, \delta_2, \delta_3, \delta_4$ as indicated in Figure 4.11, we once again carefully work out the braiding map. The motion of the poles is described in Figure 4.12. We see that

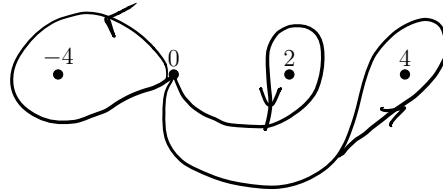
$$\varphi(\delta_1) = (\beta_1^{-1} \beta_2^{-1} \beta_3^{-1} \beta_1 \beta_2) \beta_3 (\beta_1^{-1} \beta_2^{-1} \beta_3^{-1} \beta_1 \beta_2)^{-1} \quad (4.50)$$

$$\varphi(\delta_2) = \beta_1 \beta_4 \quad (4.51)$$

$$\varphi(\delta_3) = (\beta_3^{-1} \beta_2^{-1} \beta_4 \beta_3) \beta_2^{-1} (\beta_3^{-1} \beta_2^{-1} \beta_4 \beta_3)^{-1} \quad (4.52)$$



(a) The loops γ_i .



(b) The loops δ_i .

Figure 4.11: The initial configuration.

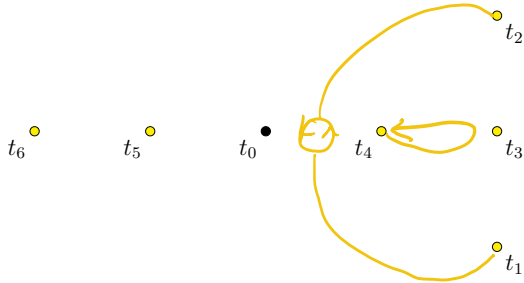
Running the Dettweiler-Wewers algorithm, we obtain the following monodromy representation:

$$\begin{aligned}
 \delta_1 \mapsto & \begin{pmatrix} 0 & 1 & 0 & -2 \\ 1 & 0 & 0 & 2 \\ 2 & -2 & 1 & 4 \\ 0 & 0 & 0 & 1 \end{pmatrix} & \delta_2 \mapsto & \begin{pmatrix} 0 & 1 & 0 & 0 \\ 1 & 0 & 0 & 0 \\ 0 & 0 & 0 & 1 \\ 0 & 0 & 1 & 0 \end{pmatrix} \\
 \delta_3 \mapsto & \begin{pmatrix} 1 & 0 & 0 & 0 \\ 4 & 1 & -2 & 2 \\ 2 & 0 & 0 & 1 \\ -2 & 0 & 1 & 0 \end{pmatrix} & \delta_4 \mapsto & \begin{pmatrix} 1 & 0 & 0 & 2 \\ 8 & -3 & 2 & 12 \\ 4 & -2 & 1 & 8 \\ -2 & 0 & 0 & -3 \end{pmatrix}
 \end{aligned} \tag{4.53}$$

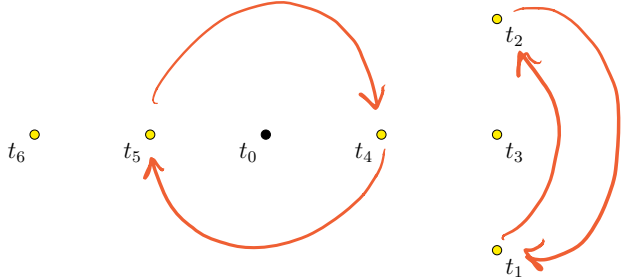
If we conjugate these monodromy matrices by the matrix

$$L = \begin{pmatrix} 0 & 0 & 1 & -1 \\ -1 & -1 & -1 & 1 \\ -1 & 0 & -1 & 0 \\ 1 & -1 & 0 & 0 \end{pmatrix},$$

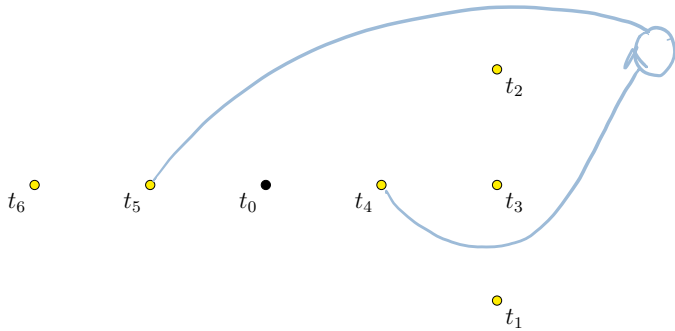
then we obtain the four monodromy matrices (more precisely, their transposes) that appear in [38].



(a) The braid $\varphi(\delta_1)$.



(b) The braid $\varphi(\delta_2)$.



(c) The braid $\varphi(\delta_3)$.

Figure 4.12: The motion of poles.

This monodromy representation is not irreducible. Indeed, the vector $v = (1, -1, 1, -1)$ is fixed by the monodromy transformations corresponding to δ_1, δ_3 and it is sent to $-v$ by the other two transformations. Thus, the parabolic cohomology local systems decomposes into the sum of a one-dimensional representation and an irreducible rank-three local system. From this, we deduce the existence of an infinite-order section to the fibration (4.48), and that the K3-surfaces have Picard rank nineteen. The fact that each $V(a)$ is in fact M_2 -polarized is shown in [38]. The 3×3 monodromy transformations corresponding to the transcendental lattices are as follows:

$$\begin{aligned} \delta_1 &\mapsto \begin{pmatrix} -2 & 3 & -2 \\ 3 & -2 & 2 \\ 6 & -6 & 5 \end{pmatrix} & \delta_2 &\mapsto \begin{pmatrix} 0 & 1 & 0 \\ 1 & 0 & 0 \\ 1 & -1 & 1 \end{pmatrix} \\ \delta_3 &\mapsto \begin{pmatrix} 1 & 0 & 0 \\ 6 & -1 & 0 \\ 3 & -1 & 1 \end{pmatrix} & \delta_4 &\mapsto \begin{pmatrix} 3 & -2 & 2 \\ 20 & -15 & 14 \\ 12 & -10 & 9 \end{pmatrix} \end{aligned} \tag{4.54}$$

Remark 24. Note that the rank one local system corresponding to the infinite-order section is *not* the trivial local system since δ_2, δ_4 acted non-trivially. It follows that the family $V(a)$ is a family of M_2 -polarized K3 surfaces that is *not* an M_2 -polarized family as defined in the previous section.

Remark 25. As is explained in [38], the elliptic surface $V(a)$ and $V(-a)$ are isomorphic via an explicit birational map. Using this, they produce an elliptic fibration structure on the family \mathcal{X}_2 for which there is an infinite-order section. Comparing this fibration with the fibration on \mathcal{X}_2 described in the previous section, we have an explicit example of two elliptic fibration structures for which the parabolic cohomology groups are different. Specifically, the parabolic cohomology local system induced by this quotient will have rank four, but will be reducible—the one-dimensional piece corresponding to the section will be the trivial local system. Nonetheless, they both contain the same irreducible rank three piece corresponding to the transcendental lattice.

Chapter 5

Isomonodromic Deformations

The original motivation of this thesis was to enhance the notion of Doran’s geometric isomonodromic deformations to a structure that was more sensitive to some of integral structures involved. Chapters 3 and 4 have demonstrated that the notion of geometric variations of local systems is a powerful tool that allows us to “replace” a family of fibrations by a family of local systems, but retain much of the structures we care about. In this chapter, we discuss the theory of isomonodromic deformations and describe how they tie in to the variation of local systems framework. We begin by discussing isomonodromy in general, and then the Schlesinger equations, which describe a particular kind of isomonodromic deformation. It is shown that geometric variations of local systems give rise to solutions of the Schlesinger equations; this solidifies the fact that geometric variations of local systems are the true “successor” to the notion of geometric isomonodromic deformations.

5.1 Isomonodromy

We begin by reviewing some of the formalism of isomonodromic deformations, specifically the Malgrange formalism discussed in [15][35]. We start with some local theory; consider a family of Fuchsian systems

$$\frac{dy}{dx} = \left(\sum_{i=1}^m \frac{A_i(t)}{x - t_i} \right) y, \quad \sum_{i=1}^m B_i(t) = 0$$

depending holomorphically on the parameter $t = (t_1, \dots, t_m)$ in a small disk around $t^0 = (t_1^0, \dots, t_m^0)$. The family is called isomonodromic if the monodromy representation does not depend on the deformation parameter t . Thus, for each t there is a fundamental matrix $Y(x, t)$ that solves the corresponding system and the monodromy matrices do not vary as

we vary t . Such a family is called an *isomonodromic family of matrices*. Set

$$S = \mathbf{P}^1 \times D(t^0) - \cup\{(x - t_i) = 0\}.$$

Then, a solution to such a system is a matrix $Y(x, t)$ depending holomorphically on both arguments. Such a solution will define a monodromy representation

$$\pi_1(S, (x_0, t^0)) \rightarrow \mathrm{GL}_p(\mathbf{C}).$$

If we let

$$\omega = \frac{dY(x, t)}{Y(x, a)},$$

then ω is a single-valued 1-form and so we may consider it as a 1-form on S . For each $g \in \pi_1(S, (x_0, t^0))$, we find

$$g^*\omega = dg^*Y(X, t)g^*Y^{-1}(x, t) = \omega.$$

Then, the Pfaffian system $dy = \omega y$ on S is completely integrable and, for each fixed $t \in D(t^0)$, it agrees with Fuchsian system. We have the following result:

Theorem ([5], Theorem 2). *The family of Fuchsian systems is isomonodromic if and only if there exists a matrix differential 1-form ω on S such that:*

1. *The 1-form can be expressed as*

$$\omega = \sum_{i=1}^m \frac{B_i(t)}{x - t_i} dx,$$

for each fixed $t \in D(t^0)$;

2. $d\omega = \omega \wedge \omega$.

More generally, we will consider meromorphic connections with logarithmic poles. Let X be a complex manifold, let Y be a smooth codimension one sub-manifold, and let E be a rank n holomorphic vector bundle over X and ∇ a flat connection on $X - Y$. The connection ∇ is called meromorphic over Y if there exists for each $y \in Y$ a neighbourhood U of y such that $E|_U$ is trivial and the connection form of ∇ with respect to a basis of sections is meromorphic on U . Further, the connection is said to have a *logarithmic pole along Y* if, in a coordinate chart (t_1, \dots, t_r) with $Y = \{t_1 = 0\}$, the connection form is given by

$$\Omega = A_1 \frac{dt_1}{t_1} + A_2 dt_2 + \dots + A_r dt_r,$$

with the A_i holomorphic.

The primary case we consider is when $X = \mathbf{P}^1$ and $Y = \{t_1^0, \dots, t_{m-1}^0, \infty\}$. Use x as parameter on \mathbf{P}^1 and consider a differential equation over X with regular singularities, i.e., a holomorphic vector bundle E^0 over X with a flat connection ∇^0 of $E|_{X-Y}$ meromorphic over Y . If the differential equation is given by

$$\frac{dy}{dx} = \left(\sum_{i=1}^m \frac{A_i(t)}{x - t_i} \right) y,$$

then the connection ∇^0 is defined by

$$\nabla(y) = dy - \left(\sum_{i=1}^m \frac{A_i(t)}{x - t_i} \right) y dx.$$

We see that this has logarithmic poles at each $x = t_i$ and also at ∞ .

Now we want to consider a global picture of isomonodromic deformations of flat connections. Let S be a complex variety, and consider deformation functions

$$t_i: S \rightarrow \mathbf{C}, \quad 1 \leq i \leq m-1$$

that describe the motion of the mobile poles. Fixing a base point $s_0 \in S$, set $t_i^0 = t_i(s_0)$. We will assume that the values of the t_i are pair-wise distinct complex numbers.

Let $X = \mathbf{P}^1 \times S$ and $Y \subseteq X$ be the smooth codimension one sub-manifold given by

$$Y = Y_1 \cup \dots \cup Y_{m-1} \cup Y_\infty\},$$

where

$$Y_i = \{(x, s) \mid (x, s) \in X, x = t_i(s)\},$$

and

$$Y_\infty = \{\infty\} \times S.$$

Definition 24. An *isomonodromic deformation*

$$(E, \nabla) \text{ of the pair } (E^0, \nabla^0)$$

with deformation space S , deformation functions t_i and base point s_0 is given by

1. a holomorphic vector bundle E over $X = \mathbf{P}^1 \times S$ of rank n ;
2. an integrable connection ∇ of $E|_{X-Y}$, meromorphic over Y for which the restriction

to $\mathbf{P}^1 \times \{s_0\}$ is our initial system

Remark 26. From this definition, it is clear that an isomonodromic deformation gives rise to a variation of local systems in the sense of [12] by considering the local system naturally attached to the flat connection.

5.2 The Schlesinger Equations

In this section, we consider a particular class of isomonodromic deformations known as *Schlesinger deformations*. Consider an isomonodromic deformation of the initial rank m Fuchsian system

$$\frac{dy}{dx} = \left(\sum_{i=1}^r \frac{A_i^0}{x - t_i^0} \right) y, \quad A_i^0 = A_i(t^0), \quad (5.1)$$

given by the 1-form

$$\omega_S = \sum_{i=1}^r \frac{A_i(t)}{x - t_i} d(x - t_i),$$

and assume the systems are *non-resonant*, which means that the eigenvalue differences of the matrices A_i are non-integers. We will say more about this condition later. As t varies, the isomonodromy condition, $d\omega_S = \omega_S \wedge \omega_S$, comes down to

$$dA_i(t) = - \sum_{j \neq i, j=1}^r \frac{[A_i(t), A_j(t)]}{t_i - t_j} d(t_i - t_j).$$

Expanding this out, we obtain an equivalent system of non-linear partial differential equations, known as the *Schlesinger equations*:

$$\frac{\partial A_i}{\partial t_j} = \frac{[A_i, A_j]}{t_i - t_j}, \quad \frac{\partial A_i}{\partial t_i} = - \sum_{i \neq j, j=1}^r \frac{[A_i, A_j]}{t_i - t_j}. \quad (5.2)$$

Here, the variable t varies in \mathcal{O}^r , the configuration space of r points on the Riemann sphere. Note the difference from \mathcal{O}_r , which classifies *subsets of r distinct points* on the Riemann sphere. In the literature, it is common to fix $t_r = \infty$, in which case we instead work with $\mathbf{C}^{r-1} - \Delta$, the configuration space of $r - 1$ points in the plane.

Because the Schlesinger equations enjoy the Painlevé property, any solution to (5.2) in a neighbourhood of the initial point $t^0 = (t_1^0, \dots, t_m^0)$ admits an analytic continuation to a holomorphic function on the universal cover [26]. Concretely, a solution to the Schlesinger equations is a collection of matrices $A_i(\tilde{t})$ depending on $\tilde{t} \in \tilde{S}$ for which the corresponding family of Fuchsian systems (5.1) is an isomonodromic deformation of the initial system with

deformation space equal to \tilde{S} .

The fundamental group $\pi_1(\mathcal{O}^r, t^0) \cong \mathcal{P}_r$, which is the *pure Hurwitz braid group*, acts on $\tilde{\mathcal{O}}^r$ by deck-transformations, and thus acts on the set of matrices as well. Let Γ be the kernel of this action so that for each $\gamma \in \Gamma$, we have

$$A_i^\gamma(\tilde{t}) = A_i(\tilde{t}), \quad i = 1, \dots, r.$$

Then, the functions A_i can be viewed as functions on the quotient $\mathcal{O}_\Gamma := \Gamma \backslash \tilde{\mathcal{O}}^r$, and we have a *global isomonodromic deformation* with deformation space \mathcal{O}_Γ and deformation functions $t_i: \tilde{\mathcal{O}}_\Gamma \rightarrow \mathcal{O}^r \rightarrow \mathbf{C}$. We refer to the cover $\mathcal{O}_\Gamma \rightarrow \mathcal{O}^r$ as the *Schlesinger cover* associated to the solution. If Γ is a subgroup of finite-index, then we call the solution a finite-branching solution. If the A_i are algebraic functions of $t \in \mathcal{O}^r$, then it is clear that the A_i analytically continue to produce a finite-branching solution. Results of Cousin [10] show that the converse is true: if we have a finite branching solution, then the matrices A_i are algebraic functions of t . We summarize this discussion as follows:

Proposition 17. *Solutions to the Schlesinger equations (5.2) with initial system (5.1) are in one-to-one correspondence with variations of the initial local system parameterized by the universal cover of the configuration space \mathcal{O}^r for which the divisor $D(t)$ is given by (t_1, \dots, t_r) .*

Algebraic solutions to the Schlesinger equations are in one-to-one correspondence with variations of the above form that factor through a finite sub-cover of the universal cover of \mathcal{O}^r .

In the beginning of this section, we assumed that the Fuchsian systems were *non-resonant*. This is an important condition in the theory of isomonodromic deformations. Indeed, there exist *resonant* isomonodromic deformations that do *not* solve the Schlesinger equations—such deformations are known as non-Schlesinger deformations. In order to account for this, a stronger notion of isomonodromy known as *isoprincipality* was developed in [27]. Every isoprincipal deformation of Fuchsian systems is isomonodromic, but not conversely; in the non-resonant case, the two notions agree with each other. Solutions to the Schlesinger equations correspond precisely to isoprincipal deformations. Thus, an isomonodromic deformation of Fuchsian systems is either isoprincipal, or else it is a non-Schlesinger deformation. This subtle distinction is important to us because the isomonodromic deformations that come from our geometric setting are resonant systems in general.

The original intent of Doran's work in [15] was to construct interesting solutions to the Schlesinger equations in the form of *geometric isomonodromic deformations*. As has been demonstrated in this thesis, considering the differential equations coming from periods up to projective normal form has the effect of eliminating a lot of interesting geometric information.

In contrast, the formalism of variation of local systems applied to families of fibred manifolds is sensitive enough to capture much of the interesting structures that vary in the family. Thus, the variations of geometric local systems considered in this thesis should be considered as a natural successor to the geometric isomonodromic deformations considered by Doran.

As far as finding interesting solutions to the Schlesinger is concerned, the framework developed in this thesis is sufficient for these purposes. Concretely, if \mathcal{V} is a variation of geometric local systems corresponding to a family of Picard-Fuchs equations, then, more than being an isomonodromic family of differential equations, the family is *isoprincipal*, in the sense of [27], as was shown in [32]. It follows that \mathcal{V} describes a solution to a particular Schlesinger equation due to the results in [27].

To be more precise, it is not, in general, the Schlesinger equations that will be relevant, but rather a system of differential equations that are derived from the Schlesinger equations. Indeed, given a variation of geometric local systems, one needs to write down the deformation functions that describe the motion of each pole, rather than work with the description of the divisor, as we have done throughout this work. Even after this is done, the number of poles may disagree with the number of deformation parameters in the Schlesinger equations, and so we may have to consider a pull-back of the Schlesinger equations.

For example, consider the variation of geometric local systems corresponding to the M_2 -polarized K3 surface-fibration on the quintic mirror family considered in Chapter 4. The corresponding isoprincipal deformation of Fuchsian systems has seven singularities, but the motion of the poles is described only in terms of one parameter. Therefore, rather than solving the Schlesinger equations for rank three Fuchsian systems with seven singular points, the relevant system of differential equations is the pull back of the Schlesinger equations along the map that sends the deformation parameter to the ordered 7-tuple of singular points. Since the five mobile poles in this example were roots of a quintic, we cannot really hope to do this explicitly, but this is enough for our purposes.

The following summarizes the above discussion:

Proposition 18. *Let \mathcal{V} be a geometric variation of local systems. Then \mathcal{V} gives rise to a solution to an isomonodromic deformation equation derived from the Schlesinger system. In particular, isomonodromic deformations arising from geometry are Schlesinger deformations.*

5.3 The Sixth Painlevé Equation

Over the course of this thesis, we have seen many different examples of geometric variations of local systems and each of them gives rise to solutions to different isomonodromic deformation equations. We end the thesis by discussing one particularly well-known isomonodromic

deformation equation derived from the Schlesinger equations known as the sixth Painlevé equation. This equation arises by considering isomonodromic deformations of rank two Fuchsian systems for which the poles are normalized to be located at $(0, t, 1, \infty)$ for $t \notin \{0, 1, \infty\}$:

$$\frac{dy}{dx} = \left(\frac{A_0}{x} + \frac{A_t}{x-t} + \frac{A_1}{x-1} \right) y = A(x, t)y, \quad (5.3)$$

and for which A_0, A_t, A_1 and $A_\infty = -(A_0 + A_t + A_1)$ are all traceless.

As explained in [34], if the top-right entry of $A(t)$ has a unique zero λ that depends on t . It can be shown that solving the Schlesinger equations subject to these normalizations is equivalent to solving the following differential equation for λ and t :

$$\begin{aligned} \frac{d^2\lambda}{dt^2} &= \frac{1}{2} \left(\frac{1}{\lambda} + \frac{1}{\lambda-1} + \frac{1}{\lambda-t} \right) \left(\frac{d\lambda}{dt} \right)^2 - \left(\frac{1}{t} + \frac{1}{t-1} + \frac{1}{\lambda-t} \right) \frac{d\lambda}{dt} \\ &+ \frac{\lambda(\lambda-1)(\lambda-t)}{t^2(t-1)^2} \left(\alpha + \beta \frac{t}{\lambda^2} + \gamma \frac{t-1}{(\lambda-1)^2} + \delta \frac{t(t-1)}{(\lambda-t)^2} \right), \end{aligned}$$

where $\alpha, \beta, \gamma, \delta$ are parameters that depend on the eigenvalues θ_i of the residues A_i .

By fixing a particular isomonodromic deformation equation, like the one above, it is a reasonable question to ask: what is the totality of solutions that come from geometry? The answer to this question was answered by Doran in [21], in which he shows that the only solutions that come from geometry are the ones derived from the five families of rational elliptic surfaces in Herfurtner's classification that do not have I_0^* fibres. If we relax the condition that the residue matrices A_i must be traceless, which amounts to considering their projective normal forms, then we obtain a whole slew of solutions to corresponding Schlesinger equation from all twelve of the families of rational elliptic surfaces found by Herfurtner. Combining the structural results on Stiller's K -equations with Doran's classification of geometric solutions to Painlevé VI, we conclude that the only solutions coming from geometry to this slightly less constrained problem are still the ones that we can derive from Herfurtner's list.

There are lots of algebraic solutions to Painlevé VI that do not come from geometry. In fact, the problem of classifying all the algebraic solutions to Painlevé VI is one that inspired many bodies of work, most notably the works of Iwasaki et. al. [25, 24], Boalch [?, 3, 4], Dubrovin-Mazzocco [?, 36], Hitchin [?], Kitaev [28], and Doran [15], to name a few, with a complete classification of the solutions, up to birational symmetries of the Painlevé VI equation, being obtained by Lisovsky-Tyhky in [33]. The classification naturally breaks into one discrete family of so-called Cayley solutions, three families of solutions (solutions that solve Painlevé VI for a continuous deformation of the $(\alpha, \beta, \gamma, \delta)$ parameters), and forty-five exceptional solutions. An interesting fact that appears by looking at the classification

is that even though the solutions coming from geometry are relatively few, the solutions derived in this manner all lied in one of the continuous families of solutions. So, while the classification of geometric isomonodromic deformations may not shed light on the full classification problem of algebraic solutions to Schlesinger equations, it may well be the case that the solutions coming from geometry will generate interesting sub-classes of solutions, as is what happened for Painlevé VI.

To the authors knowledge, the formalism of variation of local systems has not yet been applied to solutions of isomonodromic deformations. For example, we have already described how algebraic solutions to the Schlesinger equations correspond to variations of local systems parameterized by finite covers of the configuration space. One may therefore ask: what is the structure of the parabolic cohomology of the variation on the corresponding Schlesinger cover? In the context of Painlevé VI, the Schlesinger cover reduces to a finite covering $t: S \rightarrow \mathbf{P}^1 - \{0, 1, \infty\}$, i.e., a Belyi map; in this case, we refer to the curve S as the *Painlevé curve* associated to the solution. Since a complete classification of algebraic solutions to Painlevé VI is known, an interesting problem would be to determine to what extent the parabolic cohomology of a solution classifies the solution. As we saw with the five families on Herfurtners list, the parabolic cohomology changes quite a bit if we modify the projective equivalence class of the initial monodromy representation. Indeed, we observed that for each of the five families, applying a quadratic twist at two of the monodromies increased the rank of parabolic cohomology. It follows already that parabolic cohomology is therefore more sensitive than the equivalence relation that is defined in terms of birational symmetries of the Painlevé equation.

We close this section by working out one example of computing the parabolic cohomology of an algebraic Painlevé solution to demonstrate the method. We consider the first exceptional solution to Painlevé VI, using notation in [33]. This solution was originally constructed by Boalch in [4]. The corresponding Painlevé curve has genus 0 and the corresponding Belyi map is

$$t = 27 \frac{(5s - 2)^2}{(s + 5)(4s^2 - 5s + 10)^2}, \quad t - 1 = -\frac{(s + 2)^3(4s - 7)^2}{(s + 5)(4s^2 - 5s + 10)^2}.$$

By setting

$$\lambda = 2 \frac{(s^2 + s + 7)(5s - 2)}{s(s + 5)(4s^2 - 5s + 10)},$$

one can check explicitly that $\lambda = \lambda(t)$ solve Painlevé VI for parameters $(\alpha, \beta, \gamma, \delta) = (\frac{2}{18}, -\frac{2}{25}, \frac{1}{50}, \frac{4}{9})$. The initial monodromy representation can be calculated from the data in [33] to produce the 4-tuple of 2×2 monodromy matrices $\mathbf{g} = (g_0, g_t, g_1, g_\infty)$; each matrix lies in $\mathrm{SL}_2(\mathbf{Q}(\zeta))$ where ζ is a primitive 30-th root of unity; we do not display the tuple

here. We do note that each of the transformations is diagonalizable and does not have 1 as eigenvalue, from which it follows that the rank of the corresponding parabolic cohomology group is equal to four.

By using the techniques found in [4] and the explicit description of the Belyi-map, it is not difficult to find generators for the corresponding fundamental group and their images under the braiding map. In this case, $S = \mathbf{P}^1 - \{\frac{2}{5}, -2, \frac{7}{4}, -5, \frac{1}{8}(5 \pm 3i\sqrt{15}), \infty\}$ is the Riemann sphere minus 7 points. For an appropriate choice of generating loops $\gamma_1, \dots, \gamma_7$, the braiding map is computed to be

$$\begin{aligned}\gamma_1 &\mapsto \beta_2^{-2}\beta_1^{-1} \\ \gamma_2 &\mapsto \beta_2^6 \\ \gamma_3 &\mapsto \beta_2^2\beta_1^4\beta_2^{-2} \\ \gamma_4 &\mapsto \beta_2^2\beta_1^2(\beta_2^{-2}\beta_1^{-2})^2\beta_1^{-2}\beta_2^{-1} \\ \gamma_5 &\mapsto \beta_2^2\beta_1^2\beta_2^4\beta_1^{-2}\beta_2^{-2} \\ \gamma_6 &\mapsto \beta_2^2(\beta_2^{-2}\beta_1^{-2})^2\beta_2\end{aligned}$$

Applying the Dettweiler-Wewers algorithm to compute the monodromy representation for parabolic cohomology, we obtain a representation for which γ_1 corresponds to an order six transformation and the other generators map to involutions. They generate an infinite group of transformations in $\mathrm{SL}_4(\mathbf{C})$.

If we apply birational symmetries of Painlevé VI, the rank of parabolic cohomology does not change, but the corresponding monodromy representations are not globally conjugate to each other (though the tuple of transformations obtained behaves similarly to that described above). So, while the rank is invariant under the birational transformations, parabolic cohomology appears to be sensitive enough to distinguish the solutions.

The purpose of this example was simply to demonstrate some of the things that can happen, as well as to illustrate the fact that the methods of Dettweiler-Wewers are easily applicable in this situation. A complete investigation of the parabolic cohomology local systems corresponding to algebraic solutions to Painlevé VI constitutes work in progress.

Chapter 6

Conclusion/Future Work

Throughout this thesis we have demonstrated that the formalism of geometric variations of local systems is the natural framework with which to study varying “internal” fibration structures on a family of algebraic varieties equipped with an “external” fibration. Such variations of local systems are the natural generalization of Doran’s geometric isomonodromic deformations tuned to a setting in which we wish to remain sensitive to the underlying integral structures of our geometric families. More than just developing formalism, this thesis has demonstrated that it is possible to implement the Dettweiler-Wewers algorithm for many interesting families of internal fibration structures in order to compute, in a tractable manner, the monodromy representation of the corresponding local system of parabolic cohomology groups which, in turn, gives us information about the external fibration. Because the algorithm is not tethered to local systems defined over fields, we are able to work with the \mathbf{Z} -modules of cohomology groups and produce the corresponding \mathbf{Z} -valued monodromy matrices.

The next natural step is to layer on the additional structure induced by the polarizations of the variations of Hodge structures that we are studying. That is, given the *lattice* structure on each of the varying internal variations of Hodge structure, we would like to produce the lattice structure on the associated parabolic cohomology groups. Techniques to do this are described in a follow-up paper by Dettweiler-Wewers [?] and applying this in our geometric setting constitutes work in-progress.

In addition to the full exploration of the K3 surface families that one can derive from Herfurtner’s list by quadratic twist and the examination of the parabolic cohomology invariant in the context of the classification of algebraic solutions to the sixth Painlevé equation, there are two other immediate applications of the techniques developed here that will be worked on in the near future. Firstly, it is natural to continue the study of Calabi-Yau threefolds fibred by M_n -polarized K3 surfaces that served to motivate this thesis. The authors of [17]

indicated that there are many interesting families of such threefolds and indicated that certain Hurwitz curves will play a central role in the moduli-theory of such threefolds. The geometric variation of local systems framework that we developed in this thesis is that natural formalism to investigate the properties of these families. Since the families considered in [17] are all determined by families of functional invariants, it is evident that the techniques used in this thesis will allow us to perform concrete computations in this context in order to help inform the general theory. Secondly, we will take a closer look at the Dwork pencil and the iterative construction used in [19] to produce the Picard-Fuchs equation for the family of Calabi-Yau n -folds from the family of Calabi-Yau $n - 1$ -folds. In each step of their iterative construction, the internal fibration structures are determined by functional invariants of very special forms. Our hope is that we can provide an iterative construction that computes the integral monodromy matrices for each step in the Dwork-family.

Bibliography

- [1] Amnon Besser and Ron Livné. Picard-Fuchs equations of families of QM abelian surfaces. *arXiv:1202.2808*, pages 1–18, February 2012.
- [2] Joan S. Birman. *Braids, Links, and Mapping Class Groups*. Princeton University Press, 1975.
- [3] Philip Boalch. Some explicit solutions to the Riemann-Hilbert problem. *arXiv:math/0501464*, pages 1–24, January 2005.
- [4] Philip Boalch. The fifty-two icosahedral solutions to Painlevé VI. *Journal für die reine und angewandte Mathematik (Crelles Journal)*, (596):183–214, 2006.
- [5] A. A. Bolibruch. On Isomonodromic Deformations of Fuchsian Systems. *Journal of Dynamical and Control Systems*, 3(4):589–604, October 1997.
- [6] James Carlson, Stefan Müller-Stach, and Chris Peters. *Period Mappings and Period Domains*. Cambridge Studies in Advanced Mathematics. Cambridge University Press, 2 edition, August 2017.
- [7] A. Clingher, C. F. Doran, J. Lewis, and U. Whitcher. Normal Forms, K3 Surface Moduli, and Modular Parametrizations. In *Groups and Symmetries, Proceedings of the CRM Conference in Honor of John McKay*, volume 47, pages 81–98. December 2007.
- [8] Adrian Clingher and Charles Doran. Modular invariants for lattice polarized K3 surfaces. *The Michigan Mathematical Journal*, 55(2):355–393, August 2007.
- [9] Adrian Clingher, Charles F. Doran, Jacob Lewis, Andrey Y. Novoseltsev, and Alan Thompson. The 14th case VHS via K3 fibrations. In *Recent Advances in Hodge Theory: Period Domains, Algebraic Cycles, and Arithmetic*, (London Mathematical Society Lecture Note Series, pages 165–228. December 2016.

- [10] Gaël Cousin. Algebraic isomonodromic deformations of logarithmic connections on the Riemann sphere and finite braid group orbits on character varieties. *Mathematische Annalen*, 367(3):965–1005, 2017.
- [11] Pierre Deligne. *Equations Differentielles a Points Singuliers Reguliers*. Lecture Notes in Mathematics. Springer-Verlag, Berlin Heidelberg, 1970.
- [12] Michael Dettweiler and Stefan Wewers. Variation of local systems and parabolic cohomology. *Israel Journal of Mathematics*, 156(1):157, December 2006.
- [13] Igor V. Dolgachev. Mirror symmetry for lattice polarized K3 surfaces. *Journal of Mathematical Sciences*, 81(3):2599–2630, February 1996.
- [14] C. F. Doran, A. Harder, A. Y. Novoseltsev, and A. Thompson. Calabi–Yau threefolds fibred by mirror quartic K3 surfaces. *Advances in Mathematics*, 298:369–392, August 2016.
- [15] Charles F. Doran. Algebraic and Geometric Isomonodromic Deformations. *Journal of Differential Geometry*, 59(1):33–85, September 2001.
- [16] Charles F. Doran, Andrew Harder, Andrey Y. Novoseltsev, and Alan Thompson. Families of Lattice Polarized K3 Surfaces with Monodromy. *International Mathematics Research Notices*, 2015(23):12265–12318, January 2015.
- [17] Charles F. Doran, Andrew Harder, Andrey Y. Novoseltsev, and Alan Thompson. Calabi–Yau threefolds fibred by high rank lattice polarized K3 surfaces. *arXiv:1701.03279 [math]*, January 2017.
- [18] Charles F. Doran, Andrew Harder, and Alan Thompson. Hodge Numbers from Picard–Fuchs Equations. *Symmetry, Integrability and Geometry: Methods and Applications*, 13(45):23, December 2017.
- [19] Charles F. Doran and Andreas Malmendier. Calabi–Yau manifolds realizing symplectically rigid monodromy tuples. *arXiv:1503.07500 [math]*, March 2015.
- [20] Charles F. Doran and John W. Morgan. Mirror Symmetry and Integral Variations of Hodge Structure Underlying One Parameter Families of Calabi–Yau Threefolds. In *Mirror Symmetry V: Proceedings of the BIRS Workshop on Calabi–Yau Varieties and Mirror Symmetry*, pages 517–538. May 2007.

- [21] Charles Francis Doran. *Picard-Fuchs Uniformization and Geometric Isomonodromic Deformations: Modularity and Variation of the Mirror Map*. Ph.D., Harvard University, United States – Massachusetts, 1999.
- [22] Phillip A. Griffiths. The Residue Calculus and some Transcendental Results in Algebraic Geometry, I*. *Proceedings of the National Academy of Sciences of the United States of America*, 55(5):1303–1309, May 1966.
- [23] Stephan Herfurtner. Elliptic surfaces with four singular fibres. *Mathematische Annalen*, 291(2):319–342, 1991.
- [24] Michi-aki Inaba, Katsunori Iwasaki, and Masa-Hiko Saito. Dynamics of the Sixth Painlevé Equation. *Séminaires et Congrès*, 14:103–167, 2006.
- [25] Katsunori Iwasaki. On Algebraic Solutions to Painlevé VI. In *A Contribution to the Proceedings of the Conference on Exact WKB Analysis and Microlocal Analysis in RIMS, Kyoto*, pages 1–16. September 2008.
- [26] Katsunori Iwasaki, Hironobu Kimura, Shun Shimemura, and Masaaki Yoshida. *From Gauss to Painlevé: A Modern Theory of Special Functions*. Aspects of Mathematics. Vieweg+Teubner Verlag, 1991.
- [27] Victor Katsnelson and Dan Volok. Deformations of Fuchsian Systems of Linear Differential Equations and the Schlesinger System. *Mathematical Physics, Analysis and Geometry*, 9:135–186, May 2006.
- [28] A. V. Kitaev. Dessins d’Enfants, Their Deformations and Algebraic the Sixth Painlevé and Gauss Hypergeometric Functions. *arXiv:nlin/0309078*, September 2003.
- [29] K. Kodaira. On Compact Complex Analytic Surfaces, I. *Annals of Mathematics*, 71(1):111–152, 1960.
- [30] K. Kodaira. On Compact Analytic Surfaces: II. *Annals of Mathematics*, 77(3):563–626, 1963.
- [31] K. Kodaira. On the Structure of Compact Complex Analytic Surfaces, III. *American Journal of Mathematics*, 90(1):55–83, 1968.
- [32] Jacob Lewis. *Elliptic and K3 Surfaces: Normal Forms, Deformations, and Applications*. Ph.D., University of Washington, United States – Washington, 2010.

- [33] Oleg Lisovyy and Yuriy Tykhyy. Algebraic solutions of the sixth Painlevé equation. *Journal of Geometry and Physics*, 85:124–163, November 2014.
- [34] Gilbert Mahoux. Introduction to the Theory of Isomonodromic Deformations of Linear Ordinary Differential Equations with Rational Coefficients. In *The Painlevé Property*, CRM Series in Mathematical Physics, pages 35–76. Springer, New York, NY, 1999.
- [35] B. Malgrange. Sur les déformations isomonodromiques. I. Singularités régulières. *Cours de l'institut Fourier*, 17:1–26, 1982.
- [36] Marta Mazzocco. Picard and Chazy Solutions to the Painlevé VI Equation. *Mathematische Annalen*, 321:157–195, 2001.
- [37] Rick Miranda, Università di Pisa, and Dipartimento di matematica. *The Basic Theory of Elliptic Surfaces: Notes of Lectures*. ETS Editrice, Pisa, 1989. OCLC: 25560032.
- [38] Norihiko Narumiya and Hironori Shiga. The mirror map for a family of K3 surfaces induced from the simplest 3-dimensional reflexive polytope. In *Proceedings on Moonshine and Related Topics*, pages 139–161, Montréal, QC, 1999, December 2001.
- [39] K Oguiso and Tetsuji Shioda. The Mordell-Weil lattice of a rational elliptic surface. *Comment. Math. Univ. St. Pauli*, 40, January 1991.
- [40] Matthias Schuett and Tetsuji Shioda. Elliptic Surfaces. In *Algebraic Geometry in East Asia-Seoul 2008*, number 60 in Advanced Studies in Pure Mathematics, pages 51–160. 2010.
- [41] Peter F. Stiller. Elliptic Curves Over Function Fields and the Picard Number. *American Journal of Mathematics*, 102(4):565–593, 1980.
- [42] Peter F. Stiller. Differential equations associated with elliptic surfaces. *Journal of the Mathematical Society of Japan*, 33(2):203–233, April 1981.
- [43] Peter F. Stiller. The Picard numbers of elliptic surfaces with many symmetries. *Pacific Journal of Mathematics*, 128(1):157–189, 1987.
- [44] Alan Thompson, Sara Angela Filippini, and Helge Ruddat. An Introduction to Hodge Structures. In Radu Laza, Matthias Schütt, and Noriko Yui, editors, *Calabi-Yau Varieties: Arithmetic, Geometry and Physics: Lecture Notes on Concentrated Graduate Courses*, Fields Institute Monographs. Springer-Verlag, New York, 2015.

- [45] Steven Zucker. Hodge Theory with Degenerating Coefficients: L2 Cohomology in the Poincare Metric. *Annals of Mathematics*, 109(3):415–476, 1979.
- [46] Steven Zucker and David A. Cox. Intersection Numbers of Sections of Elliptic Surfaces. *Inventiones mathematicae*, 53:1–44, 1979.

Appendix A

Sage Code

This appendix contains the sage code used for the computations in this thesis. Specifically, the code for the following algorithms is included, where \mathbf{g} denotes an r -tuple of $m \times m$ monodromy matrices:

- implementation of the braiding action—given \mathbf{g} and a braid β , expressed as a word in $\beta_i^{\pm 1}$, compute the r -tuple \mathbf{g}^β ;
- constructions of the subspaces $H_{\mathbf{g}}, E_{\mathbf{g}}, W_{\mathbf{g}}$;
- implementation of the maps $\Phi(\mathbf{g}, \beta)$ and $\Psi(\mathbf{g}, h)$.

Also included in this appendix are dictionaries of the following monodromy representations:

- the monodromy representations for the eleven rigid elliptic surfaces on Herfurtner’s list with exactly one additive fibre;
- the monodromy representations for the seven families of rational elliptic surfaces with an I_0^* fibres.

Dettweiler-Wewers Algorithm

```
###In the following, the input g is an r-tuple of mxm matrices---a
monodromy representation
#Here, K is a field or ring
#This is the function phi(Beta_j,g)
def phi(j,g):
    r=len(g)
    m=g[0].nrows()
    V=K^(r*m)
    U=K^m
    Ubasis=U.basis()
    Vbasis=V.basis()
    e={}
    for i in [1..r*m]:
        e[i]=Vbasis[i-1]
    f={}
    for i in [1..m]:
        f[i]=Ubasis[i-1]
    #j will take values in 1 to r-1
    a={}
    for i in [0..r-1]:
        a[i+1]=g[i]
    #so a1 is the first monodromy matrix, etc.
    I1=[]
    I2=[]
    I3=[]
    for i in [1..m*(j-1)]:
        I1.append(list(e[i]))
    for i in [1..m]:
        I2.append(m*j*[0]+list(f[i]*a[j+1])+(r*m-m*j-m)*[0])

    for i in [1..m]:
        I2.append(m*(j-1)*[0]+list(f[i])+list(f[i]*(1-
a[j+1].inverse()*a[j]*a[j+1]))+(r*m-m*j-m)*[0])

    for i in [(m*(j+1)+1)..r*m]:
        I3.append(list(e[i]))
    return Matrix(K,I1+I2+I3)

def Psi(g,h):
    r=len(g)
    m=g[0].nrows()
    s=r*m
    U=K^m
```

```

Ubasis=U.basis()
f={}
for i in [1..m]:
    f[i]=Ubasis[i-1]
I={}
for i in [1..r]:
    I[i]=[]
for i in [1..r]:
    for j in [1..m]:
        I[i].append(m*(i-1)*[0]+list(f[j]*h)+(s-m*i)*[0])
J=[]
for i in [1..r]:
    J=J+I[i]
return Matrix(K,J)

```

#This is the "characteristic" vector that has b in the "i" position, and solves for the last position using relation (2). So, here i in [1..r-1].

#Caution, this assumes that we are solving for the last entry

```

def Chi(i,g,b):
    r=len(g)
    m=g[0].nrows()
    s=r*m
    a=1
    for j in [i..r-1]:
        a=a*g[j]
    return vector(K,m*(i-1)*[0]+list(b)+(s-m*i-m)*[0]+list(-b*a))

```

#for this guy, i in [2..r]

```

def ChiFirst(i,g,b):
    r=len(g)
    m=g[0].nrows()
    s=r*m
    a=identity_matrix(m)
    for j in [1..i-1]:
        a=a*g[j]
    return vector(K,list(-b*a.inverse())+m*(i-2)*[0]+list(b)+(s-m*i+m)*[0])

```

```

def Diag(g,b):
    r=len(g)
    m=g[0].nrows()
    s=r*m
    I=[]
    for i in [0..r-1]:

```

```

        I=I+list(b*(g[i]-1))
    return vector(K,I)

def E_Basis(g):
    m=g[0].nrows()
    U=K^m
    Ubasis=U.basis()
    f={}
    for i in [1..m]:
        f[i]=Ubasis[i-1]
    A=[]
    for i in [1..m]:
        A.append(Diag(g,f[i]))
    return A

def H_Basis(g):
    r=len(g)
    m=g[0].nrows()
    s=r*m
    B={}
    C={}
    for i in [0..r-2]:
        B[i]=(g[i]-1).image().basis()
    for i in [0..r-2]:
        C[i]=[]
        for j in B[i]:
            C[i].append(Chi(i+1,g,j))
    D=[]
    for i in [0..r-2]:
        D=D+C[i]
    return D

#These are the braiding maps
#here, i in [1..r-1]
def beta(i,g):
    r=len(g)
    m=g[0].nrows()
    s=r*m

    if i in [1..r-1]:
        A=[]
        B=[]
        C=[]
        for j in [1..i-1]:
            A.append(g[j-1])
        B=[g[i],g[i].inverse()*g[i-1]*g[i]]
        for j in [i+1..r-1]:
            C.append(g[j])

```

```

    return A+B+C
if i in [-(r-1)..-1]:
    k=i.abs()
    A=[]
    B=[]
    C=[]
    for j in [1..k-1]:
        A.append(g[j-1])
    B=[g[k-1]*g[k]*g[k-1].inverse(),g[k-1]]
    for j in [k+1..r-1]:
        C.append(g[j])
    return A+B+C

##These functions take as input a word in the braid generators. Input
the braid from left to right. For example, I=[1,-2,3] acts as
Beta1*Beta2^{-1}*Beta3
def Beta(I,g):
    a=g
    for i in I:
        a=beta(i,a)
    return a

def Phi(I,g):
    M=1
    a=g
    for i in I:
        if i>0:
            M=M*phi(i,a)
            a=beta(i,a)
        if i<0:
            M=M*phi(-i,beta(i,a)).inverse()
            a=beta(i,a)
    return M

#This conjugates a tripe.
def Conjugation_Action(g,h):
    r=len(g)
    A=[]
    for i in [0..r-1]:
        A.append(h.inverse()*g[i]*h)
    return A

```

Representation Dictionaries

#Below are the 11 monodromy representations corresponding to the 11 examples on Herfurtner's list with only one additive fibre

```
Representations={}
Representations[1]=[Matrix(ZZ,[[1,1],[-1,0]]),Matrix(ZZ,[[1,8],[0,1]])]
Representations[2]=[Matrix(ZZ,[[2,1],[-1,0]]),Matrix(ZZ,[[1,7],[0,1]])]
Representations[3]=[Matrix(ZZ,[[2,1],[-1,0]]),Matrix(ZZ,[[3,4],[-4,5]])]
Representations[4]=[Matrix(ZZ,[[1,1],[-1,0]]),Matrix(ZZ,[[3,4],[-4,5]])]
Representations[5]=[Matrix(ZZ,[[3,4],[-1,-1]]),Matrix(ZZ,[[3,1],[-4,-1]])]
Representations[6]=[Matrix(ZZ,[[4,9],[-1,-2]]),Matrix(ZZ,[[3,2],[-2,-1]])]
Representations[7]=[Matrix(ZZ,[[3,4],[-1,-1]]),Matrix(ZZ,[[1,0],[-3,1]])]
Representations[8]=[Matrix(ZZ,[[5,8],[-2,-3]]),Matrix(ZZ,[[4,3],[-3,-2]])]
Representations[9]=[Matrix(ZZ,[[3,4],[-1,-1]]),Matrix(ZZ,[[0,1],[-1,-1]])]
Representations[10]=[Matrix(ZZ,[[0,1],[-1,-1]]),Matrix(ZZ,[[1,0],[-2,1]])]
Representations[11]=[Matrix(ZZ,[[0,1],[-1,-1]]),Matrix(ZZ,[[1,0],[-3,1]])]
```

#Here, we've twisted the additive fibre

```
ModReps={}
ModReps[1]=[-Matrix(ZZ,[[1,1],[-1,0]]),Matrix(ZZ,[[1,8],[0,1]])]
ModReps[2]=[Matrix(ZZ,[[2,1],[-1,0]]),Matrix(ZZ,[[1,7],[0,1]])]
ModReps[3]=[Matrix(ZZ,[[2,1],[-1,0]]),Matrix(ZZ,[[3,4],[-4,5]])]
ModReps[4]=[-Matrix(ZZ,[[1,1],[-1,0]]),Matrix(ZZ,[[3,4],[-4,5]])]
ModReps[5]=[Matrix(ZZ,[[3,4],[-1,-1]]),Matrix(ZZ,[[3,1],[-4,-1]])]
ModReps[6]=[Matrix(ZZ,[[4,9],[-1,-2]]),Matrix(ZZ,[[3,2],[-2,-1]])]
ModReps[7]=[Matrix(ZZ,[[3,4],[-1,-1]]),Matrix(ZZ,[[1,0],[-3,1]])]
```

```

Matrix(ZZ, [[-1,1],[-2,1]],Matrix(ZZ, [[1,5],[0,1]]))
ModReps[8]=[Matrix(ZZ, [[5,8],[-2,-3]],Matrix(ZZ, [[4,3],[-3,-2]]),-
Matrix(ZZ, [[0,1],[-1,0]],Matrix(ZZ, [[1,4],[0,1]]))
ModReps[9]=[Matrix(ZZ, [[3,4],[-1,-1]],-Matrix(ZZ, [[0,1],
[-1,-1]],Matrix(ZZ, [[0,1],[-1,2]],Matrix(ZZ, [[1,6],[0,1]]))
ModReps[10]=[-Matrix(ZZ, [[0,1],[-1,-1]],Matrix(ZZ, [[1,0],
[-2,1]],Matrix(ZZ, [[-1,4],[-1,3]],Matrix(ZZ, [[1,5],[0,1]]))
ModReps[11]=[-Matrix(ZZ, [[0,1],[-1,-1]],Matrix(ZZ, [[1,0],
[-3,1]],Matrix(ZZ, [[-1,2],[-2,3]],Matrix(ZZ, [[1,3],[0,1]]))

##This creates the dictionary for the monodromy representations giving
rise to
TwistRep={}
for i in [1..11]:
    TwistRep[i]=[Matrix(ZZ, [[-1,0],[0,-1]])+ModReps[i]

Morange=Matrix(ZZ, [[1,1],[0,1]])
Mpurple=Matrix(ZZ, [[0,1],[-1,0]])
Minus=[Matrix(ZZ, [[-1,0],[0,-1]])]

#Reps[i] produces the 4-tuple of monodromy matrices representing the
homological invariant for the i-th I0^* family in Herfurtners list. -1
will always be the first entry.

Reps={}
Reps[1]=Minus+[Matrix(ZZ, [[1,0],[-1,1]],Matrix(ZZ, [[1,4],
[0,1]],Matrix(ZZ, [[3,4],[-1,-1]])]
Reps[2]=Minus+[Matrix(ZZ, [[1,0],[-2,1]],Matrix(ZZ, [[1,2],[0,1]]),-
Matrix(ZZ, [[-3,-2],[2,1]])]
Reps[3]=Minus+[Matrix(ZZ, [[1,3],[0,1]],Matrix(ZZ, [[1,1],[-1,0]]),-
Matrix(ZZ, [[0,-1],[1,-2]])]
Reps[4]=Minus+[Matrix(ZZ, [[1,2],[0,1]],-Matrix(ZZ, [[-1,-2],
[1,1]],Matrix(ZZ, [[1,0],[-1,1]])]
Reps[5]=Minus+[Matrix(ZZ, [[1,1],[0,1]],Matrix(ZZ, [[0,1],[-1,-1]]),-
Matrix(ZZ, [[-1,0],[1,-1]])]
Reps[6]=Minus+[Matrix(ZZ, [[1,1],[-1,0]],-Matrix(ZZ, [[0,-1],
[1,0]],Matrix(ZZ, [[1,1],[0,1]])]
Reps[7]=Minus+[Matrix(ZZ, [[1,1],[-1,0]],Matrix(ZZ, [[0,1],[-1,1]]),-
Matrix(ZZ, [[-1,-2],[0,-1]])]

```

Appendix B

Monodromy Representations

This appendix contains tables of monodromy representations for the parabolic cohomology associated to the families of K3 surfaces computing in Chapter 2.

- Tables B.1 and B.2 tabulate the monodromy representations for the two-parameter family of K3 surfaces obtained by performing a quadratic twist at two points smooth points a_1, a_2 ;
- table B.3 tabulate the monodromy representations for the three-parameter family of K3 surfaces obtained by performing a quadratic twist at two smooth points for each of the seven families already containing an I_0^* fibre;
- table B.4 shows the monodromy representations for the one-parameter families of K3 surfaces obtained by twisting two of the three non- I_0^* fibres in the seven I_0^* families. Column A corresponds to twisting the second and third fibre; column B corresponds to twisting the first and third; column C corresponds to twisting the first and second.

Label	γ_1	γ_2	γ_3	γ_4	γ_5
1	$\begin{pmatrix} 1 & 0 & 0 & 0 & 0 \\ 0 & 1 & 0 & 0 & 0 \\ 0 & 0 & 1 & 0 & 0 \\ -1 & 1 & 1 & 1 & 0 \\ 1 & -1 & 0 & 0 & 1 \end{pmatrix}$	$\begin{pmatrix} 1 & 0 & 0 & 0 & 0 \\ 2 & -1 & 0 & -2 & 0 \\ 2 & 0 & -1 & 0 & -2 \\ -2 & 1 & 1 & 2 & 1 \\ 1 & -1 & 0 & -1 & 1 \end{pmatrix}$	$\begin{pmatrix} 17 & 0 & 0 & 16 & -32 \\ 14 & 1 & 0 & 14 & -28 \\ 6 & 0 & 1 & 6 & -12 \\ 4 & 0 & 0 & 5 & -8 \\ 11 & 0 & 0 & 11 & -21 \end{pmatrix}$	$\begin{pmatrix} 1 & 0 & 0 & 0 & 0 \\ 1 & 0 & 1 & -2 & 0 \\ 3 & -1 & -1 & 0 & -2 \\ 0 & 0 & 0 & 1 & 0 \\ 0 & 0 & 0 & 0 & 1 \end{pmatrix}$	$\begin{pmatrix} -47 & 16 & 24 & 48 & 16 \\ -38 & 13 & 20 & 40 & 12 \\ -19 & 7 & 9 & 20 & 6 \\ -18 & 6 & 9 & 19 & 6 \\ -36 & 12 & 18 & 36 & 13 \end{pmatrix}$
2	$\begin{pmatrix} 1 & 0 & 0 & 0 & 0 \\ 0 & 1 & 0 & 0 & 0 \\ 0 & 0 & 1 & 0 & 0 \\ -2 & 1 & 1 & 1 & 0 \\ -1 & 1 & -1 & 0 & 1 \end{pmatrix}$	$\begin{pmatrix} 1 & 0 & 0 & 0 & 0 \\ 0 & 1 & 0 & 0 & 0 \\ 8 & -4 & -1 & -2 & -2 \\ -4 & 2 & 1 & 2 & 1 \\ 4 & -2 & -1 & -1 & 0 \end{pmatrix}$	$\begin{pmatrix} 1 & 0 & 0 & 0 & 0 \\ 4 & -1 & 0 & 4 & -4 \\ 0 & 0 & 1 & 0 & 0 \\ -2 & 1 & 0 & -1 & 2 \\ -2 & 1 & 0 & -2 & 3 \end{pmatrix}$	$\begin{pmatrix} 1 & 0 & 0 & 0 & 0 \\ 0 & 1 & 0 & 0 & 0 \\ 5 & -2 & -1 & -2 & -2 \\ 0 & 0 & 0 & 1 & 0 \\ 0 & 0 & 0 & 0 & 1 \end{pmatrix}$	$\begin{pmatrix} 1 & 0 & 0 & 0 & 0 \\ -14 & 7 & 4 & 12 & 4 \\ 5 & -2 & -1 & -2 & -2 \\ 0 & 0 & 0 & 1 & 0 \\ 0 & 0 & 0 & 0 & 1 \end{pmatrix}$
3	$\begin{pmatrix} 1 & 0 & 0 & 0 & 0 \\ 0 & 1 & 0 & 0 & 0 \\ 0 & 0 & 1 & 0 & 0 \\ -2 & 1 & 1 & 1 & 0 \\ -1 & 1 & -1 & 0 & 1 \end{pmatrix}$	$\begin{pmatrix} 1 & 0 & 0 & 0 & 0 \\ 0 & 1 & 0 & 0 & 0 \\ 8 & -4 & -1 & -2 & -2 \\ -4 & 2 & 1 & 2 & 1 \\ 4 & -2 & -1 & -1 & 0 \end{pmatrix}$	$\begin{pmatrix} 1 & 0 & 0 & 0 & 0 \\ 4 & -1 & 0 & 8 & -8 \\ 0 & 0 & 1 & 0 & 0 \\ -2 & 1 & 0 & -3 & 4 \\ -2 & 1 & 0 & -4 & 5 \end{pmatrix}$	$\begin{pmatrix} 1 & 0 & 0 & 0 & 0 \\ 0 & 1 & 0 & 0 & 0 \\ 5 & -2 & -1 & -2 & -2 \\ 0 & 0 & 0 & 1 & 0 \\ 0 & 0 & 0 & 0 & 1 \end{pmatrix}$	$\begin{pmatrix} 1 & 0 & 0 & 0 & 0 \\ -32 & 15 & 8 & 24 & 8 \\ 5 & -2 & -1 & -2 & -2 \\ 0 & 0 & 0 & 1 & 0 \\ 0 & 0 & 0 & 0 & 1 \end{pmatrix}$
4	$\begin{pmatrix} 1 & 0 & 0 & 0 & 0 \\ 0 & 1 & 0 & 0 & 0 \\ 0 & 0 & 1 & 0 & 0 \\ -1 & 1 & 1 & 1 & 0 \\ 1 & -1 & 0 & 0 & 1 \end{pmatrix}$	$\begin{pmatrix} 1 & 0 & 0 & 0 & 0 \\ 2 & -1 & 0 & -2 & 0 \\ 2 & 0 & -1 & 0 & -2 \\ -2 & 1 & 1 & 2 & 1 \\ 1 & -1 & 0 & -1 & 1 \end{pmatrix}$	$\begin{pmatrix} 41 & 0 & 0 & 60 & -60 \\ 36 & 1 & 0 & 54 & -54 \\ 8 & 0 & 1 & 12 & -12 \\ 6 & 0 & 0 & 10 & -9 \\ 34 & 0 & 0 & 51 & -50 \end{pmatrix}$	$\begin{pmatrix} 1 & 0 & 0 & 0 & 0 \\ 1 & 0 & 1 & -2 & 0 \\ 3 & -1 & -1 & 0 & -2 \\ 0 & 0 & 0 & 1 & 0 \\ 0 & 0 & 0 & 0 & 1 \end{pmatrix}$	$\begin{pmatrix} -109 & 30 & 60 & 120 & 60 \\ -95 & 26 & 53 & 106 & 52 \\ -23 & 7 & 12 & 26 & 12 \\ -22 & 6 & 12 & 25 & 12 \\ -99 & 27 & 54 & 108 & 55 \end{pmatrix}$
5	$\begin{pmatrix} 1 & 0 & 0 & 0 & 0 \\ 0 & 1 & 0 & 0 & 0 \\ 0 & 0 & 1 & 0 & 0 \\ -1 & 2 & 1 & 1 & 0 \\ 1 & -1 & -2 & 0 & 1 \end{pmatrix}$	$\begin{pmatrix} 1 & 0 & 0 & 0 & 0 \\ 0 & 1 & 0 & 0 & 0 \\ 6 & -6 & -1 & -4 & -2 \\ -3 & 3 & 1 & 3 & 1 \\ 6 & -6 & -2 & -4 & -1 \end{pmatrix}$	$\begin{pmatrix} 1 & 0 & 0 & 0 & 0 \\ 4 & -1 & 0 & -2 & -4 \\ 0 & 0 & 1 & 0 & 0 \\ -4 & 2 & 0 & 3 & 4 \\ 2 & -1 & 0 & -1 & -1 \end{pmatrix}$	$\begin{pmatrix} 1 & 0 & 0 & 0 & 0 \\ 0 & 1 & 0 & 0 & 0 \\ 5 & -3 & -1 & -4 & -2 \\ 0 & 0 & 0 & 1 & 0 \\ 0 & 0 & 0 & 0 & 1 \end{pmatrix}$	$\begin{pmatrix} 1 & 0 & 0 & 0 & 0 \\ -10 & 8 & 3 & 10 & 2 \\ 5 & -3 & -1 & -4 & -2 \\ 0 & 0 & 0 & 1 & 0 \\ 0 & 0 & 0 & 0 & 1 \end{pmatrix}$
6	$\begin{pmatrix} 1 & 0 & 0 & 0 & 0 \\ 0 & 1 & 0 & 0 & 0 \\ 0 & 0 & 1 & 0 & 0 \\ 2 & -2 & -2 & 1 & 0 \\ -3 & 2 & 4 & 0 & 1 \end{pmatrix}$	$\begin{pmatrix} 1 & 0 & 0 & 0 & 0 \\ 0 & 1 & 0 & 0 & 0 \\ -4 & 0 & 3 & 4 & 2 \\ 0 & 0 & 0 & 1 & 0 \\ 8 & 0 & -4 & -8 & -3 \end{pmatrix}$	$\begin{pmatrix} 1 & 0 & 0 & 0 & 0 \\ -6 & 3 & 4 & 4 & 4 \\ 0 & 0 & 1 & 0 & 0 \\ 0 & 0 & 0 & 1 & 0 \\ 6 & -2 & -4 & -4 & -3 \end{pmatrix}$	$\begin{pmatrix} 1 & 0 & 0 & 0 & 0 \\ 0 & 1 & 0 & 0 & 0 \\ -5 & 2 & 3 & 4 & 2 \\ 5 & -2 & -2 & -3 & -2 \\ 0 & 0 & 0 & 0 & 1 \end{pmatrix}$	$\begin{pmatrix} 1 & 0 & 0 & 0 & 0 \\ 16 & -5 & -8 & -12 & -4 \\ -5 & 2 & 3 & 4 & 2 \\ -11 & 4 & 6 & 9 & 2 \\ 0 & 0 & 0 & 0 & 1 \end{pmatrix}$

Table B.1: Monodromy matrices for the two-parameter family of K3 surfaces generated by the eleven entries on Herfurtnier's list with exactly one additive fibre. (Entries 1-6)

Label	γ_1	γ_2	γ_3	γ_4	γ_5
7	$\begin{pmatrix} 1 & 0 & 0 & 0 & 0 \\ 0 & 1 & 0 & 0 & 0 \\ 0 & 0 & 1 & 0 & 0 \\ 0 & 0 & 1 & 1 & 0 \\ -1 & 1 & -2 & 0 & 1 \end{pmatrix}$	$\begin{pmatrix} 1 & 0 & 0 & 0 & 0 \\ 0 & 1 & 0 & 0 & 0 \\ 2 & 0 & -1 & -4 & -2 \\ -1 & 0 & 1 & 3 & 1 \\ 2 & 0 & -2 & -4 & -1 \end{pmatrix}$	$\begin{pmatrix} 1 & 0 & 0 & 0 & 0 \\ 4 & 5 & 0 & 0 & -12 \\ 2 & 2 & 1 & 0 & -6 \\ -1 & -1 & 0 & 1 & 3 \\ 2 & 2 & 0 & 0 & -5 \end{pmatrix}$	$\begin{pmatrix} 1 & 0 & 0 & 0 & 0 \\ 0 & 1 & 0 & 0 & 0 \\ 1 & 1 & -1 & -4 & -2 \\ 0 & 0 & 0 & 1 & 0 \\ 0 & 0 & 0 & 0 & 1 \end{pmatrix}$	$\begin{pmatrix} 1 & 0 & 0 & 0 & 0 \\ -14 & -1 & 12 & 48 & 12 \\ -6 & 0 & 5 & 20 & 4 \\ 0 & 0 & 0 & 1 & 0 \\ -7 & -1 & 6 & 24 & 7 \end{pmatrix}$
8	$\begin{pmatrix} 1 & 0 & 0 & 0 & 0 \\ 0 & 1 & 0 & 0 & 0 \\ 0 & 0 & 1 & 0 & 0 \\ 0 & -2 & -2 & 1 & 0 \\ 0 & 2 & 3 & 0 & 1 \end{pmatrix}$	$\begin{pmatrix} 1 & 0 & 0 & 0 & 0 \\ 0 & 1 & 0 & 0 & 0 \\ -4 & 2 & 5 & 6 & 4 \\ 0 & 0 & 0 & 1 & 0 \\ 6 & -3 & -6 & -9 & -5 \end{pmatrix}$	$\begin{pmatrix} 1 & 0 & 0 & 0 & 0 \\ -4 & 5 & 6 & 6 & 6 \\ 0 & 0 & 1 & 0 & 0 \\ 0 & 0 & 0 & 1 & 0 \\ 4 & -4 & -6 & -6 & -5 \end{pmatrix}$	$\begin{pmatrix} 1 & 0 & 0 & 0 & 0 \\ 0 & 1 & 0 & 0 & 0 \\ -4 & 4 & 5 & 6 & 4 \\ 4 & -4 & -4 & -5 & -4 \\ 0 & 0 & 0 & 0 & 1 \end{pmatrix}$	$\begin{pmatrix} 1 & 0 & 0 & 0 & 0 \\ 8 & -7 & -9 & -12 & -6 \\ -4 & 4 & 5 & 6 & 4 \\ -4 & 4 & 5 & 7 & 2 \\ 0 & 0 & 0 & 0 & 1 \end{pmatrix}$
9	$\begin{pmatrix} 1 & 0 & 0 & 0 & 0 \\ 0 & 1 & 0 & 0 & 0 \\ 0 & 0 & 1 & 0 & 0 \\ 3 & -3 & -3 & 1 & 0 \\ 4 & -3 & -6 & 0 & 1 \end{pmatrix}$	$\begin{pmatrix} 1 & 0 & 0 & 0 & 0 \\ 0 & 1 & 0 & 0 & 0 \\ 0 & -2 & 3 & 4 & -2 \\ 0 & 1 & -1 & -1 & 1 \\ 0 & -2 & 2 & 4 & -1 \end{pmatrix}$	$\begin{pmatrix} -11 & 8 & 8 & 4 & 0 \\ -10 & 7 & 8 & 6 & -2 \\ -6 & 4 & 5 & 2 & 0 \\ -4 & 3 & 2 & 1 & 1 \\ -7 & 5 & 4 & 1 & 2 \end{pmatrix}$	$\begin{pmatrix} 1 & 0 & 0 & 0 & 0 \\ 0 & 1 & 0 & 0 & 0 \\ -2 & 1 & 3 & 4 & -2 \\ 4 & -2 & -4 & -7 & 4 \\ 4 & -2 & -4 & -8 & 5 \end{pmatrix}$	$\begin{pmatrix} -29 & 20 & 26 & 28 & -12 \\ -21 & 16 & 17 & 18 & -8 \\ -17 & 11 & 16 & 18 & -8 \\ 1 & -2 & 1 & -1 & 2 \\ 1 & -2 & 1 & -2 & 3 \end{pmatrix}$
10	$\begin{pmatrix} 1 & 0 & 0 & 0 & 0 \\ 0 & 1 & 0 & 0 & 0 \\ 0 & 0 & 1 & 0 & 0 \\ 0 & 0 & 1 & 1 & 0 \\ 0 & -1 & 1 & 0 & 1 \end{pmatrix}$	$\begin{pmatrix} 1 & 0 & 0 & 0 & 0 \\ 4 & -1 & 0 & -6 & 0 \\ 4 & 0 & -1 & -4 & -2 \\ -2 & 0 & 1 & 3 & 1 \\ 0 & -1 & 1 & -1 & 2 \end{pmatrix}$	$\begin{pmatrix} 11 & 0 & 0 & 0 & -20 \\ 2 & 1 & 0 & 0 & -4 \\ 2 & 0 & 1 & 0 & -4 \\ 7 & 0 & 0 & 1 & -14 \\ 6 & 0 & 0 & 0 & -11 \end{pmatrix}$	$\begin{pmatrix} 1 & 0 & 0 & 0 & 0 \\ 4 & -1 & 3 & -6 & 0 \\ 4 & -1 & 2 & -4 & -2 \\ 0 & 0 & 0 & 1 & 0 \\ 0 & 0 & 0 & 0 & 1 \end{pmatrix}$	$\begin{pmatrix} -29 & -10 & 20 & 20 & 20 \\ -2 & 0 & 1 & 4 & -2 \\ -6 & -1 & 3 & 6 & 2 \\ -24 & -8 & 16 & 17 & 16 \\ -18 & -6 & 12 & 12 & 13 \end{pmatrix}$
11	$\begin{pmatrix} 1 & 0 & 0 & 0 & 0 \\ 0 & 1 & 0 & 0 & 0 \\ 0 & 0 & 1 & 0 & 0 \\ 0 & 0 & -3 & 1 & 0 \\ 0 & -1 & -3 & 0 & 1 \end{pmatrix}$	$\begin{pmatrix} 1 & 0 & 0 & 0 & 0 \\ -2 & -1 & 4 & 2 & 0 \\ 0 & 0 & 3 & 4 & -2 \\ 0 & 0 & -1 & -1 & 1 \\ -1 & -1 & 1 & -1 & 2 \end{pmatrix}$	$\begin{pmatrix} 5 & 0 & 8 & 16 & -12 \\ 2 & 1 & 4 & 8 & -6 \\ 2 & 0 & 5 & 8 & -6 \\ -1 & 0 & -2 & -3 & 3 \\ 2 & 0 & 4 & 8 & -5 \end{pmatrix}$	$\begin{pmatrix} 1 & 0 & 0 & 0 & 0 \\ -2 & -1 & 7 & 2 & 0 \\ 0 & -1 & 6 & 4 & -2 \\ 0 & 2 & -10 & -7 & 4 \\ 0 & 2 & -10 & -8 & 5 \end{pmatrix}$	$\begin{pmatrix} -7 & -6 & -4 & -20 & 12 \\ 0 & -1 & -1 & -2 & 0 \\ -2 & -2 & -3 & -8 & 4 \\ 4 & 4 & 8 & 17 & -8 \\ 0 & 1 & 6 & 6 & -1 \end{pmatrix}$

Table B.2: Monodromy matrices for the two-parameter family of K3 surfaces generated by the eleven entries on Herfurter's list with exactly one additive fibre. (Entries 7-11)

Label	A		B		C		
	σ_0	σ_1	σ_0	σ_1	σ_0	σ_1	
1	$\begin{pmatrix} 1 & 0 & 0 \\ 0 & 1 & 0 \\ 0 & 2 & -1 \end{pmatrix}$	$\begin{pmatrix} 1 & -8 & 4 \\ -1 & 1 & -2 \\ 0 & 0 & 1 \end{pmatrix}$	$\begin{pmatrix} 1 & 0 & 0 \\ -2 & 1 & 4 \\ -1 & 0 & 1 \end{pmatrix}$	$\begin{pmatrix} -3 & 2 & 4 \\ 0 & 1 & 0 \\ -2 & 1 & 3 \end{pmatrix}$	$\begin{pmatrix} 1 & 0 & 0 \\ 1 & 3 & -2 \\ 0 & 2 & -1 \end{pmatrix}$	$\begin{pmatrix} 3 & 4 & 0 \\ 1 & 3 & -2 \\ 4 & 8 & -3 \end{pmatrix}$	$\begin{pmatrix} 3 & 4 & 0 \\ -2 & -3 & 0 \\ -2 & -2 & -1 \end{pmatrix}$
	$\begin{pmatrix} 1 & 0 & 0 \\ 0 & 1 & 0 \\ -2 & -2 & -1 \end{pmatrix}$	$\begin{pmatrix} 5 & 4 & 2 \\ -10 & -7 & -4 \\ -2 & -2 & -1 \end{pmatrix}$	$\begin{pmatrix} 1 & 0 & 0 \\ 0 & 1 & -2 \\ 2 & 0 & 1 \end{pmatrix}$	$\begin{pmatrix} -1 & 2 & -2 \\ 0 & 1 & 0 \\ 0 & 0 & 1 \end{pmatrix}$	$\begin{pmatrix} 1 & 0 & 0 \\ 0 & 1 & -2 \\ -2 & 0 & 1 \end{pmatrix}$	$\begin{pmatrix} 1 & 2 & 0 \\ 0 & 3 & -2 \\ 0 & 2 & -1 \end{pmatrix}$	$\begin{pmatrix} 1 & 2 & 0 \\ 0 & -1 & 0 \\ -2 & -2 & -1 \end{pmatrix}$
3	$\begin{pmatrix} 1 & 0 & 0 \\ 0 & 1 & 0 \\ 1 & -1 & -1 \end{pmatrix}$	$\begin{pmatrix} -31 & 48 & -24 \\ -22 & 34 & -17 \\ -7 & 11 & -6 \end{pmatrix}$	$\begin{pmatrix} 1 & 0 & 0 \\ 0 & 1 & 0 \\ -1 & 3 & 3 \end{pmatrix}$	$\begin{pmatrix} 1 & 0 & -8 \\ 2 & -1 & -2 \\ 0 & 0 & -7 \end{pmatrix}$	$\begin{pmatrix} 1 & 0 & 0 \\ 3 & 1 & 0 \\ 5 & -1 & 1 \end{pmatrix}$	$\begin{pmatrix} -1 & 2 & -2 \\ 3 & 0 & -1 \\ 8 & -5 & 3 \end{pmatrix}$	$\begin{pmatrix} -1 & 2 & -2 \\ 0 & 6 & -7 \\ 0 & 5 & -6 \end{pmatrix}$
	$\begin{pmatrix} 1 & 0 & 0 \\ 0 & 1 & 0 \\ 1 & -1 & -1 \end{pmatrix}$	$\begin{pmatrix} 1 & 4 & -8 \\ 0 & 1 & -2 \\ 1 & 2 & -5 \end{pmatrix}$	$\begin{pmatrix} 1 & 0 & 0 \\ 0 & 1 & 0 \\ 0 & -2 & 1 \end{pmatrix}$	$\begin{pmatrix} -3 & 4 & 4 \\ 0 & 1 & 2 \\ -2 & 2 & 3 \end{pmatrix}$	$\begin{pmatrix} 1 & 0 & 0 \\ 2 & 1 & 0 \\ 1 & -1 & 1 \end{pmatrix}$	$\begin{pmatrix} -1 & 0 & -2 \\ 2 & -1 & 0 \\ 3 & -1 & 3 \end{pmatrix}$	$\begin{pmatrix} -1 & 0 & -2 \\ 0 & -1 & -4 \\ 0 & 0 & 1 \end{pmatrix}$
5	$\begin{pmatrix} 1 & 0 & 0 \\ 0 & 1 & 0 \\ 1 & -1 & -1 \end{pmatrix}$	$\begin{pmatrix} 1 & 8 & -8 \\ 0 & 1 & -1 \\ 1 & 4 & -5 \end{pmatrix}$	$\begin{pmatrix} 1 & 0 & 0 \\ 0 & 1 & 0 \\ -1 & 2 & 1 \end{pmatrix}$	$\begin{pmatrix} 17 & 0 & -24 \\ 4 & -1 & -4 \\ 10 & 1 & -15 \end{pmatrix}$	$\begin{pmatrix} 1 & 0 & 0 \\ -1 & 1 & 0 \\ 0 & 1 & 1 \end{pmatrix}$	$\begin{pmatrix} -1 & 0 & -2 \\ -1 & -1 & -1 \\ 0 & 1 & 2 \end{pmatrix}$	$\begin{pmatrix} -1 & 0 & -2 \\ 0 & -1 & 1 \\ 0 & 0 & 1 \end{pmatrix}$
	$\begin{pmatrix} 1 & 0 & 0 \\ 0 & 1 & 0 \\ 0 & 0 & 1 \end{pmatrix}$	$\begin{pmatrix} -1 & 2 & 0 \\ 4 & 5 & -8 \\ 2 & 3 & -4 \end{pmatrix}$	$\begin{pmatrix} 1 & 0 & 0 \\ 0 & 1 & 0 \\ 0 & -1 & 1 \end{pmatrix}$	$\begin{pmatrix} -1 & 2 & 0 \\ -4 & -11 & 8 \\ -4 & -6 & 6 \end{pmatrix}$	$\begin{pmatrix} 1 & 0 & 0 \\ 0 & 2 & -1 \\ 0 & -1 & 1 \end{pmatrix}$	$\begin{pmatrix} -1 & 0 & -4 \\ -2 & -2 & -7 \\ 1 & 1 & 4 \end{pmatrix}$	$\begin{pmatrix} -1 & 0 & -4 \\ 0 & -1 & -1 \\ 0 & 0 & 1 \end{pmatrix}$
6	$\begin{pmatrix} 1 & 0 & 0 \\ 0 & 1 & 0 \\ 0 & 0 & 1 \end{pmatrix}$	$\begin{pmatrix} -7 & 0 & 0 \\ -8 & -3 & 4 \\ -6 & -1 & 1 \end{pmatrix}$	$\begin{pmatrix} 1 & 0 & 0 \\ 0 & 1 & 0 \\ -1 & 0 & 1 \end{pmatrix}$	$\begin{pmatrix} 1 & 0 & 0 \\ -8 & 1 & 4 \\ -2 & 0 & 2 \end{pmatrix}$	$\begin{pmatrix} 1 & 0 & 0 \\ 2 & -1 & -3 \\ -1 & 1 & 2 \end{pmatrix}$	$\begin{pmatrix} 5 & 0 & -12 \\ 4 & 1 & -4 \\ 3 & 0 & 0 \end{pmatrix}$	$\begin{pmatrix} 5 & 0 & -12 \\ 3 & -1 & -6 \\ 2 & 0 & -5 \end{pmatrix}$
	$\begin{pmatrix} 1 & 0 & 0 \\ 0 & 1 & 0 \\ 0 & 0 & 1 \end{pmatrix}$	$\begin{pmatrix} -3 & 0 & 0 \\ -2 & -5 & 4 \\ -2 & -5 & 4 \end{pmatrix}$	$\begin{pmatrix} 1 & 0 & 0 \\ 0 & 1 & 0 \\ 3 & -1 & -1 \end{pmatrix}$	$\begin{pmatrix} 1 & 0 & 0 \\ -8 & 1 & 4 \\ -2 & 0 & 2 \end{pmatrix}$	$\begin{pmatrix} 1 & 0 & 0 \\ 3 & -1 & -1 \\ -1 & 0 & 1 \end{pmatrix}$	$\begin{pmatrix} 5 & 0 & -12 \\ 7 & -2 & -15 \\ 0 & 1 & -1 \end{pmatrix}$	$\begin{pmatrix} 5 & 0 & -12 \\ 3 & -1 & -6 \\ 2 & 0 & -5 \end{pmatrix}$
7	$\begin{pmatrix} 1 & 0 & 0 \\ 0 & 1 & 0 \\ 0 & 0 & 1 \end{pmatrix}$	$\begin{pmatrix} -3 & 0 & 0 \\ -2 & 0 & 0 \\ -3 & 0 & 0 \end{pmatrix}$	$\begin{pmatrix} 1 & 0 & 0 \\ 0 & 1 & 0 \\ -1 & 0 & 1 \end{pmatrix}$	$\begin{pmatrix} 1 & 0 & 0 \\ -8 & 1 & 4 \\ -2 & 0 & 2 \end{pmatrix}$	$\begin{pmatrix} 1 & 0 & 0 \\ 2 & -1 & -3 \\ -1 & 1 & 2 \end{pmatrix}$	$\begin{pmatrix} 5 & 0 & -12 \\ 7 & -2 & -15 \\ 0 & 1 & -1 \end{pmatrix}$	$\begin{pmatrix} 5 & 0 & -12 \\ 3 & -1 & -6 \\ 2 & 0 & -5 \end{pmatrix}$
	$\begin{pmatrix} 1 & 0 & 0 \\ 0 & 1 & 0 \\ 0 & 0 & 1 \end{pmatrix}$	$\begin{pmatrix} -3 & 0 & 0 \\ -2 & 0 & 0 \\ -3 & 0 & 0 \end{pmatrix}$	$\begin{pmatrix} 1 & 0 & 0 \\ 0 & 1 & 0 \\ -1 & 0 & 1 \end{pmatrix}$	$\begin{pmatrix} 1 & 0 & 0 \\ -8 & 1 & 4 \\ -2 & 0 & 2 \end{pmatrix}$	$\begin{pmatrix} 1 & 0 & 0 \\ 2 & -1 & -3 \\ -1 & 1 & 2 \end{pmatrix}$	$\begin{pmatrix} 5 & 0 & -12 \\ 7 & -2 & -15 \\ 0 & 1 & -1 \end{pmatrix}$	$\begin{pmatrix} 5 & 0 & -12 \\ 3 & -1 & -6 \\ 2 & 0 & -5 \end{pmatrix}$

 Table B.4: The monodromy representations for the one-parameter families of K3 surfaces obtained by twisting two non- I_0^* fibres in the I_0^* -families.